Remote sensing of crop inventories and crop model simulations for irrigation management along the Guyana coastal plains

Guia Marie M. Mortel

Department of Bioresource Engineering

McGill University, Montreal

A thesis submitted to McGill University in partial fulfillment of the requirements for the degree of Master of Science

ABSTRACT

Updated, localized, and specific information on agricultural land area, crops planted, and irrigation requirements contribute to better irrigation planning and management. To this end, parameters and methods for a crop inventory and simulation of crop water productivity at the Guyana coastal lands were investigated. A supervised classification using Landsat8, Sentinel2, and RADARSAT/RCM C-Band was evaluated. For an inventory of both sugarcane and rice, the optical-radar fusion of Sentinel2 and RCM provided the highest accuracy (sugarcane: users accuracy [UA] = 95%, producers accuracy [PA] = 100%; and rice UA = 100%, PA = 95%), compared to single image products. Supervised classification using Sentinel2-RCM images for May, June and Oct 2021, and Jan 2022 showed good prediction with an accuracy of 82 - 87%, and kappa at 0.80 – 0.85. The crop stage at image acquisition impacts the accuracy of classification. The highest accuracy for rice was obtained at the vegetative, reproductive, and mature stages while for sugarcane, the highest accuracy was at tillering and maximum canopy phase.

The crop (rice, sugarcane and vegetables) simulations of water productivity were performed with the AquaCrop model and used both location-specific soil and weather data as well as AquaCrop default values. General field information and calibrated parameters are from the literature. The following irrigation thresholds based on the water holding capacity at the root zone (WHR) were tested: 50 to 120% WHR for rice, 40 to 100%WHR for sugarcane and 40 to 100% WHR for vegetables. The scenarios of 80%WHR for rice, 50%WHR for sugarcane and 40%WHR for vegetables have the lowest irrigation requirements without incurring significant difference (at $p>0.05$) in yield. These irrigation scenarios are recommended for irrigation water distribution during dry periods. Results of both the crop inventory and crop modelling provide important inputs into large-scale agricultural water planning and management in wet tropical regions.

RESUME

Des informations actualisées, localisées et spécifiques sur la superficie des terres agricoles, les cultures plantées et les besoins en irrigation contribuent à une meilleure planification et gestion de l'irrigation. Dans ce but, nous avons étudié les paramètres et les méthodes d'inventaire des cultures, ainsi que des simulations de l'efficacité de l'utilisation de l'eau sur les terres côtières de la Guyane. Une classification supervisée utilisant Landsat8, Sentinel2, et RADARSAT/RCM C-Band a été évaluée. Pour un inventaire de la canne à sucre et du riz, la fusion optique-radar de Sentinel2 et de RCM a fourni la plus grande précision pour la canne à sucre (précision des utilisateurs [UA] = 95 %, précision des producteurs [PA] = 100 %) et pour le riz (UA = 100 %, PA = 95 %), comparativement à l'utilisation d'images individuelles. La classification supervisée à l'aide d'images fusionnées Sentinel2-RCM pour mai, juin et octobre 2021, ainsi que pour janvier 2022, a montré une bonne prédiction avec une précision de 82 à 87 % et un kappa de 0,80 à 0,85. Le stade de la culture au moment de l'acquisition de l'image a un impact sur la précision de la classification. La plus grande précision pour le riz a été obtenue aux stades végétatif, reproductif et mature, tandis que pour la canne à sucre, la plus grande précision a été obtenue au stade du tallage et de la canopée maximale.

Les simulations de la productivité de l'eau des cultures (riz, canne à sucre et légumes) ont été réalisées avec le modèle AquaCrop et ont utilisé à la fois des données pédologiques et météorologiques spécifiques au site et les valeurs par défaut d'AquaCrop. Les informations générales sur les champs et les paramètres calibrés proviennent de la littérature. Les seuils d'irrigation suivants ont été testés : 50 à 120% de la capacité de rétention d'eau à la zone racinaire (WHR) pour le riz, 40 à 100%WHR pour la canne à sucre et 40 à 100% WHR pour les légumes. Les scénarios de 80 % de la capacité de rétention d'eau au niveau des racines pour le riz, de 50 %

pour la canne à sucre et de 40 % pour les légumes présentent les besoins d'irrigation les plus faibles sans entraîner de différence significative (à $p>0,05$) dans le rendement. Ces scénarios d'irrigation sont recommandés pour la distribution de l'eau d'irrigation pendant les périodes sèches. Les résultats de l'inventaire des cultures et de la modélisation des cultures fournissent des données importantes pour la planification et la gestion de l'eau agricole à grande échelle dans les régions tropicales humides.

ACKNOWLEDGEMENTS

My journey in McGill started when Dr. Chandra Madramootoo accepted me under his guidance. For this and his guidance, instruction and support throughout the years, I am immensely grateful. I am grateful for his mentoring, and his unique and thoughtful perspective on my thesis, the future of the agriculture sector, navigating through the academic and professional world, and continuous learning and improvement.

I would like to express my gratitude to the McGill community who supported, advised and taught me within the last two years. Special thanks to Naresh Thangaraju, Samuel Ihuoma and lab mates at the Water Innovation Lab for their advice on the thesis methods and navigating academic requirements at McGill. Many thanks to Dr. Adamchuk and Dr. Grant Clark for building up my knowledge of GIS, remote sensing, modelling and simulations. I am also grateful for the steady and reliable support of Wendy Ouellette, Shirley Mongeau and Christiane Trudeau.

Dr. Vern Singhroy has been an important contributor to the work on the crop inventory. I am thankful for his assistance in acquiring satellite data, for his insights on the methods and results, for taking photos of rice and sugarcane farms in Guyana, and for his guidance in presenting the tables and figures in the manuscript.

Simulation and remote sensing analysis require a lot of good-quality data. In this aspect, I am grateful for the detailed and rigorous work of Dr. Madramootoo, Raffaela Maria Pilati de Carvalho, Larissa Jarvis and Dr. Felexce Ngwa for the data collection of weather and the soil information at Guyana; and to Dr. Heather McNairn of Agriculture and Agri-Food Canada and the Landsat and Sentinel teams for allowing access to the satellite data used in this study.

I acknowledge the gracious fellowship provided by the Macdonald Stewart Foundation under the Liliane and David M. Stewart Fellowship in Water Resources and financial support from the International Development Research Centre (IDRC), Government of Canada through Global Affairs Canada, and the Natural Sciences and Engineering Research Council of Canada (NSERC). I am also thankful for McGill University's GREAT award for its support of my participation in the 2022 CSBE/SCGAB AGM and Technical Conference at Charlottetown.

Last but not the least, I wish to show my appreciation to my family and friends who have been a continuous pillar of support and encouragement throughout this journey.

CONTRIBUTION OF AUTHORS

Guia Marie Mortel is the principal author of this work, which was supervised by Dr. Chandra A. Madramootoo of McGill University. The conceptualization of the thesis was led by Dr. Madramootoo. The methodology was developed by Mortel, in consultation with Dr. Madramootoo. The data on soil and weather data were provided by Dr. Chandra Madramootoo. Ms. Mortel conducted the data gathering, processing of satellite images, model parameterization, crop simulation and statistical analysis. The results were interpreted by Mortel and Dr. Madramootoo. Ms. Mortel drafted the thesis and the four manuscripts, which were further reviewed and edited by Dr. Madramootoo. Dr. Vern Singhroy, a co-author of the manuscript presented in Chapter III, was involved in its conceptualization, interpretation of results, and review of the manuscript. Dr. Viacheslav Adamchuk, a co-author of the manuscript presented in Chapter III, was involved in its data analysis and interpretation of results.

A. Manuscripts

Chapter III: **Mortel, G.M.M.**, Madramootoo, C. A. Singhroy, V., Adamchuk, V.I. (2022). Classification of rice and sugarcane areas using optical-radar fusion. [Manuscript in preparation].

Chapter IV: **Mortel, G.M.M.**, Madramootoo, C. A. (2022). Optimizing water productivity of rice in tropical coastal plains heavy clay soil. [Manuscript in preparation].

Chapter V: **Mortel, G.M.M.**, Madramootoo, C. A. (2022). Improving water productivity of surface irrigated sugarcane estates in the Guyana coastal plains. [Manuscript in preparation].

Chapter VI: **Mortel, G.M.M.**, Madramootoo, C. A. (2022). Development of irrigation water strategies to intensify vegetable production in Guyana. [Manuscript in preparation].

B. Papers presented at conferences

1. **Mortel, G.M.M**, Madramootoo, C.A., Singhroy, V. RADARSAT/RCM for determining crop inventories in coastal Guyana. 2022 CSBE/SCGAB AGM and Technical Conference. July 2022.
2. **Mortel, G.M.M**., Madramootoo, C.A. Irrigation management for intensive vegetable production in Guyana. 2022 CSBE/SCGAB AGM and Technical Conference. July 2022.

TABLE OF CONTENTS

LIST OF FIGURES

LIST OF TABLES

LIST OF ABBREVIATIONS

AAFC	Agriculture and Agri-Food Canada
ANOVA	analysis of variance
AOI	areas of interest
AWD	alternate wetting and drying
BBP	Black Bush Polder
CCo	initial canopy cover
CC_t	effective canopy cover at a time, t
CCx	maximum canopy cover
CDC	canopy decline coefficient
CGC	canopy growth coefficient
CSA	Canadian Space Agency
DAP	days after planting
DAT	days after transplanting
Dr	depletion of water at the root zone
ESA	European Space Agency
ETc	crop evapotranspiration
ETo	reference evapotranspiration
FAO	Food and Agriculture Organization of the United Nations
FC	field capacity
GFC	Guyana Forestry Commission
GLSC	Guyana Lands & Surveys Commission
GRDB	Guyana Rice Development Board

GuySuCo	Guyana Sugar Corporation
HI	harvest index
HIo	reference harvest index
I	irrigation applied
I&D	irrigation and drainage
kc	crop coefficient
kc_{end}	crop coefficient at the late-season stage
kc_{ini}	crop coefficient at the initial stage
kc_{max}	maximum crop coefficient
kc_{mid}	crop coefficient at mid-season
Ks	stress coefficient
Ks_{aer}	water stress due to poor aeration
Ksat	saturated hydraulic conductivity
$Ks_{b,c}$	cold stress affecting biomass production
$Ks_{exp,w}$	water stress coefficient affecting canopy expansion
$Ks_{pol,c}$	cold stress affecting pollination
$Ks_{pol,h}$	heat stress affecting pollination
Ks_{sen}	water stress for early canopy senescence
Ks_{sto}	water stress coefficient affecting stomatal closure
MBE	mean bias error
MC_{vol}	moisture content by volume
NAREI	National Agricultural Research & Extension Institute
NASA	National Aeronautics and Space Administration

NDVI	Normalized Difference Vegetation Index
NSERC	Natural Sciences and Engineering Research Council of Canada
OA	overall accuracy
OECD	Organisation for Economic Co-operation and Development
PA	producer’s accuracy
p_{lower}	lower threshold for a stress coefficient
psto	threshold of Dr for water stress affecting stomatal closure
p_{upper}	upper threshold for a stress coefficient
PWP	permanent wilting point
R	rainfall received
RAW	readily available water
RCM	RADARSAT Constellation Mission
RH_{min}	minimum relative humidity
RMSE	root mean square error
RMSEn	percent root mean square error
SAR	synthetic aperture radar
SAT	saturation
TAW	total available water
Tn	daily minimum temperature
Tx	daily maximum temperature
u_2	wind speed at 2 meters height
UA	user’s accuracy
UA	user’s accuracy

UAV	unmanned aerial vehicles
UKCEH	UK Centre for Ecology & Hydrology
USACE	US Army Corps of Engineers
USDA	US Department of Agriculture
USGS	United States Geological Survey
WHR	water holding capacity at the root zone
WP	water productivity
WP*	normalized water productivity
WP_{et}	simulated water productivity for evaporation and transpiration
Y	yield
Ze	effective rooting depth
Z_{soil}	depth of the soil restrictive layer
$Z_{watertable}$	depth of the water table
Zx	maximum rooting depth

CHAPTER I: GENERAL INTRODUCTION

1. Background of the study

Agroecosystems are at risk of experiencing drought or waterlogging without an established irrigation and drainage system. To have sustainable yields, with minimal abiotic stress, large agricultural systems must have a well-designed water management system. The crop area and irrigation water requirements are important for water management planning and design. The irrigation water requirement is the amount of water needed to satisfy crop evapotranspiration needs and water losses incurred in the field such as soil evaporation, runoff, and deep percolation. It gives irrigation managers information on the volume of water which needs to be routed to a service area. The water requirement is usually measured or simulated at field or plant level at a unit depth of water required per unit area. To scale up the crop water requirements of an irrigation system, the service area also needs to be known.

The service area can be determined by regular reporting and accounting of planted and harvested fields. For wider irrigation and drainage systems and management such as at the regional and national level, a faster and more reliable means of monitoring the crop area ought to be established. Crop inventories through remote sensing have been developed and implemented in several countries for monitoring at a large scale. This study uses the latest developments in satellite technology and remote sensing to monitor rice and sugarcane inventories along the Guyana coastal lands.

Guyana was chosen for this study because the technologies mentioned above are still in their infancy in the country. Moreover, Guyana is in a transitional stage as it shifts from its extensive monocropping of sugarcane into more diversified agriculture. Sugarcane has been its major crop since the 19th century, but due to declining demand from the European Union and the

United States (Mitchell, 2006), and competition from subsidized beet sugar in European countries (McGowan, 2008), there was less demand for sugarcane. The abandoned farms are slowly being converted into other high value crops due to the government's agricultural diversification program. This crop diversification makes use of the existing expansive irrigation and drainage infrastructure, the high fertility of these coastal soils and abundant rainfall.

Knowledge of the crop water requirements of sugarcane, rice and various vegetables would be helpful for water resources management and planning. Moreover, much of Guyana's canals and irrigation and drainage infrastructure has been designed with drainage and navigation as a priority. Improvements in the infrastructure's design from an irrigation perspective would support more resilient agriculture, considering climate change. Climate scenarios for Guyana's coastal region suggest decreasing annual total rainfall and increasing intensity of flooding and drought (Government of Guyana, 2012). The agriculture sector needs to implement water-saving practices and improve the performance of existing irrigation and drainage systems.

2. Objectives of the research

This thesis aims to contribute to improvements in Guyana's agricultural water management through the following specific research objectives:

i. Develop a methodology for an operational crop inventory by comparing the suitability of Landsat8, Sentinel2, RCM and optical-radar fusion as image inputs (Chapter III);
ii. Evaluate the applicability of AquaCrop for modelling rice growth and water productivity (Chapter IV);
iii. Investigate irrigation deficit scenarios and their impact on the yield and water productivity of sugarcane (Chapter V);
iv. Recommend a water management scenario for higher vegetable productivity (Chapter VI).

CHAPTER II: COMPREHENSIVE REVIEW OF RELEVANT LITERATURE

1. Agricultural and climatological characteristics of the Guyana coastal land

Guyana is a country in South America, nestled between 1° to 9 °N and 56° to 62° W. For several decades, sugarcane has been its major crop, with the management of its farms held by the government since 1976 through the Guyana Sugarcane Corporation (1999). However, due in part to the declining preferential sales of the European Union and the United States (Mitchell, 2006), and competition from subsidized beet sugar from European countries (McGowan, 2008), the production of sugarcane has decreased remarkably. Nearly 400 sugarcane estates had encompassed the coastal plains of Guyana at its peak production in the 19th century (GuySuCo, 1999) but as of 2018, only three estates remain (GuySuCo, 2018). The exports, which amounted to USD 123 million in 2011 fell to USD 27.7 million in 2019 (Singh, 2021). Rice production has been the second major crop of Guyana since the 20th century (McGowan 2008). It has been increasing steadily, contributing to 5% of the total GDP by 2013 (Ministry of Agriculture, 2013). Rice is cultivated in Regions 2, 3, 4, 5 and 6, shown in Figure 2.1, and covers approximately 90,000 ha (Ministry of Agriculture 2013).

Figure 2.1. Primary rice-producing regions in Guyana (reprinted from Mahdu, 2019).

Aside from the reasons cited for sugarcane's decline, the agriculture sector also experienced symptoms of Dutch disease caused by the booming gold, diamond and oil industries (Bubbico et al., 2020), persistent labour issues (GuySuCo, 2018), the deterioration of the irrigation and drainage system and access roads, absentee owners, and patches of high salinity areas (GLSC, 2013). These led to the contraction of agriculture and further abandonment of agricultural lands. In Region 6, cultivated lands (53,000 ha) are almost as wide as abandoned lands (44,000 ha) of which 82% is publicly owned (GLSC, 2004).

The soils of the coastal farmlands of Guyana are mostly rich clayey and silty soils. From the coast and stretching 32 km inland, the soil is hydraquents or marine phase front land soil; meanwhile areas closer to the rivers are fluvaquents or riverain soils. Both are classified as good to moderate agricultural land with poor drainage (Braun & Derting, 1964; GLSC, 2013). Agriculture is limited near the coast since the soils further inland are medihemist soils which are bog soils of very high acidity, extremely low fertility and acid sulphate toxicity (GLSC, 2013).

The climate at the coast and the upper half of Guyana is tropical rainforest (Peel et al., 2007). The wet climate at the coast allows for two high-yielding cropping seasons. Crops can be planted all year round.

Both the soil and the climate are suitable for agriculture and support high yields. Moreover, the area has four major rivers (Essequibo, Demerara, Berbice and Corentyne Rivers) which divide the coastal plains and provides freshwater from the backlands; and plentiful narrow rivers and streams such as the Mahaica, Mahaicony, Abary and Canje rivers (USACE, 1998). However, even with the presence of these rivers, areas near the coastline of Guyana have large quantities of brackish water all year round due to the tidal influence along the river and streams (USACE, 1998). Wide and shallow reservoirs called conservancies were constructed further inland to catch and store fresh water. Canals, discharge regulators and gates were also installed to deliver fresh water from the conservancy to the farms.

The fertile soil, wet climate, availability of freshwater for irrigation, and existence of an established and expansive I&D system encourage agriculture and point to a high potential for agriculture to thrive in Guyana. However, agriculture has been solely focused on sugarcane for a very long time, and a shift to other crops, such as vegetables, will require not only a shift in the crops produced, but also a shift in the farmers' and government's thinking, priorities, and the design, planning and management of infrastructures and systems.

2. Crop water management of tropical agricultural systems

The water management measures such as water harvesting, soil moisture conservation, irrigation improvements, and a combination of these measures can contribute to an increase in the global kcal production by at least 18% for the low implementation scenario, and at most 60% for the maximum implementation (Jägermeyr et al., 2016). Crop water management is important for all levels of agriculture production: for the farmers to get high sustainable yields and improved productivity, and the national and global interest in keeping food security for the next years in light of the growing population and a more erratic climate.

In the tropics, which lie between the Tropic of Cancer and the Tropic of Capricorn, cold temperature is not a limiting factor to production, but the high temperature increases evaporation, and the precipitation is not well distributed all year round (Hoffman et al., 1990). The monsoons bring in heavy rainfall but the intensity, start and end of a monsoon season varies annually. The key characteristics therefore of crop water management for tropical agriculture are the storage of water during the wet months, reduction of water losses during the dry months, and productivity improvements.

Reduction of water losses in the field contributes to higher water productivity (WP). As an efficiency parameter, higher WP values can be achieved by obtaining better yields and reducing inputs and losses. There are several ways to reduce losses such as by controlling soil evaporation through mulching and closer plant spacing and using systems with fewer conveyance losses and application inefficiencies, e.g., drip irrigation. Various mulching media such as straw (Biswal et al., 2022), composted coir pith, sugarcane trash (Dhanapal et al., 2019) and plastic film (Chai et al., 2022) have been tried and their impact on the yield and water productivity have been studied.

The water use efficiency can also be improved by developing better varieties (Dou et al., 2016; Poddar et al., 2022), inducing water stress to promote fruit formation, using deficit irrigation or alternate-wetting and drying, and modifying the irrigation methods such as using alternate or fixed furrow irrigation instead of the convention furrow irrigation (Abera et al., 2020; Bayisa et al., 2021).

Water-saving methods such as deficit irrigation and alternate wetting and drying (AWD) has been around for several years. The current trend of research on these technologies involves their comparison with other irrigation regimes such as continuous flooding and saturation (Blango et al., 2019; Dou et al., 2016; Poddar et al., 2022), identification of soil-water thresholds to minimize yield losses (Akinro et al., 2012; Bayisa et al., 2021; Vélez-Sánchez et al., 2022), and the scheduling of varying levels of applied water stress or soil-water thresholds for different crop phenological stages (Brar & Singh, 2022; Dingre et al., 2021; Elsheikh, 2015).

The water management strategies discussed above are tested and measured at the field or farm level. To scale up the impact of these strategies to the requirements at a larger scale such as for a town or an irrigation service area, the production area must be known.

3. Monitoring of crop production area

A crop inventory which uses remote sensing satisfies the requirements for monitoring a large expanse done at frequent intervals and low labour needs. Remote sensing information can be obtained either from satellite images or from UAVs. In this paper, remote sensing implies the images obtained from satellites. Several satellites have been deployed in the past decades as humanity's knowledge of space exploration grew. These satellites take images of the earth's surface at a constant schedule and collect different information depending on their specifications. Sensors on board the satellites capture images from different wavelengths of the electromagnetic spectrum. Some, such as Landsat (USGS, 2022), Sentinel-2 (ESA, 2022a), and MODIS (NASA, 2022a) provide data from the optical, infrared and ultraviolet range, while others such as the RADARSAT Constellation Mission (CSA, 2021), Sentinel-1 (ESA, 2012), NISAR (NASA, 2022b), and TerraSAR-X (ESA, 2022b) provide data from the radar L, X or C-bands. These sensors differ further by their spectral resolution, which is the range of wavelengths they were designed to receive; the radiometric resolution which is their sensitivity to the wavelengths; and spatial resolution which is the area equivalent to one-pixel size in the satellite image. Moreover, each of these satellites has specific paths around the earth which determines their temporal resolution or the frequency that an image is captured in a location. Various satellite images or data products are available for use with each one having its own set of specifications, data archive length, preprocessing, availability, and costs.

Before a crop inventory is established, the most suitable satellite products and processing methods have to be determined first. The design of an inventory depends on the purpose, the target final product, characteristics of the location, objects to be identified, frequency of data collection, and also financial constraints. When the target of the inventory is general vegetation, the area can be distinguished from adjacent water bodies, and urban areas by the RGB, near-infrared, red edge bands (Chen et al., 2021; Feranec et al., 2000; Waser & Schwarz, 2006). When the targets of the inventory are specific vegetation covers such as trees, crops or grass, satellites which provide more spectral bands greatly assist in distinguishing the minute differences in the spectral reflectance of crops such as done by (Marais-Sicre et al., 2020; Pfitzner et al., 2022; Verma et al., 2019).

The location of the crop inventory and desired frequency of monitoring determines the suitable satellite sources. In the tropics where cloud cover is a concern, radar images are more reliable sources as they can retrieve information through thick layers of clouds. Given the frequency of cloudy days in the tropics, and the return frequency (every 12 or 14 days) of optical satellites, few to no clear images can be obtained in a year. A large-scale crop inventory poses another concern since several cloudless images have to be available to create a mosaic image. Finally, the cost of acquiring satellite images is an important factor to ensure the smooth and regular operation of crop inventories.

4. Identification of crop water requirement

The irrigation water requirement can be computed from the crop water requirement and the production area. The crop water requirement is measured or simulated at the plant level and it is equivalent to the needs of a crop for evapotranspiration (Hoffman et al., 1990). Quantifying evapotranspiration, however, is complicated. Not only does evapotranspiration vary between crops, but also between climate, varieties and cultivars, and different crop stages. A standard or reference evapotranspiration was established to create a baseline evapotranspiration value, usually of alfalfa or other short grasses. The computation of the ETo is altogether a separate set of modelling. It can be measured using evaporation pans or computed from the Penman-Monteith, Hargreaves, Blaney-Criddle, and several other methods (Hoffman et al., 1990).

The ETo accounts for the impact of climate and location on ETc, whereas the crop coefficient accounts for the evapotranspiration of the target crop relative to the reference grass. As the crops mature, the kc also varies. This factor is considered in ETc computations by using a different kc value for the initial stage (kc_{ini}), mid-season (kc_{mid}) and late season (kc_{end}) stage (Allen et al., 1998) The crop transpiration is computed from the ETo and the crop coefficient, as shown in Equation 1.

$$ETc = kc * ETo \qquad \text{(Eq. 1)}$$

Theoretically, crop transpiration would represent all of the crop's water needs. But in a farm, evapotranspiration and delivery of water comes with losses incurred from the application of irrigation, evaporation, run-off and storage and movements of water within the soil. Crop models seek to simulate the interactions between the crop, climate, soil, water and management practices, and predict the impact of these interactions on the crop's growth, yield and environment.

One of these crop growth models is AquaCrop (FAO, 2018), which is notable for its simple design and usability to a wide range of practitioners. AquaCrop is a water-based model wherein the availability of water drives growth (Steduto et al., 2009). The translation of water to yield is governed by three equations: computation of the water required for evapotranspiration (in Equation 2), conversion of the water transpired into biomass (in Equation 3) and partitioning of the above-ground biomass into yield and non-marketable biomass (in Equation 4).

$$ETc = kc * ETo * CC_t \qquad \text{(Eq. 2)}$$

$$B = WP^* * Tr \qquad \text{(Eq. 3)}$$

$$Y = HI * B \qquad \text{(Eq. 4)}$$

Wherein the ETc is the crop evapotranspiration (mm day^{-1}); kc is the crop coefficient (unitless); ETo is the reference crop evapotranspiration (mm day^{-1}); CC_t is the effective canopy cover at time t (%); B is the aboveground biomass (kg); WP* is the normalized water productivity (kg m^{-3}); Y is the yield (kg); HI is the harvest index (unitless)

The values of all of the parameters in the three core equations are adjusted by the input parameters, the presence of stresses, the extent of canopy cover over time, and the effective depth of the root zone. There are three components or modules which are simulated separately in AquaCrop: soil available water, root deepening and canopy development. The parameter values contributed by each component to the core equations are shown in Figure 2.2.

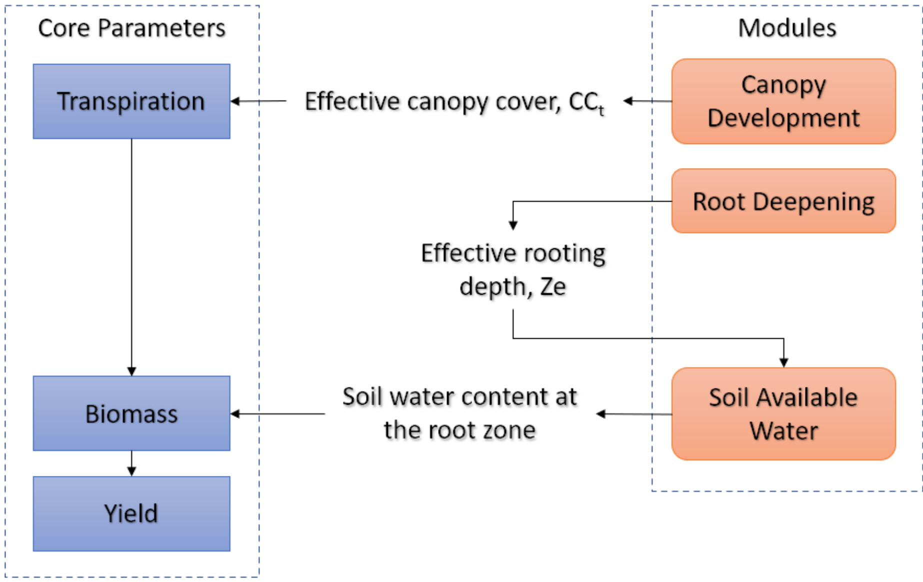

Figure 2.2. Simplified core simulation computations, modules and parameters in AquaCrop

The canopy development module provides the effective canopy cover used in Equation 2. Meanwhile, the root deepening module simulates root growth and provides the effective rooting depth which is further used in the soil available water module. Lastly, the soil available water module's main output is the soil water content at the root zone. Water uptake is either equal to the crop transpiration requirement in Equation 2, or the available water at the root zone, whichever is smaller.

AquaCrop does not model the processes behind crop stress. Instead, the values of the stress coefficients (Ks) are determined by the values of indicator parameters and their relationship to stress thresholds, as shown in Table 2.1. Several stress coefficients are used to represent water stress due to drought, water stress from waterlogging, cold stress, heat stress, nutrient deficiency stress, and salinity stress. The Ks values indicated the severity of stress wherein values closer to '1' are for unstressed or optimal conditions and values nearer to '0' represents stressed conditions.

The stress coefficients are incorporated into the core equations or modules depending on the parameter they modify.

Table 2.1. Stresses considered in AquaCrop and their indicators, thresholds, stress coefficient, and effect on parameters.

Stress coefficient (K_s)	Indicator	Parameter Modified
A. Water Stress		
water stress affecting canopy expansion ($Ks_{exp,w}$)	fraction of water depletion at the root zone (Dr)	canopy growth coefficient (CGC), harvest index (HI)
water stress affecting stomatal closure (Ks_{sto})	fraction of water depletion at the root zone (Dr)	crop evapotranspiration (ETc), harvest index (HI)
water stress for early canopy senescence (Ks_{sen})	fraction of water depletion at the root zone (Dr)	Senescence phase, canopy decline coefficient (CDC)
water stress due to poor aeration (Ks_{aer})	percent air in soil pore volume	crop evapotranspiration (ETc)
B. Temperature stress		
cold stress affecting pollination ($Ks_{pol,c}$)	Daily minimum temperature (T_n)	harvest index (HI)
cold stress affecting biomass production ($Ks_{b,c}$)		Biomass (B)
heat stress affecting pollination ($Ks_{pol,h}$)	Daily maximum temperature (T_x)	harvest index (HI)
C. Soil Fertility Stress		
soil fertility stress coefficients	soil available Nitrogen, Phosphorus, Potassium	CGC, maximum canopy cover (CCx), normalized water productivity (WP^*)
D. Soil salinity stress		
salinity stress affecting stomatal closure (Ks_{sto})	electrical conductivity (ECe)	CGC, CC_x, CDC

* p_{lower} and p_{upper} are thresholds defined for each stress coefficient and indicator

AquaCrop has been used extensively since its dissemination. A review by (Salman et al., 2021) has shown that the research using AquaCrop can be divided into development, evaluation and application. The works on development include the addition of new features such as the assimilation of remote-sensing data (Corbari et al., 2021; Han et al., 2020), AquaCrop-GIS (Lorite et al., 2013), and programming into other languages (Camargo Rodriguez & Ober, 2019). Evaluation activities, meanwhile, are parametrization, calibration, validation and testing studies of different crops at various locations (Sandhu et al., 2015; Wellens et al., 2022). Lastly, the application of AquaCrop constitutes studies of crop response to agronomic management practices (Ahmadzadeh Araji et al., 2019; Bahmani & Eghbalian, 2018), impact assessment to crop production by environmental changes (Alvar-Beltrán et al., 2021; Raoufi & Soufizadeh, 2020), and support to policymaking through the simulation of hypothetical scenarios and interventions (Karandish & Hoekstra, 2017; Zhuo et al., 2016).

AquaCrop is suitable for this thesis as it has already established its use for large-scale applications such as those for climate change impact assessment and policy support. Its use of conservative and default parameters; and templates for grains/fruit-producing crops, leafy vegetables and root/tuber crops, make it applicable when information on the numerous model parameters is limited. A comprehensive review of crop parameters for field crops (Pereira, Paredes, Hunsaker, et al., 2021), vegetables (Pereira, Paredes, López-Urrea, et al., 2021) and tree and vine fruit crops (Rallo et al., 2021) has confirmed that the standard crop parameters released in FAO56 (Allen et al., 1998) is still in agreement with the result of recent crop parameter studies. The review released updated FAO56 standard crop parameters to incorporate the results of the new studies. Moreover, the parameters adjusted to the standard climate (minimum relative humidity RH_{min} = 45% and wind speed at 2 meters height u_2 = 2 m s^{-1}) (Allen et al., 1998; Pereira, Paredes, López-Urrea, et al., 2021) were also provided to improve the transferability of crop coefficients for simulation at other locations.

BRIDGING TEXT

Research objective 1 aims to develop a methodology for a crop inventory for rice and sugarcane. The study is discussed in Chapter III. Several satellite images taken on different dates were tested. The suitability of these data inputs, the date of acquisition and optical-radar fusion were explored to come up with a set of methods or guidance for establishing a crop inventory in the country.

This study is in preparation for submission to the *International Journal of Applied Earth Observation and Geoinformation*. The paper is co-authored by Guia Marie M. Mortel, Dr. Chandra Madramootoo, Dr. Vern Singhroy and Dr. Viacheslav Adamchuk. The contributions of each author are mentioned on page 7.

CHAPTER III

Classification of rice and sugarcane crop patterns using optical-radar fusion

Abstract

Crop inventory has been traditionally conducted using optical satellites. In recent years, the use of synthetic aperture radar has extended the applicability of remote sensing by providing a textural basis for classification in both day and night-time, and over cloud-covered areas. We explore the applicability of optical-radar fusion for a crop inventory of sugarcane and rice in the coastal plains of Guyana in South America. Land use in Guyana has changed considerably. A crop inventory could provide insight into the extent of the land use change and identify alternative cropping patterns for abandoned land. A most recent set of images and acquisition dates were evaluated to distinguish between rice and sugarcane. Supervised classification using single-sensor, single-date images showed better performance with Sentinel2 (81% overall accuracy), compared to Landsat8 and RADARSAT Constellation Mission (RCM). Landsat8 is suitable for the mapping of sugarcane areas, and Sentinel2 is suitable for rice. However, for the simultaneous classification of both crops, the Sentinel2-RCM (accuracy of 84% and kappa of 0.82) is better than single-sensor classifications using only Landsat8, Sentinel2 and RCM. Better class accuracies were observed for rice when most of the fields are at the vegetative, reproductive, and mature stages. For sugarcane, the tillering, grand growth, and early maturity stages are most suited for a crop inventory. The results provide a basis for the design of an operational system for the mapping of rice and sugarcane areas in Guyana and other tropical regions.

1. Introduction

Monitoring crop area production is essential for various planning activities. In the context of agricultural water management, crop area information, alongside irrigation requirements, is necessary to calculate the volume of water to be released to farms. Accurate data on the area planted provides a more exact estimate of irrigation allocations.

Remote sensing is a common approach for large-scale crop monitoring. National crop inventories, such as in the US (USDA, 2019), Canada (AAFC, 2022) and the UK (UKCEH, 2022) rely on optical and radar satellite images (MODIS, Landsat-5, AWiFS, DMC, Sentinel1, Sentinel2 and Radarsat2) to generate crop area information. The general process of an inventory or classification is by running a trained algorithm over a set of satellite images for a target area. Satellite images will have differing data and resolution accuracy depending on the satellite, sensor and wavebands selected. The trained algorithm, meanwhile, can be prepared using supervised or unsupervised classification.

A few global annual crop mapping and forecasting services also exist such as the Crop Explorer by the USDA Foreign Agricultural Service (2022), Crop Watch bulletins by the Institute of Remote Sensing and Digital Earth of the Chinese Academy of Sciences (CropWatch, 2022), Monitoring Agricultural ResourceS by the European Commission (2022), and the Global Information and Early Warning System on Food and Agriculture by FAO (2022).

Due to the importance of rice to the food security of many cultures around the world, some institutions have produced country-wide maps specifically for rice. For example, the Philippine Rice Information System provides a country-wide map of areas planted with rice and their estimated yield during each cropping season using Sentinel1A images and the ORYZA crop model (Alosnos et al., 2019; PHILRICE, 2022). Research on methods for mapping rice areas has also been done at the global scale to map rainfed, irrigated and paddy croplands using MODIS, climate date, and existing statistical crop surveys and inventories (Salmon et al., 2015). Other country- or region-wide mapping studies have been done in West Indonesia (Sianturi et al., 2018; Thorp and

Drajat, 2021), the Mekong River Delta in Vietnam (Bouvet and Le Toan, 2011; Kontgis et al., 2015), and China (Wei et al., 2022; Zhan et al., 2021).

Mapping of sugarcane areas is operational at the national level in Brazil through the Canasat Project which provides annual maps of sugarcane cultivation areas and harvested fields using multitemporal and multispectral images from Landsat and the China-Brazil Earth Resources Satellite (CBERS) (Canasat, 2022; Rudorff et al., 2010). Sugarcane mapping studies have also been done in Guangxi, China (J. Wang et al., 2020); Longzhou, China (Wang et al., 2019); southeast India (S. Wang et al., 2020); and in Sao Paulo Brazil using object-based image analysis (Luciano et al., 2019).

1.1. Classification using optical and SAR satellite images

High spectral resolution sensors can pick up subtle variations between different crops or land cover subclasses (Qin et al., 2022; Hamzeh et al., 2016; Pfitzner et al., 2022). In addition to the bands provided by high spectral images, indexes also improve classification by providing an additional value for classification. The Normalized Difference Vegetation Index (NDVI) is one of the common indexes used to indicate vegetation health (De Oto et al., 2019; Feng et al., 2022; Ihuoma and Madramootoo, 2019; ILRI, 2022.). A comparison by Zhi et al. (2017) on vegetation indexes has showed NDVI to be the optimal optical index for identifying rice phenology as compared to 11 other indexes such as the enhanced vegetation index, simple ratio and chlorophyll index. NDVI values above 1 or below zero are usually indicative of non-vegetated areas, and are thus, also helpful in distinguishing vegetation.

In recent years, there is increasing use of radar sensors for crop inventory (AAFC, 2022; Homayouni et al., 2019; Pei et al., 2011; UKCEH, 2022). The active transmission of SAR satellites allows sensors to use its energy to illuminate and thus detect and record images at any time. Clouds, and other less dense matter, do not interact with the SAR signals, making SAR appealing for remote sensing studies over regularly clouded areas such as the tropics. One of these SAR data sources is the RADARSAT Constellation Mission (RCM) which consists of three small synthetic aperture radar (SAR) satellites flying in a constellation configuration. It was launched in June 2019, and new applications of the products are currently being developed. The RCM provides compact polarization. In this configuration, the signal transmits waves at circular or compact polarizations and receives the backscatter either along H or V vectors (Touzi and Côté, 2019). Recent results have shown that the multi-frequency and compact polarimetric images from RCM, when combined with fully polarimetric data, were useful for estimating soil moisture conditions, improving ship detection and classification, and mapping geological structures (Singhroy et al., 2021). This study is a first for mapping tropical crops using RCM.

1.2. Remote sensing in Guyana

Cloud cover is a challenge to remote sensing activities in Guyana. It is overcast for most of the year, and partly cloudy for the rest. A review of Landsat8 images from 1990 to 2009 identified only 280+ viable cloud-free images, in which more than 70% were taken between August to November (GFC and Poyry Forest Industry [PFI], 2011). Its climate has two rainy seasons: one from December to January, and a wetter season from April to August (US Army Corps of Engineers [USACE], 1998). The two rainy seasons dictate the start of the two main planting periods. The first season of rice is planted between May and June, while the second season is from November to December (Guyana Rice Development Board [GRDB], 2022). Sugarcane is mostly planted during the second season.

A national forest inventory (GFC and PFI, 2011) has been conducted in Guyana. Other remote-sensing studies done are the detection of artisanal gold mining in forests (Stoll et al., 2022), mapping of mangrove areas (Nedd et al., 2021) and identifying episodes of coastline advance and retreat (Ahmad and Lakhan, 2012). Time-series radar and Landsat data fusion techniques were used to estimate coastline changes and map land cover along the coastal areas (Singhroy, 1996, 1995; Singhroy et al., 2021).

There is currently no methodology for an operational crop inventory in Guyana. To contribute to filling this gap, this study will evaluate the suitability of Landsat8, Sentinel2, RCM and optical-radar fusion as image inputs for the crop inventory. Furthermore, we will also test the performance of the classification for varying acquisition dates. This study seeks to address the following research objectives:

i. Analysis of the performance of classifying rice and sugarcane areas using single-date images from Landsat8, Sentinel2 and RCM;
ii. Assess the accuracy of classification using a combination of optical and radar data;
iii. Establish the considerations for deciding the image acquisition date for the crop inventory.

2. Methodology

2.1. Site selection

Guyana is located between 1.18° and 8.44° N, with the Atlantic Ocean at its north, and Venezuela, Brazil and Suriname at its borders. Its major crops are rice and sugarcane, which are grown along the Atlantic seacoast stretching from the Pomeroon River to the Corentyne River. These agricultural lands comprise 1.54% of the total land and contribute around 16.8% to the national GDP (Bank of Guyana, 2020). Most of the rice is grown at West Berbice in Region 5, Essequibo in Region 2, and Frontlands in Region 6 (GRDB, 2016b). Meanwhile, the major sugarcane estates are Albion/ Port Mourant in Region 6, Blairmont in Region 5 and Uitvlught in

Region 3 (GuySuCo, 2018).

West of the Berbice river from the Number 40 to Waterloo villages was selected for the classification. The site encompasses parts of Region 5 and Region 6 and has a good mix of sugarcane estates, rice fields, and other land use. Two areas-of-interest (AOI) (in Figure 3.1) were selected: one for training near Bush Lot village, and one for testing at Waterloo village. Figure 3.2 shows the rice and sugarcane crops in the testing and training areas on June 25th, 2022. The fields followed the regular planting schedule and represented the usual field view during June.

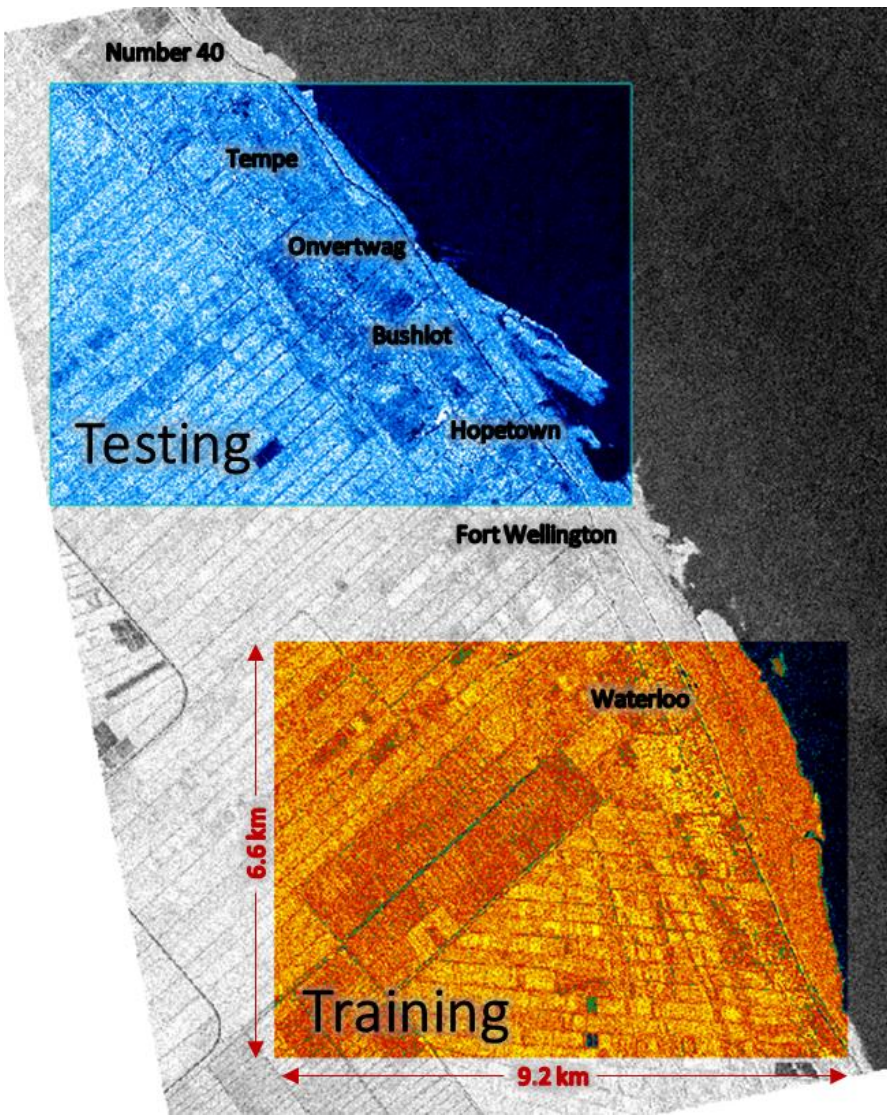

Figure 3.1. Area-of-interest used for training and testing.

Figure 3.2. Rice (A) and sugarcane (B) fields at the study site in June.

2.2. Satellite data and pre-processing

Images covering the coastline from Number 40 to Waterloo villages were acquired for May, June and October 2021, and January 2022. The final set of selected images for Landsat8, Sentinel2 and RCM are shown in Table 3.1.

Table 3.1. Final selection of images for each satellite per acquisition month.

Month	Landsat8	Sentinel 2	RCM
May	2021-04-29	2021-05-12	2021-05-02
June	2019-05-26	2021-06-11	2021-06-10
October	2021-10-06	2021-10-09	2021-10-01
January	2022-01-08	2022-01-12	2022-01-08

Landsat 8 Operational Land Imager is an optical satellite, designed and managed by the NASA and the US Geological Survey (USGS) from 1972 to the present. It provides reflectance for 11 bands at 15, 30, and 100 km spatial resolution at a revisit time of 16 days (USGS, 2022). Meanwhile, Sentinel2 is managed by the European Space Agency. It provides data on visible light, and infrared bands at 10, 20 and 60 m spatial resolution at a revisit of 10 days per satellite or 5 days for the whole constellation (ESA, 2022). The RCM, meanwhile, provides SAR images using

its fully polarimetric capabilities, in addition to single-polarization (HH, HV, VV), conventional (HH-HV, VV-VH, and HH-VV), and hybrid (i.e., compact) dual polarization. The RCM is designed to transmit and receive C-band at 12 days frequency per satellite or 4 days for the whole constellation at a spatial resolution of 3 to 100m depending on the imaging mode (CSA, 2021).

2.2.1. Preprocessing

The RCM images were C-band RCH and RCV, taken at 5 m resolution. Radiometric correction, multi-look, speckle filtering and terrain correction were performed. For Landsat8, images from the Level2 Collection2 Tier1 were used. Collection 2 images have been corrected with terrain correction, radiometric calibration, and radiometric saturation; Level2 images are products taken at a 76' solar zenith angle, thus reducing shadows in the image; and Tier 1 are scenes of the highest available data quality (USGS, 2022). The scenes were projected to WGS 1984 UTM Zone 21N. The Sentinel2 images, meanwhile, were Level 1C Top-of-the-atmosphere. The bands at 10 meters resolution were used along with the infrared bands at 20 meters resolution, as shown in Table 3.2. Atmospheric correction was done to convert from 1C to 1A Bottom-of-the-Atmosphere. For both Landsat8 and Sentinel2, the NDVI was calculated, and all the bands were stacked.

Table 3.2. Bands used and their spatial and spectral resolution

Satellite	**Landsat8**	**Sentinel 2**	
Spatial resolution	30 meters	10 meters	20 meters
Bands used (Code and wavelength)	B1: 435 – 451 nm, ultra-blue B2: 452 – 512 nm, blue B3: 512 – 590 nm, green B4: 636 – 673 nm, red B5: 851 – 879 nm, NIR B6: 1,566 – 1,651 nm, SWIR1 B7: 2,107 – 2,294 nm, SWIR2	B2: 490 nm, blue B3: 560 nm, green B4: 665 nm, red B8: 842 nm, VNIR	B5: 705 nm, VNIR B6: 740 nm, VNIR B7: 783 nm, VNIR B8a: 865 nm, NIR B11: 1610 nm, SWIR1 B12: 2190 nm, SWIR2

Satellite	Landsat8	Sentinel 2
Computed Index	NDVI	NDVI

2.2.2. Generating reference images and criteria for rice and sugarcane

Sample points were generated all over the AOIs. They were manually classified and then confirmed with experts familiar with the area. In the satellite images, sugarcane fields were observed to have a very distinct pattern, as seen in Appendix A. Rows can be identified, especially in high-resolution images. Deep furrows appear every two rows. The whole field, which averages six ha, is bisected by an in-field collector drain (GuySuCo, 2022). The farm irrigation canals are wider and are easily distinguishable in satellite images. Meanwhile, a rice field (Figure 3.3 A) can range from 0.5 to 6 ha. Regardless of the field dimensions, rice farms are significantly smaller than sugarcane farms. Because rice is planted by broadcast or by closely spaced rows, it appears as uniform green bands in satellite images. The false-colour images using SWIR - NIR - Red (Landsat8: B6-B5-B4, Sentinel2: B11-B8a-B4) were also used to differentiate between soil and flooded fields; and soil and newly planted crops. The reference images and criteria shown in Appendix A were used to help classify each sample point.

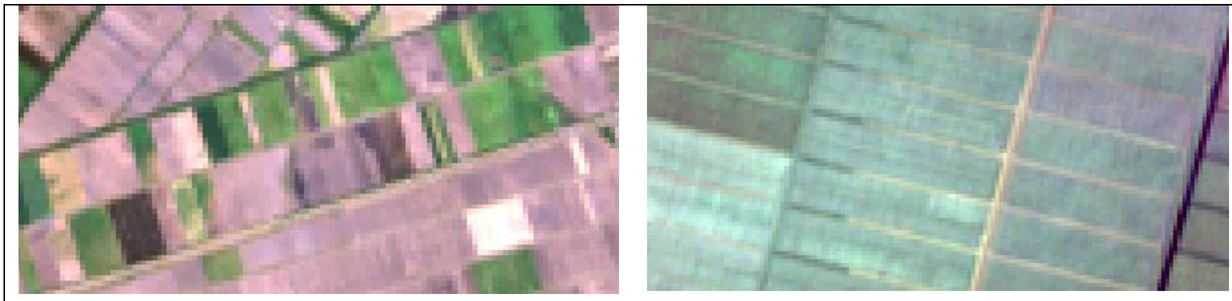

a. Rice fields

b. Sugarcane fields

Figure 3.3. Rice (a) and sugarcane (b) fields, as observed from satellite images

2.3. Image classification and accuracy analysis using single satellite images

Supervised classification is a method of identifying a pixel's class based on statistical similarities between its band values and those of training points with a known class. An image was selected for Landsat8 (2021-04-29), Sentinel2 (2021-05-12) and RCM (2021-05-02). Each of the three images was clipped with the AOI for training and used for supervised classification. Several training points were manually identified for each of the 10 classes: rice, sugarcane, mixed vegetation, grassland, soil, cloud shadow, clouds, water, forest and settlements. To extract meaningful information from the satellite data, a spectral-based pattern recognition algorithm is used. It is chosen over object-oriented algorithms because of its use of the spectral information at each pixel to identify its class. Moreover, it is available in many free and open-source software, or commonly used GIS processing software. This allows an easier replication or adoption of the methods in this study. The maximum likelihood, a spectral-based algorithm, assigns pixels to a class based on their band fit with the normal distribution of each class's band (Casella and Berger, 2002). It was used for its rapid processing and low computing resource requirement. The probability threshold was set to zero to force the program to classify all pixels. The classification algorithm was run using the training images and the training points. The classified images were then smoothed and aggregated using majority analysis with kernel size 7.

Once the classification of the training image was acceptable by visual inspection, a statistical analysis was done to check its accuracy. First, the supervised classification was run for the whole image using the trained set of algorithms, training points and parameters. The classified image was then clipped with the testing AOI. Random sample points were generated, and the actual class of each point was checked by referring to several sources: true-colour image, false-colour image, Google Earth, ESRI World Imagery, and confirmation with field photos and experts.

Satellite imagery had been used to validate the class of the sample points when field validation is not possible, such as when the study period is in the past and land use has changed considerably such as forest degradation (Chen et al., 2021), land cover change (Feranec et al., 2000; Li et al., 2021), and cropping pattern changes (Lunetta et al., 2010) over several years; or the locations are expensive for field validation such as remote islands (Hanintyo et al., 2021), caribou areas for lichen cover monitoring (Jozdani et al., 2021) or tracking forest fires (Sifakis et al., 2004).

A confusion matrix was generated to compare the actual with the predicted class. The optical image which produced the highest accuracy was stacked with the RCM image for the optical-radar fusion. A similar procedure for training and accuracy analysis was carried out on this image to determine the performance of the fusion as compared to single-sensor images.

2.4. Multi-date image classification and accuracy analysis

The sensor which gave the highest accuracy between Landsat8 and Sentinel2 was fused with RCM and used for the analysis on varying image acquisition dates. Images were downloaded for May, June and October 2021, and January 2022. Preprocessing was done as described in Section 2.2, and classification training and testing as in Section 2.3.

The results of each acquisition date were overlayed with the crop calendar for rice and sugarcane to determine the performance of the classification across the crops' various growth stages. The crop calendar is based on the pattern of land cover change observed across the four images; the known growth duration of the crop; and the usual planting period of rice and sugarcane. Both sugarcane and rice fields are flooded weeks before planting to control weeds. A sequence of bare soil, flooded fields and vegetation indicates the start of a cropping season.

SNAP and its Sen2Cor processor were used for pre-processing; ENVI Version 5.6.1 for the supervised classification and most of the data transformation and analysis; and ArcGIS for the creation and processing of random sample points.

3. Results and Discussion

3.1. Classification using single-sensor images

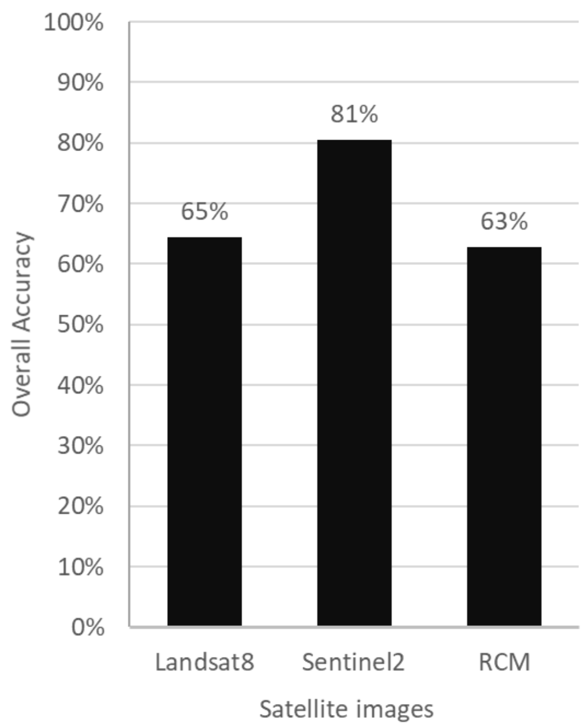

Figure 3.4. The overall accuracy of classification using various satellite images

The classification using single-date, single-sensor images from Landsat8, Sentinel2 and RCM achieved an average overall accuracy with Sentinel2 at 81% (kappa coefficient = 0.78) as shown in Figure 3.4. The overall accuracy (OA) is the percentage of true positive over the total testing points for all classes, while the kappa coefficient compares the performance of the classification to random. A kappa coefficient of zero means that the classification is as good as a random classification. The overall accuracy and kappa coefficient of the classifications using the three satellites compare well with similar crop inventories, as shown in Table 3.3. An overall accuracy ranging from 60 to 90% was obtained by other studies for single image classifications using optical satellites (SPOT, Landsat8, Sentinel2). Classifications using an individual SAR image have been proved to be inaccurate with at most 66% overall accuracy. A time series of SAR images or a combination of SAR with other satellite images are more promising methods for classifications using SAR.

Table 3.3. Overall accuracy of a single image classification using optical or SAR images

Author/s	Satellite	Overall accuracy (%)	Location	Classes
A. Optical				
Blickensdörfer et al. (2022)	Sentinel2 + Landsat8	67 – 70	Germany	Various crops
Yan et al. (2021)	Sentinel2	79 – 81	Sanjiang Plain, Chian	Various crops
Marais-Sicre et al. (2020)	Formosat-2	56	Toulouse, France	Various crops
Steinhausen et al. (2018)	Sentinel2	85 – 87	Chennai Basin, India	Land cover including agriculture
Cai et al. (2018)	Landsat	60 – 90	Illinois, USA	Corn and soybean
Zhu et al. (2012)	Landsat	78 – 87	Eastern Massachusetts	Land cover including agriculture
McNairn et al. (2009)	SPOT Landsat	77 – 81 67 – 72	Canada	Various crops
B. SAR				
Blickensdörfer et al. (2022)	SAR: Sentinel1	63 – 66	Germany	Various crops
Marais-Sicre et al. (2020)	TerraSAR Radarsat-2 Alos	42 49 – 55 35	Toulouse, France	Various crops
Idol et al. (2016)	SAR: Radarsat2	39 - 62	Wad Mani, Sudan	Land cover including agriculture
Zhu et al. (2012)	SAR: PALSAR	31	Eastern Massachusetts	Land cover including agriculture

The land cover complexity of Guyana prevents getting very high values for overall accuracy and kappa coefficient. A single class, such as mixed vegetation, encompassed a diverse subset, such as abandoned sugarcane farms, vegetable gardens, shrubbery, mangroves, and coconut plantations. There are also wetland vegetation areas which were classified either in the mixed vegetation or the water class depending on the intensity of aquatic plant growth. With the large scope of each class, the statistical measurements of the band will average out over the subclasses in its scope. Specifying a class, such as rice and sugarcane, assists in more accurately obtaining the class spectral reflectance and band statistics. It has also been shown that when the landscape becomes more heterogenous, vegetation indexes play a more important than spectral bands in the classification (Zhang et al., 2021).

3.2. Classification by optical-radar fusion

3.2.1. Overall accuracy (OA) of classification

The overall accuracy of Sentinel2 is generally good for an inventory. A higher accuracy can be achieved by testing different methods of image preprocessing, classification methods, and sets of input images. For this study, we tested different satellite images, fusion of optical and radar, and varying acquisition dates to improve the overall and class accuracies achieved.

Between the two optical satellites, Sentinel2 was chosen to be fused with RCM, not only for its higher overall accuracy and kappa coefficient but also because of its high spatial and spectral resolution. The classification using Sentinel2-RCM produced an overall accuracy (84%) and kappa coefficient (0.82) which are higher than the single data images. The accuracy obtained compared well with similar crop inventory studies using optical-radar fusion such as Sentinel2 – Sentinel1 (UKCEH, 2022); Sentinel1 - Sentinel2 - Landsat8 (Blickensdörfer et al., 2022); Landsat8 – MODIS - Sentinel1 (Ajadi et al., 2021); and Formosat2 with TerraSAR, Radarsat-2 and Alos (Marais-Sicre et al., 2020) which have reported between 71 to 95% overall accuracy. The Sentinel2-RCM fusion also gave better class accuracy for rice (UA = 100%, PA = 95%) and sugarcane (UA = 95%, PA = 100%).

Sentinel2 had low class accuracy for sugarcane due to misclassification with mixed vegetation. By fusing RCM with Sentinel2, the two classes were more easily distinguished as reflected in the improved accuracy of the class.

3.2.2. Class accuracy for rice and sugarcane classification

A classification's performance for each class is described by the class accuracies: user's accuracy and producer's accuracy. The user of a map is concerned about the map's reliability, i.e., how often is the map correct when it shows that an area is under sugarcane. It is expressed as the user's accuracy (UA) and is computed as in Equation 1. Meanwhile, map producers are concerned about the maps' truthfulness with reality, and how often the map correctly captures the areas of the class. The producer's accuracy (PA) is given in Equation 2.

Equation 1. $$user's\ accuracy\ (UA) = \frac{True\ Positive}{Predicted\ Positive}\ or\ 1 - \frac{False\ Positive}{Predicted\ Positive}$$

Equation 2. $$producer's\ accuracy\ (PA) = \frac{True\ Positive}{Actual\ Positive}\ or\ 1 - \frac{False\ Negative}{Actual\ Positive}$$

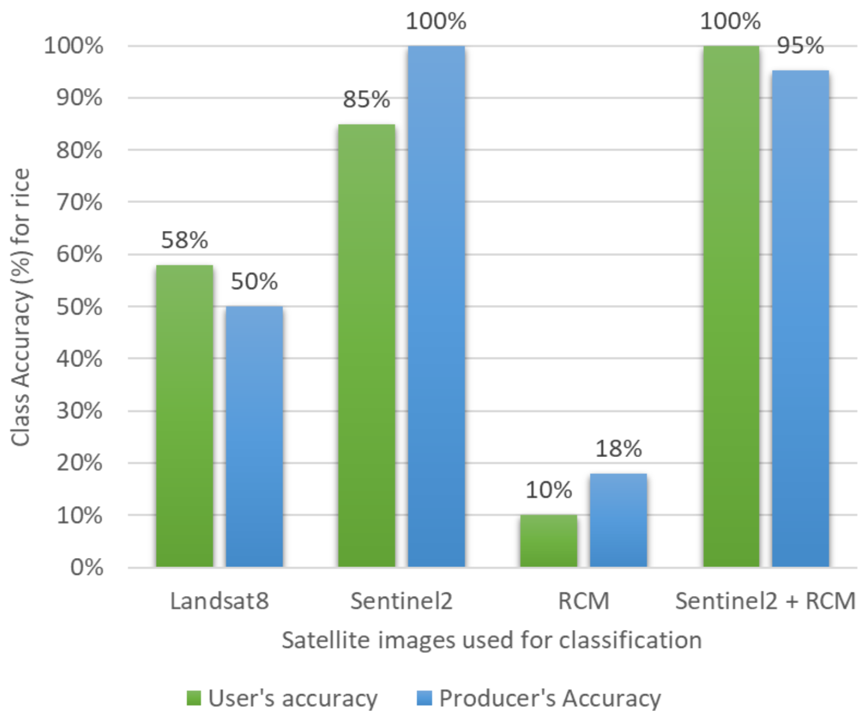

Figure 3.5. Class accuracy for rice using various single-date satellite images for classification

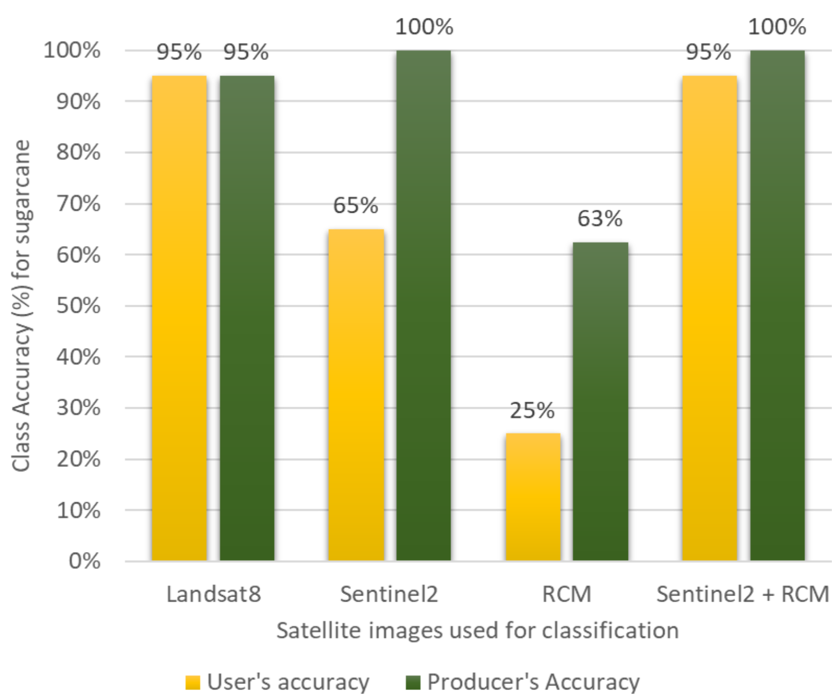

Figure 3.6. Sugarcane class accuracy using various satellite images

Landsat8 performed well for sugarcane (Figure 3.6: UA = 95%, PA = 95%), but not for rice (Figure 3.5: UA = 58%, PA = 50%). Most of the rice areas were misclassified as grass, and vice-versa. The low spatial resolution of Landsat8 is not suitable for some of the rice fields of Guyana, which can be as narrow as 25 meters. Whereas Sentinel2 was able to capture the rice areas with a PA of 100% and UA of 85% because of its higher spatial and spectral resolution compared to Landsat8. However, it did not perform adequately for sugarcane. Some abandoned and overgrown sugarcane farms were detected and falsely classified under sugarcane. Without a high smoothing and aggregation kernel size, areas within sugarcane fields were classified under grassland or mixed vegetation. The higher pixel resolution of Sentinel 2 makes the classification detect granular non-uniformity within the fields and the sparse cover between crop rows. Spatial resolution is highly influenced by the target features to be classified. Larger plantations and crops planted with wide row spacings, such as sugarcane, are better classified using lower spatial resolution. Meanwhile, narrow plots and fields with narrow row spacing, such as rice fields are better identified using higher spatial resolution.

Classification using a single-date RCM image showed inferior performance for both crops with class accuracies ranging from 10 to 62%. Sugarcane was misclassified with the grass and forest class, and rice was misclassified with grass, even at a high smoothing kernel size. The very high spatial resolution of RCM poses the same problem using Sentinel2 for sugarcane, wherein non-uniformity within the fields and between rows was detected. Further work needs to be conducted to explore the different polarimetric bands of RCM and time series to improve the separation of rice sugar cane grass and forest. Moreover, classification by radar uses a land cover's structure and surface texture to classify each pixel instead of reflectance at the visible light and infrared region. Most of the vegetation classes will have nearly the same roughness. Lastly, the

RCM classification was done using only two bands: C-Band RCH and C-Band RCV. This gives the algorithm less basis for classification when using RCM images as compared to Landsat and Sentinel2 which have more 7 and 10 bands, respectively. The maximum likelihood algorithm, and most other classification algorithms, rely on the statistics of each band to determine a pixel's class. Fewer bands, therefore, provide less basis to accurately classify a pixel. In the same way, using more bands such as when fusing optical and radar, would be beneficial since data from the visible, infrared and radio wave parts of the spectrum could be used. While RCM could be used to identify vegetation, water, and urban areas, single-date RCM images could not be used on their own to differentiate between vegetation classes.

3.3. Effect of the acquisition date and crop stage on accuracy

Sentinel2-RCM fusion was used for the classification and accuracy analysis by date because of its better performance compared to the single-sensor classifications. It performed well for May, June and October 2021, and January 2022 and had a consistent OA (82 to 87%) and kappa coefficient (see Table 3.4).

Table 3.4. Overall accuracy and kappa of classification for each acquisition date

Acquisition Date	**2021-MAY**	**2021-JUNE**	**2021-OCT**	**2022-JAN**
Overall accuracy (OA)	84.00%	82.73%	86.67%	86.11%
Kappa coefficient	0.8221	0.8063	0.8500	0.8438

3.3.1. Higher accuracy was obtained at the vegetative, reproductive, and mature stages of rice

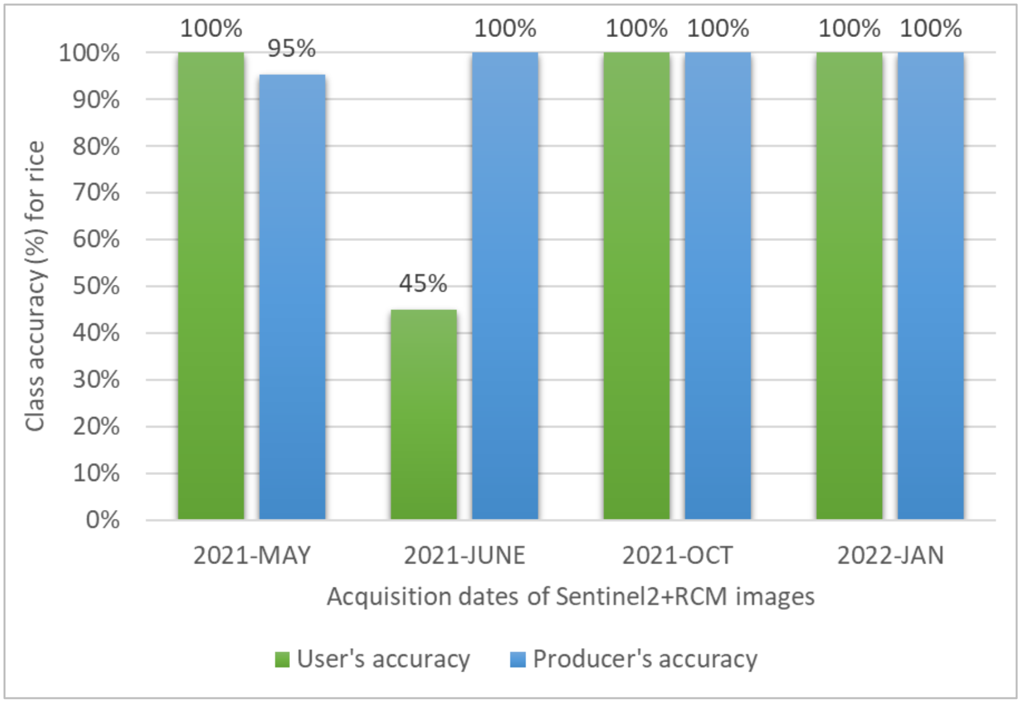

Figure 3.7. Classification accuracy of rice using Sentinel2-RCM at various acquisition dates.

The class accuracy for rice was inconsistent and dipped to 45% UA in June (see Figure 3.7). Most of the misclassification is with the grassland class. This is because the rice is in its early stages of growth and has similar backscatter as the grassland. Upon overlaying a crop calendar of rice with the class accuracies by date, we observe that the June image coincides with when most of the fields were flooded, cultivated or newly planted fields. This is because the rice seeding is conducted in flooded fields - about 3 cm of water over the soil. The classification misidentified newly planted fields with grassland, indicating that it is best to avoid this crop stage when doing the crop inventory. Not only are there insufficient planted fields to get a good estimate of the total planted area, but also the rice in the fields is too young, short, and sparse to be spectrally distinct from grass. In addition, during June, the rice fields vary between bare soil, flooded fields and fields with rice crops at about 6 cm high. This clearly can lead to misclassification because each farmer's plots have different management in the early stages. At the late vegetative and reproductive stages, rice crops have a more distinct and consistent backscatter and reflectance (Verma et al., 2019).

Therefore, good accuracies were obtained when most of the rice fields are at the late vegetative, reproductive, and ripening stages which range from 21 to 109 days after planting based on the growth duration of the GRDB10 variety (in Table 3.5). GRDB10 is the most common variety grown in Guyana followed by GRDB9 and G98-22-4 (GRDB, 2016b).

Table 3.5. Rice growth duration based on GRDB10 variety.

Crop stage	Days after Planting (DAP)
Dormancy and Tillering	0 to 21
Late vegetative	21 to 57
Reproductive	57 to 87
Ripening/ Mature	87 to 109

Note: Data from GRDB, 2016c.

The usual peak rice planting period in Guyana is May to June for the first season and December for the second season. Following this schedule, the June image in Figure 3.8 is supposed to show most fields at the newly planted or vegetative stages. However, most of the fields observed were flooded, thus indicating late planting. The light blue areas in Figure 9 show shallow muddy water and the black areas show deeper standing water. Climate reviews and weather reports confirmed that a weak La Nina was present (Hydrometeorological Service of Guyana, 2021). There was severe flooding on May 20, 2021 (OCHA, 2021). This could have hindered the supply of farm inputs as farmers wait for the water to drain to a suitable level for either land preparation or planting.

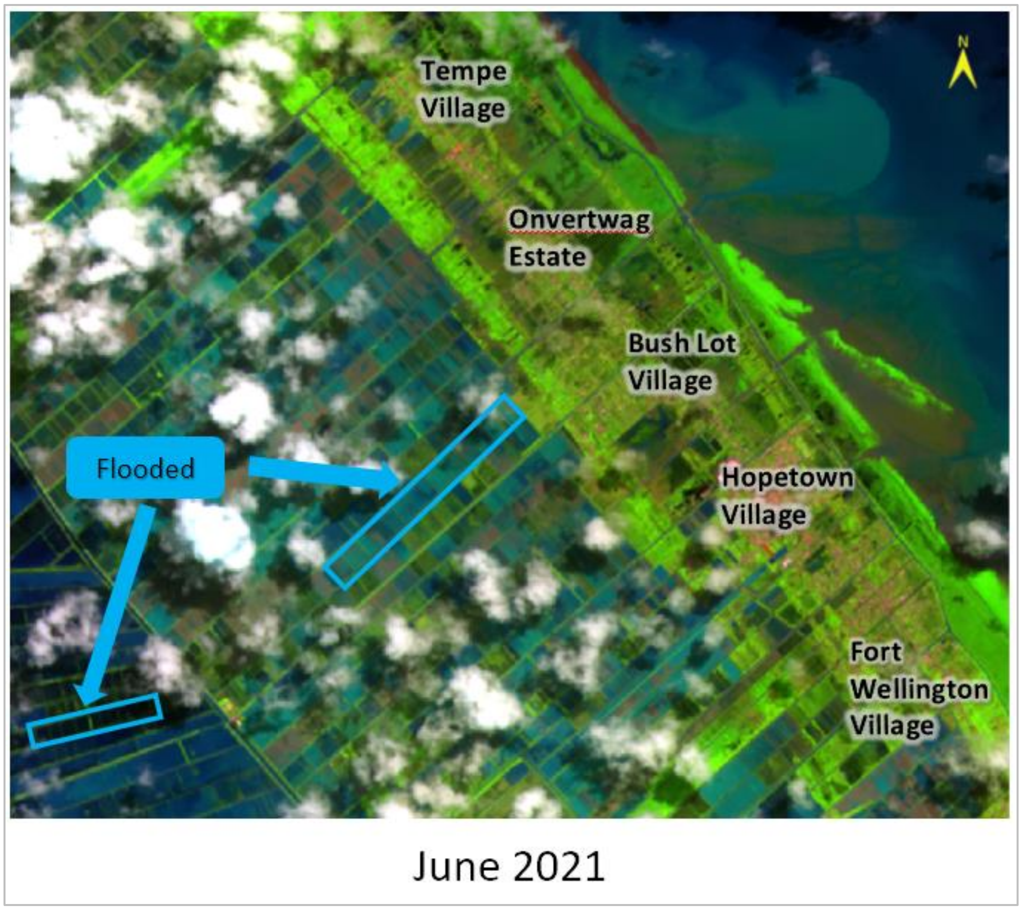

* Flooded fields are in blue, bare soil in brown and vegetated areas in green.)

Figure 3.8. False colour image (SWIR-NIR-Red) of rice areas in June 2021.

3.3.2. Higher accuracy was obtained at tillering, grand growth, and early maturity stages for sugarcane

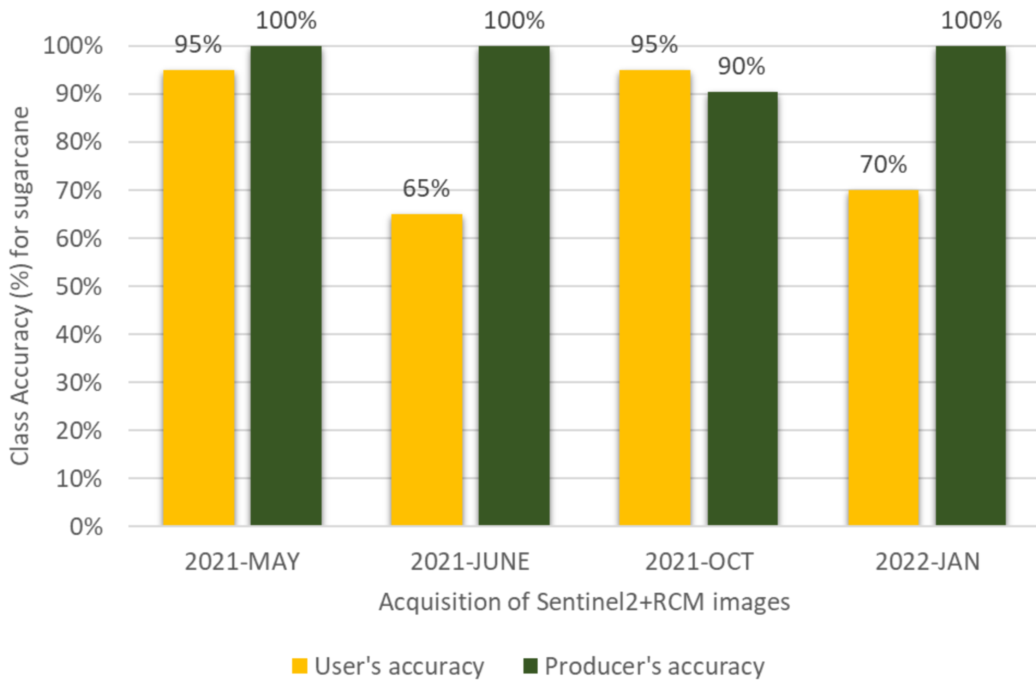

Figure 3.9. Classification accuracy of sugarcane using Sentinel2-RCM at various image acquisition dates

The classification of sugarcane fields produced lower class accuracy when the June and January images were used (See Figure 3.9.). June coincides with late maturity and harvest, and January with the establishment stage. Sugarcane's establishment phase occurs within 60 days after planting and was misclassified with grassland, in the same way as grassland was misclassified with newly planted rice. The late maturity and harvested stages of sugarcane were misclassified with mixed vegetation. Better accuracies are observed when the crop is at tillering, grand growth, and early maturity stages which occur 3 to 13 months after planting (in Table 3.6).

Table 3.6. Sugarcane growth stage duration.

Crop Stage	Months after Planting (DAP)	
	New Plant	Ratoon
Establishment	0 to 2	0 to 1
Tillering	3 to 4	2 to 3
Grand Growth	5 to 10	4 to 9
Early maturity and ripening	11 to 12	10 to 11
Late maturity	13 to 14	12 to 13

Note: Data from Eastwood, 2009; Gaj, 2014; Molijn et al., 2019

The classification also shows that sugarcane field activities are not synchronous within each block, or group of fields, and do not follow the usual crop calendar. There were also areas which fit the sugarcane field pattern but were classified as mixed vegetation. Upon closer inspection, these areas were indeed overgrown and are abandoned sugarcane fields.

3.3.3. Recommended image acquisition dates for the crop classification inventory of rice and sugarcane

The image acquisition date is indeed an important consideration when designing an annual crop inventory program. Figure 3.10 shows the rice and sugarcane areas identified by the multi-date classification for May, June and October 2021 and January 2022. When the acquisition date coincides with land preparation, very few fields are identified. To get a complete picture of the crop areas for each season or annually, the images must be acquired when suitable crop stages are present in the field. The mapped areas of each image can also be added-up into one map. However, the false positives from each image will be included in the final crop area. A temporal analysis can be done to identify the planted areas more accurately across several images.

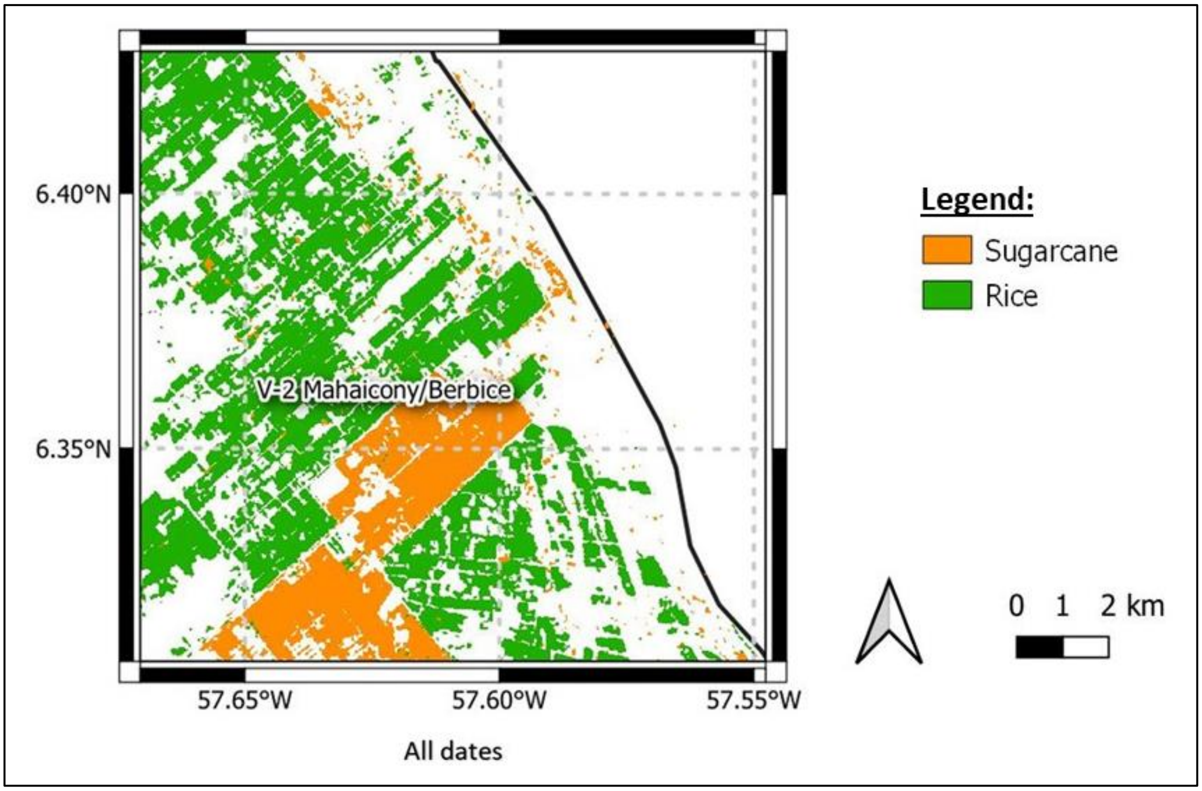

Figure 3.10. Mapped rice and sugarcane areas using the multi-date fusion of Sentinel2 and RCM compiled from the different acquisition dates.

The major crop stage or field activity is an indicator of the best months to acquire images. The plot of the rice and sugarcane calendar in Table 3.7 shows the range of crop growth stages which can be observed for each month based on the usual planting period. The stages suitable for a crop inventory for rice and sugarcane are the dominant stages in the field from January to March and June to August which represent crop maturity. Acquisition of images during these months is thus recommended if planting follows the usual cropping calendar. Otherwise, the date of image acquisition can be adjusted depending on the prevailing cropping calendar in the area.

Table 3.7. Guideline for satellite image acquisition months for crop inventory of rice and sugarcane in Guyana

Crop	Stage	Months											
		J	F	M	A	M	J	J	A	S	O	N	D
Rice	Bare Soil			x	x						x	x	
	Flooded			x	x	x					x	x	x
	Tillering	x			x	x	x					x	x
	Late vegetative [a]	x	x			x	x	x					x
	Reproductive [a]	x	x	x			x	x	x				
	Ripening [a]		x	x	x			x	x	x			
	Harvested			x	x				x	x	x		
		J	**F**	**M**	**A**	**M**	**J**	**J**	**A**	**S**	**O**	**N**	**D**
Sugarcane - First Crop	Bare Soil									x	x	x	
	Establishment										x	x	x
	Tillering [a]	x	x										x
	Grand growth [a]		x	x	x	x	x	x	x				
	Early Maturity [a]								x	x	x		
	Late Maturity										x	x	x
	Harvested											x	x
- Ratoon	Establishment											x	x
	Tillering [a]	x	x										x
	Grand growth [a]		x	x	x	x	x	x	x				
	Early Maturity [a]								x	x	x		
	Late Maturity										x	x	x
	Harvested											x	x

[a] Stages suitable for conducting the crop inventory of sugarcane and rice

4. Conclusion

We compared the performance of Landsat8, Sentinel2 and RCM for crop inventory of rice and sugarcane in Guyana. The results have shown that when single-image data is used, the optical-radar fusion of Sentinel2 and RCM is better than single-sensor classifications using Landsat8, Sentinel2 and RCM. The different class accuracies of rice and sugarcane for Landsat8 and Sentinel2 have also shown the importance of the target class's features such as farm size, uniformity, and planting pattern. Landsat8 is suitable for classifying sugarcane areas, and Sentinel2 for rice. However, to conduct an inventory for rice and sugarcane simultaneously, the optical-radar fusion of Sentinel2 and RCM is more efficient and provides better results.

Analysis by acquisition date has helped identify the crop stages which are most suitable for conducting a crop inventory: the vegetative, reproductive and mature stages for rice (2 to 4 months after planting); and tillering, grand growth and early maturity stages for sugarcane (3 to 12 month after planting).

5. Recommendations

Based on the findings of this study, the following recommendations are made:

1. With optical-radar fusion, specifically Sentinel2-RCM for a crop inventory of rice and sugarcane, improvements to the classification can be done by exploring algorithms such as Random Forest or Decision Tree, or by using multi-date imagery during the mature stages of the crops.

2. Given that Guyana is covered with clouds for most of the year, and few images are available for most months, multitemporal analysis can be explored to improve accuracy, detect field activities, and capture areas planted in the other season. An inventory for each region is more suitable to get cloudless images over an area.

3. Other techniques for gathering cloudless images such as mosaicking and augmentation with images from UAVs can also be explored. The UAV images which cover a small area can be used as low-level field verification of large areas covered by the satellite images.

4. The application of optical and radar fusion can also be explored for the inventory of other crops or land cover classes.

6. Acknowledgements

We thank Dr. Heather McNairn and Dr. Laura Dingle-Robertson of AAFC and the Landsat and Sentinel teams for providing the satellite data used in this study. We are also grateful to the NAREI for giving further insights into the cropping pattern in Guyana. We acknowledge the support of the NSERC and a fellowship to the senior author by the Liliane and David Macdonald Stewart Foundation under the Liliane and David M. Stewart Fellowship in Water Resources.

7. References

AAFC, 2022. Annual crop inventory [WWW Document]. Gov. Can. URL https://agriculture.canada.ca/atlas/aci/ (accessed 7.12.22).

Ahmad, S.R., Lakhan, V.C., 2012. GIS-Based Analysis and Modeling of Coastline Advance and Retreat Along the Coast of Guyana. Mar. Geod. 35, 1–15. https://doi.org/10.1080/01490419.2011.637851

Ajadi, O.A., Barr, J., Liang, S.-Z., Ferreira, R., Kumpatla, S.P., Patel, R., Swatantran, A., 2021. Large-scale crop type and crop area mapping across Brazil using synthetic aperture radar and optical imagery. Int. J. Appl. Earth Obs. Geoinformation 97, 102294. https://doi.org/10.1016/j.jag.2020.102294

Alosnos, E., Asilo, S., Mabalay, M., Quilang, E., de Dios, J., 2019. Operationalization of Philippine Rice Information System (PRISM): revolutionizing agriculture through ICT and satellite-based crop monitoring. Philippine Rice Research Institute, Nueva Ecija, Philippines.

Bank of Guyana, 2020. Annual Report 2020 (Annual Report). Bank of Guyana, Georgetown, Guyana.

Blickensdörfer, L., Schwieder, M., Pflugmacher, D., Nendel, C., Erasmi, S., Hostert, P., 2022. Mapping of crop types and crop sequences with combined time series of Sentinel-1, Sentinel-2 and Landsat 8 data for Germany. Remote Sens. Environ. 269, 112831. https://doi.org/10.1016/j.rse.2021.112831

Bouvet, A., Le Toan, T., 2011. Use of ENVISAT/ASAR wide-swath data for timely rice fields mapping in the Mekong River Delta. Remote Sens. Environ. 115, 1090–1101. https://doi.org/10.1016/j.rse.2010.12.014

Cai, Y., Guan, K., Peng, J., Wang, S., Seifert, C., Wardlow, B., Li, Z., 2018. A high-performance and in-season classification system of field-level crop types using time-series Landsat data and a machine learning approach. Remote Sens. Environ. 210, 35–47. https://doi.org/10.1016/j.rse.2018.02.045

Canasat, 2022. Canasat - Home [WWW Document]. Canasat - Sugarcane Crop Monit. Braz. URL http://www.dsr.inpe.br/laf/canasat/en/ (accessed 8.9.22).

Casella, G., Berger, R., 2002. Statistical Inference, 2nd ed. ed, Duxbury Advanced Series. the Wadsworth Group, California, USA.

Chen, S., Woodcock, C.E., Bullock, E.L., Arévalo, P., Torchinava, P., Peng, S., Olofsson, P., 2021. Monitoring temperate forest degradation on Google Earth Engine using Landsat time series analysis. Remote Sens. Environ. 265, 112648. https://doi.org/10.1016/j.rse.2021.112648

CropWatch, 2022. Methodology [WWW Document]. CropWatch. URL http://www.cropwatch.com.cn/htm/en/methodology.shtml (accessed 8.8.22).

CSA, 2021. RADARSAT Constellation Mission [WWW Document]. Can. Space Agency. URL https://www.asc-csa.gc.ca/eng/satellites/radarsat (accessed 7.13.22).
De Oto, L., Vrieling, A., Fava, F., de Bie, K. (C. A.J.M.), 2019. Exploring improvements to the design of an operational seasonal forage scarcity index from NDVI time series for livestock insurance in East Africa. Int. J. Appl. Earth Obs. Geoinformation 82, 101885. https://doi.org/10.1016/j.jag.2019.05.018
Eastwood, D., 2009. Agriculture Operations Guidelines.
ESA, 2022. Sentinel-2 MSI User Guide [WWW Document]. Sentin. Online. URL https://sentinels.copernicus.eu/web/sentinel/user-guides/sentinel-2-msi (accessed 7.12.22).
European Commission, 2022. Monitoring Agricultural ResourceS (MARS) [WWW Document]. Eur. Comm. Sci. Hub. URL https://joint-research-centre.ec.europa.eu/monitoring-agricultural-resources-mars_en (accessed 8.8.22).
FAO, 2022. Earth Observation - Home [WWW Document]. Food Agric. Organ. Unted Nations. URL https://www.fao.org/giews/earthobservation/ (accessed 8.8.22).
Feng, A., Zhou, J., Vories, E.D., Sudduth, K.A., 2022. Quantifying the effects of soil texture and weather on cotton development and yield using UAV imagery. Precis. Agric. 23, 1248–1275. https://doi.org/10.1007/s11119-022-09883-6
Feranec, J., Šúri, M., Ot'ahel', J., Cebecauer, T., Kolář, J., Soukup, T., Zdeňková, D., Waszmuth, J., Vâjdea, V., Vîjdea, A.-M., Nitica, C., 2000. Inventory of major landscape changes in the Czech Republic, Hungary, Romania and Slovak Republic 1970s – 1990s. Int. J. Appl. Earth Obs. Geoinformation 2, 129–139. https://doi.org/10.1016/S0303-2434(00)85006-0
Gaj, N., 2014. An analysis of the hydrology of a sugarcane field in Guyana (Master of Science Thesis). McGill University, Montreal, Canada.
GFC, Poyry Forest Industry, 2011. GFC REDD+ MRVS Year1 Interim Report (Interim Measures No. Year 1). Guyana Foresty Commission and Poyry Forest Industry.
GRDB, 2022. National Advisory on Sowing Period for Rice for 2022 [WWW Document]. Guyana Rice Dev. Board. URL https://grdb.gy/national-advisory-on-sowing-period-for-rice-3/ (accessed 7.13.22).
GRDB, 2016a. Agronomy [WWW Document]. Guyana Rice Dev. Board. URL https://grdb.gy/agronomy-of-rice/ (accessed 7.13.22).
GRDB, 2016b. 2016 Annual Report (annual report). Guyana Rice Development Board, Georgetown, Guyana.
GRDB, 2016c. Rice Breeding Programme in Guyana (brochure). Guyana Rice Development Board, Georgetown, Guyana.
GuySuCo, 2022. Field layouts [WWW Document]. Guyana Sugarcane Corp. Inc. URL https://www.guysuco.gy/index.php?option=com_k2&view=item&id=44:field-layouts&Itemid=101&lang=en (accessed 7.13.22).
GuySuCo, 2018. Annual Report 2018 (annual report). Guyana Sugar Corporation, Georgetown, Guyana.
Hamzeh, S., Naseri, A.A., AlaviPanah, S.K., Bartholomeus, H., Herold, M., 2016. Assessing the accuracy of hyperspectral and multispectral satellite imagery for categorical and Quantitative mapping of salinity stress in sugarcane fields. Int. J. Appl. Earth Obs. Geoinformation 52, 412–421. https://doi.org/10.1016/j.jag.2016.06.024
Hanintyo, R., Susilo, E., Pradisty, N.A., Surana, I.N., 2021. Chlorophyll-a and total suspended matter retrieval and comparison of C2RCC neural network algorithms on Landsat 8 data

over Wangi-Wangi Island, Indonesia, in: Proceedings. Presented at the Seventh Geoinformation Science Symposium 2021, Society of Photo-Optical Instrumentation Engineers (SPIE), Yogyakarta, Indonesia, pp. 150–158. https://doi.org/10.1117/12.2617375

Homayouni, S., McNairn, H., Hosseini, M., Jiao, X., Powers, J., 2019. Quad and compact multitemporal C-band PolSAR observations for crop characterization and monitoring. Int. J. Appl. Earth Obs. Geoinformation 74, 78–87. https://doi.org/10.1016/j.jag.2018.09.009

Hydrometeorological Service of Guyana, 2021. Drought Monitoring Bulletin (Bulletin No. Issue#45), Drought Monitoring Bulletin. Ministry of Agriculture, Tihmeri, Guyana.

Idol, T., Haack, B., Mahabir, R., 2016. An evaluation of Radarsat-2 individual and combined image dates for land use/cover mapping. Geocarto Int. 31, 1108–1122. https://doi.org/10.1080/10106049.2015.1120351

Ihuoma, S.O., Madramootoo, C.A., 2019. Sensitivity of spectral vegetation indices for monitoring water stress in tomato plants. Comput. Electron. Agric. 163, 104860. https://doi.org/10.1016/j.compag.2019.104860

ILRI, n.d. Imdex-Based Livestock Insurance [WWW Document]. Index-Based Livest. Insur. URL https://ibli.ilri.org/ (accessed 9.23.22).

Jozdani, S., Chen, D., Chen, W., Leblanc, S.G., Prévost, C., Lovitt, J., He, L., Johnson, B.A., 2021. Leveraging Deep Neural Networks to Map Caribou Lichen in High-Resolution Satellite Images Based on a Small-Scale, Noisy UAV-Derived Map. Remote Sens. 13, 2658. https://doi.org/10.3390/rs13142658

Kontgis, C., Schneider, A., Ozdogan, M., 2015. Mapping rice paddy extent and intensification in the Vietnamese Mekong River Delta with dense time stacks of Landsat data. Remote Sens. Environ. 169, 255–269. https://doi.org/10.1016/j.rse.2015.08.004

Li, C., Xian, G., Zhou, Q., Pengra, B.W., 2021. A novel automatic phenology learning (APL) method of training sample selection using multiple datasets for time-series land cover mapping. Remote Sens. Environ. 266, 112670. https://doi.org/10.1016/j.rse.2021.112670

Luciano, A.C. dos S., Picoli, M.C.A., Rocha, J.V., Duft, D.G., Lamparelli, R.A.C., Leal, M.R.L.V., Le Maire, G., 2019. A generalized space-time OBIA classification scheme to map sugarcane areas at regional scale, using Landsat images time-series and the random forest algorithm. Int. J. Appl. Earth Obs. Geoinformation 80, 127–136. https://doi.org/10.1016/j.jag.2019.04.013

Lunetta, R.S., Shao, Y., Ediriwickrema, J., Lyon, J.G., 2010. Monitoring agricultural cropping patterns across the Laurentian Great Lakes Basin using MODIS-NDVI data. Int. J. Appl. Earth Obs. Geoinformation 12, 81–88. https://doi.org/10.1016/j.jag.2009.11.005

Marais-Sicre, C., Fieuzal, R., Baup, F., 2020. Contribution of multispectral (optical and radar) satellite images to the classification of agricultural surfaces. Int. J. Appl. Earth Obs. Geoinformation 84, 101972. https://doi.org/10.1016/j.jag.2019.101972

McGowan, W., 2008. The beginnings of rice cultivation in Guyana (Part 2). Stabroek News.

McNairn, H., Champagne, C., Shang, J., Holmstrom, D., Reichert, G., 2009. Integration of optical and Synthetic Aperture Radar (SAR) imagery for delivering operational annual crop inventories. ISPRS J. Photogramm. Remote Sens. 64, 434–449. https://doi.org/10.1016/j.isprsjprs.2008.07.006

Molijn, R.A., Iannini, L., Vieira Rocha, J., Hanssen, R.F., 2019. Sugarcane Productivity Mapping through C-Band and L-Band SAR and Optical Satellite Imagery. Remote Sens. 11, 1109. https://doi.org/10.3390/rs11091109

Nedd, G.A., Oyedotun, T.D.T., Simard, M., 2021. Evaluation of Spatio-Temporal Dynamics of Guyana's Mangroves Using SAR and GEE. Earth Syst. Environ. https://doi.org/10.1007/s41748-021-00277-8

OCHA, 2021. Guyana: Floods - May 2021 | ReliefWeb [WWW Document]. Reliefweb. URL https://reliefweb.int/disaster/fl-2021-000066-guy (accessed 5.10.22).

Pei, Z., Zhang, S., Guo, L., McNairn, H., Shang, J., Jiao, X., 2011. Rice identification and change detection using TerraSAR-X data. Can. J. Remote Sens. 37, 151–156. https://doi.org/10.5589/m11-025

Pfitzner, K., Bartolo, R., Whiteside, T., Loewensteiner, D., Esparon, A., 2022. Multi-temporal spectral reflectance of tropical savanna understorey species and implications for hyperspectral remote sensing. Int. J. Appl. Earth Obs. Geoinformation 112, 102870. https://doi.org/10.1016/j.jag.2022.102870

PHILRICE, 2022. PRISM Core Activities [WWW Document]. Philipp. Rice Inf. Syst. PRISM. URL https://prism.philrice.gov.ph/aboutus/core-activities/ (accessed 8.8.22).

Qin, H., Zhou, W., Yao, Y., Wang, W., 2022. Individual tree segmentation and tree species classification in subtropical broadleaf forests using UAV-based LiDAR, hyperspectral, and ultrahigh-resolution RGB data. Remote Sens. Environ. 280, 113143. https://doi.org/10.1016/j.rse.2022.113143

Rudorff, B.F.T., Aguiar, D.A., Silva, W.F., Sugawara, L.M., Adami, M., Moreira, M.A., 2010. Studies on the Rapid Expansion of Sugarcane for Ethanol Production in São Paulo State (Brazil) Using Landsat Data. Remote Sens. 2, 1057–1076. https://doi.org/10.3390/rs2041057

Salmon, J.M., Friedl, M.A., Frolking, S., Wisser, D., Douglas, E.M., 2015. Global rain-fed, irrigated, and paddy croplands: A new high resolution map derived from remote sensing, crop inventories and climate data. Int. J. Appl. Earth Obs. Geoinformation 38, 321–334. https://doi.org/10.1016/j.jag.2015.01.014

Sianturi, R., Jetten, V.G., Sartohadi, J., 2018. Mapping cropping patterns in irrigated rice fields in West Java: Towards mapping vulnerability to flooding using time-series MODIS imageries. Int. J. Appl. Earth Obs. Geoinformation 66, 1–13. https://doi.org/10.1016/j.jag.2017.10.013

Sifakis, N., Paronis, D., Keramitsoglou, I., 2004. Combining AVHRR imagery with CORINE Land Cover data to observe forest fires and to assess their consequences. Int. J. Appl. Earth Obs. Geoinformation 5, 263–274. https://doi.org/10.1016/j.jag.2004.06.004

Singhroy, V., 1996. Interpretation of SAR Images for Coastal Zone Mapping in Guyana. Can. J. Remote Sens. 22, 317–328. https://doi.org/10.1080/07038992.1996.10855187

Singhroy, V., 1995. SAR integrated techniques for geohazard assessment. Adv. Space Res., Natural Hazards: Monitoring and Assessment Using Remote Sensing Technique 15, 67–78. https://doi.org/10.1016/0273-1177(95)00076-Q

Singhroy, V., Fobert, M.-A., Li, J., Blais-Stevens, A., Charbonneau, F., Das, M., 2021. Advanced Radar Images for Monitoring Transportation, Energy, Mining and Coastal Infrastructure, in: Singhroy, V. (Ed.), Advances in Remote Sensing for Infrastructure Monitoring, Springer Remote Sensing/Photogrammetry. Springer International Publishing, Cham, Switzerland, pp. 3–40. https://doi.org/10.1007/978-3-030-59109-0_1

Steinhausen, M.J., Wagner, P.D., Narasimhan, B., Waske, B., 2018. Combining Sentinel-1 and Sentinel-2 data for improved land use and land cover mapping of monsoon regions. Int. J. Appl. Earth Obs. Geoinformation 73, 595–604. https://doi.org/10.1016/j.jag.2018.08.011

Stoll, E., Roopsind, A., Maharaj, G., Velazco, S., Caughlin, T.T., 2022. Detecting gold mining impacts on insect biodiversity in a tropical mining frontier with SmallSat imagery. Remote Sens. Ecol. Conserv. 8, 379–390. https://doi.org/10.1002/rse2.250

Thorp, K.R., Drajat, D., 2021. Deep machine learning with Sentinel satellite data to map paddy rice production stages across West Java, Indonesia. Remote Sens. Environ. 265, 112679. https://doi.org/10.1016/j.rse.2021.112679

Touzi, R., Côté, S., 2019. Calibration of RCM Compact Modes. Presented at the IGARSS 2019 - 2019 IEEE International Geoscience and Remote Sensing Symposium, pp. 5752–5755. https://doi.org/10.1109/IGARSS.2019.8898396

UKCEH, 2022. UKCEH Land Cover plus: Crops [WWW Document]. UKCEH Land Cover Plus Crops. URL https://www.ceh.ac.uk/data/ceh-land-cover-plus-crops-2015#product (accessed 7.12.22).

USACE, 1998. Water Resources Assessment of Guyana (Assessment). US Army Corps of Engineers, Guyana.

USDA, 2022. Rice Explorer [WWW Document]. USDA Foreign Agric. Serv. URL https://ipad.fas.usda.gov/cropexplorer (accessed 8.8.22).

USDA, 2019. 2017 Agricultural Atlas Maps. Census of Agriculture.

USGS, 2022. Landsat Frequently Asked Questions [WWW Document]. USGS - Mapp. Remote Sens. Geospatial Data. URL https://www.usgs.gov/landsat-missions/landsat-frequently-asked-questions (accessed 7.12.22).

Verma, A., Kumar, A., Lal, K., 2019. Kharif crop characterization using combination of SAR and MSI Optical Sentinel Satellite datasets. J. Earth Syst. Sci. 128, 230. https://doi.org/10.1007/s12040-019-1260-0

Wang, J., Xiao, X., Liu, L., Wu, X., Qin, Y., Steiner, J.L., Dong, J., 2020. Mapping sugarcane plantation dynamics in Guangxi, China, by time series Sentinel-1, Sentinel-2 and Landsat images. Remote Sens. Environ. 247, 111951. https://doi.org/10.1016/j.rse.2020.111951

Wang, M., Liu, Z., Ali Baig, M.H., Wang, Y., Li, Y., Chen, Y., 2019. Mapping sugarcane in complex landscapes by integrating multi-temporal Sentinel-2 images and machine learning algorithms. Land Use Policy 88, 104190. https://doi.org/10.1016/j.landusepol.2019.104190

Wang, S., Di Tommaso, S., Faulkner, J., Friedel, T., Kennepohl, A., Strey, R., Lobell, D.B., 2020. Mapping Crop Types in Southeast India with Smartphone Crowdsourcing and Deep Learning. Remote Sens. 12, 2957. https://doi.org/10.3390/rs12182957

Wei, P., Chai, D., Huang, R., Peng, D., Lin, T., Sha, J., Sun, W., Huang, J., 2022. Rice mapping based on Sentinel-1 images using the coupling of prior knowledge and deep semantic segmentation network: A case study in Northeast China from 2019 to 2021. Int. J. Appl. Earth Obs. Geoinformation 112, 102948. https://doi.org/10.1016/j.jag.2022.102948

Yan, S., Yao, X., Zhu, D., Liu, D., Zhang, L., Yu, G., Gao, B., Yang, J., Yun, W., 2021. Large-scale crop mapping from multi-source optical satellite imageries using machine learning with discrete grids. Int. J. Appl. Earth Obs. Geoinformation 103, 102485. https://doi.org/10.1016/j.jag.2021.102485

Zhan, P., Zhu, W., Li, N., 2021. An automated rice mapping method based on flooding signals in synthetic aperture radar time series. Remote Sens. Environ. 252, 112112. https://doi.org/10.1016/j.rse.2020.112112

Zhang, H., Wang, Y., Shang, J., Liu, M., Li, Q., 2021. Investigating the impact of classification features and classifiers on crop mapping performance in heterogeneous agricultural landscapes. Int. J. Appl. Earth Obs. Geoinformation 102, 102388. https://doi.org/10.1016/j.jag.2021.102388

Zhi, Y., Yun, S., Kun, L., Qingbo, L., Long, L., Brisco, B., 2017. An improved scheme for rice phenology estimation based on time-series multispectral HJ-1A/B and polarimetric RADARSAT-2 data. Remote Sens. Environ. 195, 184–201. https://doi.org/10.1016/j.rse.2017.04.016

Zhu, Z., Woodcock, C.E., Rogan, J., Kellndorfer, J., 2012. Assessment of spectral, polarimetric, temporal, and spatial dimensions for urban and peri-urban land cover classification using Landsat and SAR data. Remote Sens. Environ., Remote Sensing of Urban Environments 117, 72–82. https://doi.org/10.1016/j.rse.2011.07.020

8. Appendix

Appendix A. Reference guide for classification of rice, sugarcane, and mixed vegetation.

Crop and criteria	Reference Image
RICE - Green in False Colour (SWIR-NIR-Red) - Mostly uniform green colour of the field - No visible furrow - Either square or a narrow rectangle	 
SUGARCANE - Green in False Colour (SWIR-NIR-Red) - Large rectangular parcel with rectangular plots - Plots separated by a canal - Rows of crops visible in plots (Sentinel2) - Rough grainy green, mostly uniform shade - Canals are either seen as water or soil	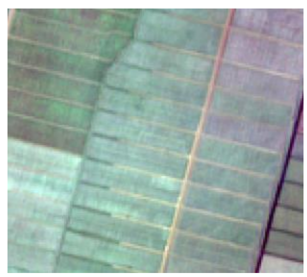 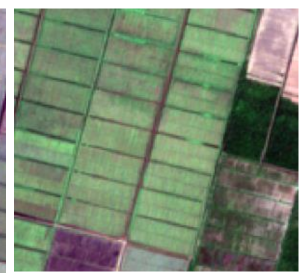

MIXED VEGETATION
- Green in False Colour (SWIR-NIR-Red)
- If in a non-agricultural area:
    - grainy or rough shades of green
    - Irregular shape
- If in an agricultural area:
    - Abandoned farms: grainy green, distinct non-uniformity, bare soil patches present, irrigation lines are overgrown
    - Vegetables: uniform green with one furrow, no sub-plots
	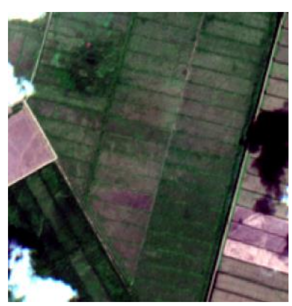 

BRIDGING TEXT

Chapter III discussed the methodology for a crop inventory in Guyana. With a full inventory over Guyana or a conservancy service area, the areas planted with rice and sugarcane can be identified and measured. This crop inventory is an important input to estimate irrigation requirements. The other important factor is the crop water requirement which will be obtained using simulations in AquaCrop. Chapter IV discusses how AquaCrop was used to simulate yield at a regional scale, and the impact of several irrigation scenarios on yield and farm water consumption for rice.

This study is in preparation for submission to *Agricultural Water Management*. The paper is co-authored by Guia Marie M. Mortel and Dr. Chandra Madramootoo. The contributions of each author are mentioned on page 7.

CHAPTER IV

Optimizing water productivity of rice in a tropical coastal plains heavy clay soil

Abstract

Rice (*Oryza sativa*) is an important staple crop in many parts of the world. In this paper, we used AquaCrop to investigate the response of rice growth to various irrigation scenarios in the Guyana coastal plains. AquaCrop was calibrated using field climate and soil data, estimated parameters and regional reports of yield from 2005 to 2008 for two seasons: Season 1 (planting from April to June) and Season 2 (from November to January). The most sensitive parameters during calibration were the days to maturity, weed coverage and crop coefficient at the maximum canopy. After calibration, the simulated yield was validated using reported yields from 2009 to 2012. The validation showed that AquaCrop and the parameters used were adequate for yield simulations (RMSEn = 5.46 to 6.43%, RMSE = 0.1 to 0.23 ton/ha, MBE = 0.05 to 0.14 ton/ha). The calibrated parameters were then used in irrigation management simulations with 50, 60, 70, 80, 90, 100, 110 and 120% water holding capacity at the rootzone (WHR), for which irrigation commences at the indicated %WHR and stops when field capacity (100%WHR) is reached. For the 100, 110, and 120% WHR, irrigation was continuous to maintain the indicated %WHR. A one-way ANOVA of the yields (at a = 0.05) show that there is a statistically significant difference in yield among the eight scenarios, and no significant difference between the yields obtained from Season 1 and Season 2 crops. Among the eight irrigation scenarios, the yield is reduced for the 50, 60, and 70% WHR with a significant difference (at a = 0.05) from the yields obtained from 90, 100, 110 and 120%WHR. The water-saving scenario of 80%WHR can be used when irrigation is limited.

1. Introduction

1.1. Rice cultivation in Guyana

Rice cultivation is a priority to ensure food security in countries with rice-based diets. Globally, approximately 54 kg per capita, is consumed annually (OECD and FAO, 2022). These consumption values are expected to increase by 1.1% yearly as driven by the increasing population in Asia, Latin America and the Caribbean, and increasing per capita consumption in Africa (OECD and FAO, 2022). In Guyana, rice is the 2nd major crop after sugarcane and has approximately 560,000 tons harvested annually of which 19% goes to domestic supply and 81% to exports (Guyana Rice Development Board [GRDB], 2016a). The dominant varieties used in Guyana are GRDB10, GRDB9, G98-22-4, G98-196 and G98135 (GRDB, 2016b). The rice farms span along Guyana's coast facing the Atlantic Ocean to the north. The top rice-producing areas are Essequibo in Region 2, West Berbice in Region 5, and the Frontlands in Region 6 (GRDB, 2016a). Region 6, the area of the study site, has around 52, 874 (18%) ha of cropland of which 6.73% of the total land area or 19,396 ha are planted with rice (GLSC, 2004). Meanwhile, around 7% of Region 6's total land area is barren overgrown rice croplands which were abandoned mainly because of the absence of enough irrigation and drainage facilities in the area (GLSC, 2004).

The soil over most of the agricultural lands is a rich alluvial clay to silty clay hydraquent which stretches 32 km inland and is often associated with poor drainage (GLSC, 2013). Four major river systems on the coastal plains provide irrigation and drainage: the Corentyne River, the Berbice River, the Demerara River and the Essequibo River (USACE, 1998).

Irrigation for rice fields is controlled by conservancies, which are shallow reservoirs providing irrigation and flood control (USACE, 1998). Each conservancy collects rainwater within the catchment and releases it through several sluice gates which route water to consumers or major rivers (Bovolo, 2014). The rehabilitation of drainage and irrigation systems and access dams has long been identified as a focus area for agricultural development, especially for the coastal region (GLSC, 2013). A survey of Guyana's rice farmers by Mahdu (2019) found that around 39% of the respondents pump water into their fields because of the absence of an irrigation system or the very low water level in the nearby irrigation canal.

When irrigation water enters the farms, it goes into basins enclosed by soil bunds of at least 20 cm high. The fields are flooded after land preparation and drained 2 – 3 days after planting (GRDB, 2020, 2016c). After the initial draining, the fields are flooded again every 6 to 7 days which is a practice akin to AWD. The fields are also drained for the application of fertilizers and post-emergence herbicides, and harvest (GRDB, 2020). Continuous flooding is not performed unless it is needed to control weeds. In this method, called Pin-Point irrigation, the fields are flooded again from 5 DAP and kept flooded until harvest (Roel et al., 1999) with at least 7 cm of standing water as recommended by the GRDB (2016c).

Planting is done before the start of the wet season which occurs from April to August and from December to January (USACE, 1998). As such, there are two main planting seasons: April to June and November to January which we refer to as Season 1 and Season 2, respectively.

1.2. Simulating rice growth using the AquaCrop model

Due to the importance of rice in many parts of the tropical world, it is often the focus of crop modelling studies using the AquaCrop, DSSAT-CERES and ORYZA models. AquaCrop is selected for this study because of its suitability for rice simulations in large-scale applications such as for a cluster of farms or regions. Large-scale applications of AquaCrop tend to be used for climate change impact simulations using projected scenarios such as the 'Adapting irrigation to climate change (AICCA)' project of the FAO and IFAD which modelled the response of irrigated and rainfed rice and maize for the West Africa region (Salman et al., 2021); and wheat and sugarcane yield simulations along the Indus River Basin in Pakistan (Alvar-Beltrán et al., 2021).

AquaCrop is based on three fundamental equations representing the physical process and relationships between the accumulated transpiration, biomass, and yield. Crop growth is driven by water, and the first basic computation is for evapotranspiration based on the percent canopy cover at any time (t), evapotranspiration (ETo) and crop coefficient (kc). A main accessibility feature of AquaCrop is its use of the effective canopy cover which can be more easily estimated visually as compared to the leaf area index. The model is also simplified by its use of stress coefficients and indicator thresholds. This reduces the number of required crop parameters and eliminates the modular simulation of processes such as the nutrient cycle, stomatal response to water stress, ion transport, stress signalling pathways, flowering, pollination, and waterlogging.

For example, the stomatal response to water stress is represented by the water stress coefficient (ks), as shown in Figure 4.e. It ranges from 1 for unstressed to 0 for fully stressed. The coefficient value is based on the fraction of soil water depletion in the rootzone (Dr). The stomatal stress is determined by a threshold (psto) value of Dr above which the crop starts to experience water stress and below which is readily available water (RAW). Above psto, the water stress coefficient becomes less than 1. The psto is a crop-dependent parameter with some crops, such as sugarcane, able to extract water more easily in drier soils, while some, such as rice and hot pepper, have lower psto values.

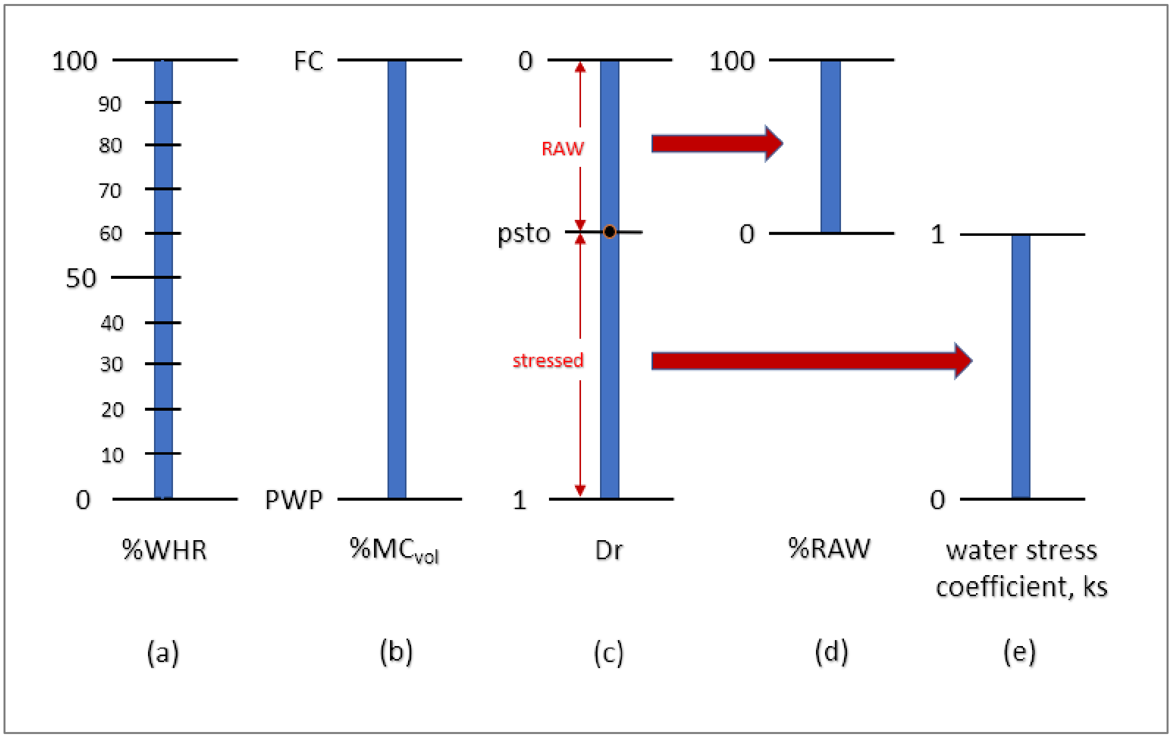

* a = water holding content at the rootzone, b = moisture content by volume, c = Dr, fraction of water depletion at the rootzone, psto = threshold of Dr, d = readily available water, e = water stress coefficient

Figure 4.1. Relationship between units of measure of soil water content.

The depletion at the rootzone (Dr) is the inverse of the water holding capacity at the rootzone (%WHR) (in Figure 4.1a-c). A 100%WHR refers to zero depletion and moisture content at field capacity, while 0%WHR is the moisture content at the permanent wilting point and the maximum Dr of 1, as illustrated in Figure 4.1a. The WHR, as shown in Equation 1, is the water content (in mm) in the root zone between the soil moisture content (%MC_{vol}) at field capacity (FC) and permanent wilting point (PWP). To prevent confusion between the different water content terms, WHR will be used throughout this paper to describe soil water content

$$WHR = (\%MC_{vol,FC} - \%MC_{vol,PWP}) \times root\ zone\ depth \quad (1)$$

Several studies have calibrated and validated AquaCrop parameters to model rice growth such as on the timing of transplanting of rainfed paddy rice in Lao (Kim et al., 2021), drying-wetting cycle in eastern China (Xu et al., 2019), and simulating the impact of climate change in sub-tropical environments (Raoufi and Soufizadeh, 2020), among many others. A comprehensive review of AquaCrop modelling studies from 2009 to 2019 found that around 10% of the studies were devoted to rice (Salman et al., 2021).

AquaCrop provides a crop template for paddy rice, the detailed contents of which are published in the AquaCrop Reference Manual (Raes et al., 2018). The parameters are based on the contributions of several scientists who have tested and calibrated these parameters (Steduto et al., 2012). A comprehensive review by Pereira et. al (2021) has released an updated set of crop parameters for AquaCrop based on several rice studies which have satisfied the criteria for defining crop parameters, producing accurate measurements, and satisfying transferability requirements. Updated values for the crop coefficient at the initial stage (kc_{ini}), middle of the season (kc_{mid}) and end of the season (kc_{end}); maximum root depth (Zx); and fraction of soil water depletion (p_{sto}) were provided. For flooded rice with dry seeding, the work of Alberto et al. (2014) in Los Baños, Philippines; Linquist et al. (2015) in California, USA; and Diaz et al. (2019) in the Rio Grande do Sul, Brazil have been used in the updated set of parameters.

Building upon the comprehensive studies done to determine the crop parameters for rice, we evaluated the applicability of AquaCrop for modelling rice growth at Black Bush Polder in Region 6, along the Guyana coastal plains. Various irrigation scenarios were simulated and based on the crop response; irrigation scenarios were recommended for the optimal use of water resources.

2. Methodology

2.1. Data and preparation of simulation files

The study location is at Black Bush Polder, Guyana (6°4’58” N, 57°15’57” W). It is near the coast and the outlet of the Corentyne River. BBP is also part of Region 6, which is one of Guyana's top rice-producing regions with approximately 20,000 hectares of rice land (GLSC, 2004). Irrigation water is supplied by the Berbice and Canje Rivers.

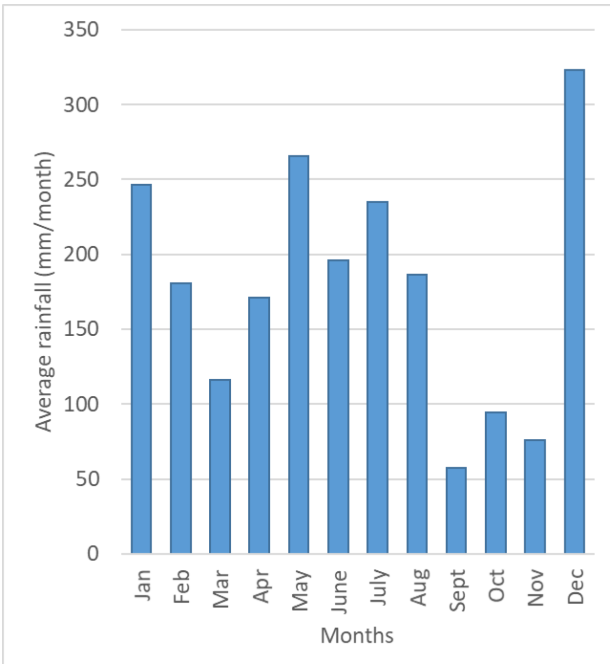

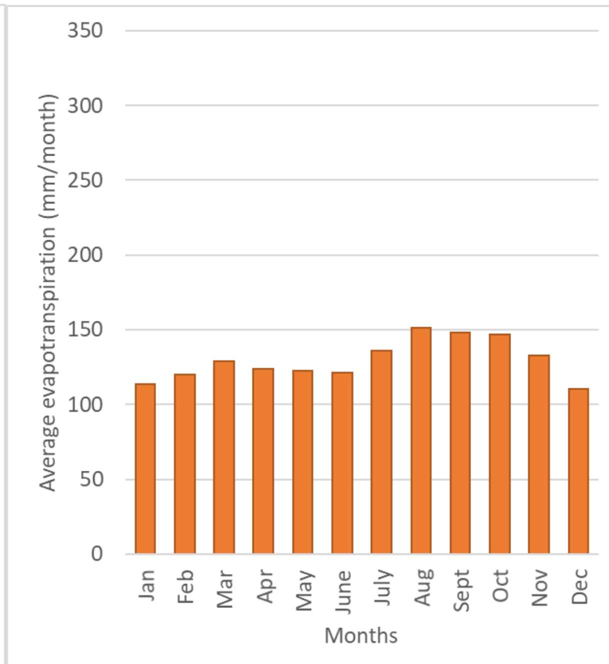

Figure 4.2. Average monthly rainfall and evapotranspiration at BBP (2005 to 2012).

The data used for the AquaCrop climate file was obtained from the set-up of a field automatic weather station which had measured daily rainfall, minimum and maximum temperature, sunshine hours, and wind speed at 2 meters from 2005 to 2012. Two peak rainy months occur, one around May and another in December, as shown in Figure 4.2. The driest months, which are between September and November, have an average monthly rainfall ranging from 57 to 94 mm. The monthly rainfall varies from the average by 50 to 200 mm. The greatest variability is observed for December until March, and May to June, which are also notably the rainy months.

The daily ETo was computed by the AquaCrop ETo calculator based on the FAO Penman-Monteith equation. The ETo averages 130 mm/month, with the highest values coinciding with the driest months. The ETO varies from the monthly average by 10 to 35 mm/month. The highest variability is observed from March to April. Meanwhile, the monthly temperatures were consistent with the minimum temperature ranging from 24.6 to 26.1°C and the maximum temperature from 30.6 to 32.9°C. The input for the annual mean atmospheric CO_2 used the dataset of the Mauna Loa Observatory as provided within AquaCrop (FAO, 2018a; Raes et al., 2018).

The soil data were obtained from soil core samples taken from 3 locations in the field at 150, 300 and 450mm depth. The soil is clayey and made up of 2% sand, 34% silt and 64% clay. It has a $\%MC_{vol}$ at PWP ranging from 32 to 35% and a $\%MC_{vol}$ at FC from 49 to 51%. The soil is under the frontland clay soil group common to the whole coastal plain of Guyana (Braun and Derting, 1964) and is characterized by deep, gray, poorly drained clayey and silty soils. More specifically, the soil type is the drained phase of Corentyne clay. It is a swampland soil prone to waterlogging during heavy rains but has high fertility (GLSC, 2004).

Other parameters used for the irrigation, field management and initial conditions files are based on informant interviews and reports of agronomic practices as discussed in Section 1.1. Meanwhile, the crop file was based on the AquaCrop paddy rice growing-degree-days. The growth schedule was first converted from growing-degree-days to calendar days using the local weather file. Then, some of the parameters were modified based on the varietal characteristic information of GRDB 10, and local agronomic reports. The GRDB10, the most common variety used, is a semidwarf with vigorous vegetative growth and high tillering ability. It has a potential grain yield of 6.8 to 7 tons/ha and matures within 106 to 112 DAP (GRDB, 2016d). A simulation file was created for the Season 1 crop and one for Season 2.

2.2. Calibration and validation

Once the input files were prepared, AquaCrop (FAO, 2018b) was run from 2005 to 2008. The resulting dry yield was converted to fresh yield by using a conversion factor of 80%. This comes from the GRDB (2016c) recommended harvest moisture of 18 to 21% moisture content. The yield of rice for 2009 – 2012 was provided in the GRDB annual reports and reported by region. The average yields for Region 6 were used for calibrating the simulation parameters. The calibration was done by adjusting parameter values to minimize the root mean square error, percent RMSE and mean bias error. The parameters calibrated were mostly non-conservative, and the values used ranged only within reported min-max values or within 10% of the default.

Validation was conducted using the final set of calibrated parameters from 2009 to 2012. Simulated yield and calibrated yield were statistically compared. Once the statistical analysis is acceptable, the parameters were further used for irrigation scenario simulations.

2.3. Irrigation management scenario simulations

The irrigation scenarios were set at 50%, 60%, 70%, 80%, 90%, 100%, 110% and 120% WHR. The percentage values correspond to the %WHR thresholds at which an irrigation input is triggered in the model. Since the AquaCrop irrigation file for generating an irrigation schedule takes RAW depletion as input, the conversion at Equation 2 was used.

$$RAW\ depletion = \ (1 - WHR)/psto \qquad (2)$$

For the 50 to 90% WHR scenarios, the irrigation input is equal to the amount required to bring back the soil moisture content to field capacity; while for the 100 to 120% WHR scenarios, the input is equal to the amount necessary to maintain the soil moisture. An illustration of the different scenario thresholds and irrigation inputs is shown in Figure 4.3.

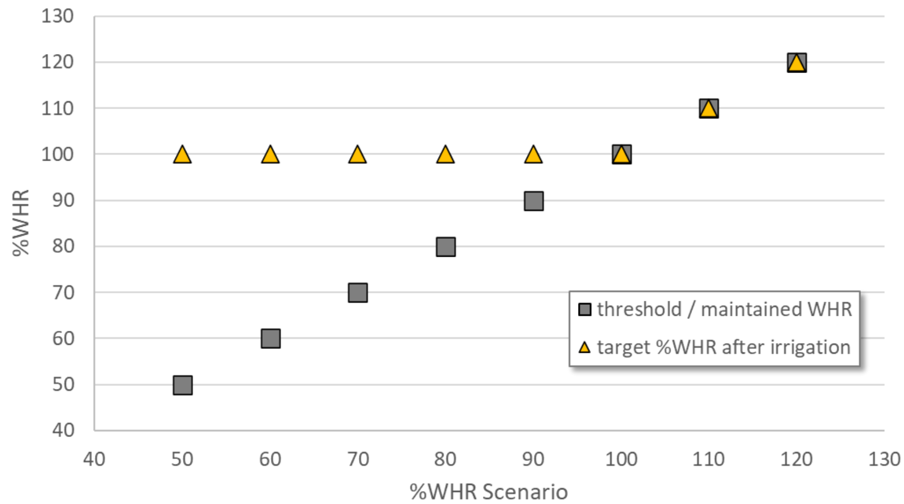

Figure 4.3. Threshold and irrigation target %WHR for each scenario.

Using the crop parameters obtained after calibration, yields at varying irrigation scenarios were simulated. A one-way ANOVA and pairwise t-test were then conducted to check the significance of the results.

3. Results and Discussion

3.1. Calibration and validation

Data for each of the parameters were obtained either through field-measured values, local data sources, or related literature. There were 11 parameters calibrated of which the days to maturity, weed coverage and crop coefficient at maximum canopy (kc_{max}) were the most sensitive. The range of values used for these three parameters (shown in Table 4.) resulted in a 5 to 10% change in the RMSEn. The values used for days to maturity were between 106 to 112 DAP based on the varietal characteristics of GRDB10. Meanwhile, for the weed coverage parameter, between 10 to 15% values were tested for the kc_{max} parameter, values between 1.0 to 1.12 were tested during the sensitivity analysis. These values fall around the updated crop coefficients from Pereira et al. (2021). The least sensitive parameters were the soil curve number, sowing rate, maximum effective rooting depth, and initial water depth between bunds. Changing these parameters did not affect the simulations.

Table 4.1. Sensitivity of the simulated yield to some calibrated parameters.

Parameter calibrated	Range of values used	Change in RMSEn (%)
Days from planting to maturity	106 to 112 DAP	7 to 10%
Weed coverage	0 to 15%	7%
Crop coefficient (kc_{max})	1 to 1.12	5%
Duration of flowering	15 to 18 days	0 to 5%
Reference harvest index (HIo)	41 to 45%	2%
Days to max rooting depth	30 to 44 days	0 to 2%
Maximum canopy cover (CCx)	85 to 99%	0.2 to 2%

The sensitivity of the simulated yield with the parameters on the days to maturity, weed coverage and kc_{max}, indicates that field measurements of these values would significantly improve the simulations. Field measurements of the psto would also be very helpful to the simulations. The psto is valuable for determining RAW and the water stress coefficient, as shown in Figure 4. and Equation 2. The final calibrated parameters are as in Table 4.2. The full list of the simulation parameters can be found in Table 4.A1.

Table 4.2. Simulation parameters and the values used.

Parameter	Value	Source
Soil:		
Saturated hydraulic conductivity (Ksat)	35.0 mm/day	AQ
Curve Number (CN)	77	AQ, Cal
Crop:		
Type of planting method	direct sowing	F
Sowing rate	134.50 kg seed/ha	F, Cal
Maximum canopy cover (CCx)	85%	AQ, Cal
Canopy decline (CDC)	13.8%/day	F
Days to emergence	21 DAP	F
Days to maturity	112 DAP	F, Cal
Duration of flowering	15 days	AQ, Cal
Days to flowering	77 DAP	F
Max effective rooting depth (Zx)	0.50 m	AQ, Cal
Days to max root depth	44 days	AQ, Cal

Parameter	Value	Source
Crop coefficient at CCx (Kc_{max})	1	AQ, Cal
Water Productivity (WP*)	19.0 g/m2	Con
Reference Harvest Index (HIo)	41%	AQ, Cal
Management:		
Irrigation Method for rice	Basin	F
Water Quality for BBP	0.0 dS/m	F
Soil covered by mulches	None, 0%	F
Soil bund height for rice	0.20 m	F
Weed cover for rice	15%	F, Cal
Simulation:		
Planting Search Window for S1	May	F
Planting Search Window for S2	Nov	F
Initial Soil Water for rice	At Saturation	F
Initial Water Depth between bunds for rice	100 mm	F, Cal
Initial salinity for BBP	0.02 dS/m	F

* Key: Cal = Calibrated, M = Measured, F = Localized field observation or information, Con = Conservative parameter, Lit = Literature, AQ = AquaCrop default

After calibration, the simulated yield had a good agreement with the actual reported yield as shown in Table 4.3. The final RMSE, RMSEn and MBE for both Season 1 and Season 2 were deemed to be acceptable at a yield error threshold of 0.43 tons per hectare.

Table 4.3. Agreement between simulated and actual dry yield (ton/ha) after calibration

	Yield (ton/ha)				RMSE	RMSEn	MBE
Year	2005	2006	2007	2008	(ton/ha)	%	(ton/ha)
Acceptable at:					<0.43	<10	<0.43
Season 1							
Actual Yield	3.1	3.7	2.9	2.8	0.25	8.11	+0.06
Simulated Yield	3.2	3.3	3.3	3.2			
Season 2							
Actual Yield	3.1	3.4	3.6	3.7	0.24	6.94	-0.13
Simulated Yield	3.2	3.1	3.3	3.2			

The set of calibrated parameters was validated using the 2009 to 2012 dataset, and the simulated yields, in Table 4.4, further confirmed that the parameters were acceptable and could be used for large-scale simulation. The validation also confirmed that in the absence of field-calibrated crop parameters, AquaCrop simulations need at least location-specific soil and weather data to produce acceptable yield estimates. The good performance of the model during calibration and validation gives us the assurance that the model can also be used to estimate yield for other water holding capacities.

Table 4.4. Agreement between simulated and actual dry yield (ton/ha) after validation.

Simulation	Yield (ton/ha)				RMSE	RMSEn	MBE
	2009	2010	2011	2012	ton/ha	%	ton/ha
Acceptable at:					<0.43	<10	<0.43
Season 1							
Actual Yield	3.2	3.2	2.8	3.4	0.17	5.46	+ 0.05
Simulated Yield	3.2	3.3	3.3	3.3			
Season 2							
Actual Yield	3.6	3.8	3.4	n/a	0.23	6.43	- 0.14
Simulated Yield	3.2	3.3	3.1	n/a			

3.2. Irrigation management scenarios

3.2.1 Relationship of yield with irrigation scenarios and crop season

Since the statistical analysis of the validation was acceptable, we then proceeded with the irrigation scenarios simulations. A simulation was performed for each of the eight irrigation scenarios for the two planting seasons from 2005 to 2012. A one-way ANOVA of the yields shows that there is a significant difference between the yields of the various irrigation scenarios ($p = 2.2e^{-16}$ at $a = 0.05$). However, there was no significant difference in yield between rice planted in Season 1 and Season 2. This might be because both seasons are the two wet seasons in BBP. Furthermore, the average amount of rainfall received within one whole crop season is nearly similar in Season 1 and Season 2, as shown in Figure 4.4. For the succeeding analysis, Season 1 and Season 2 will be aggregated.

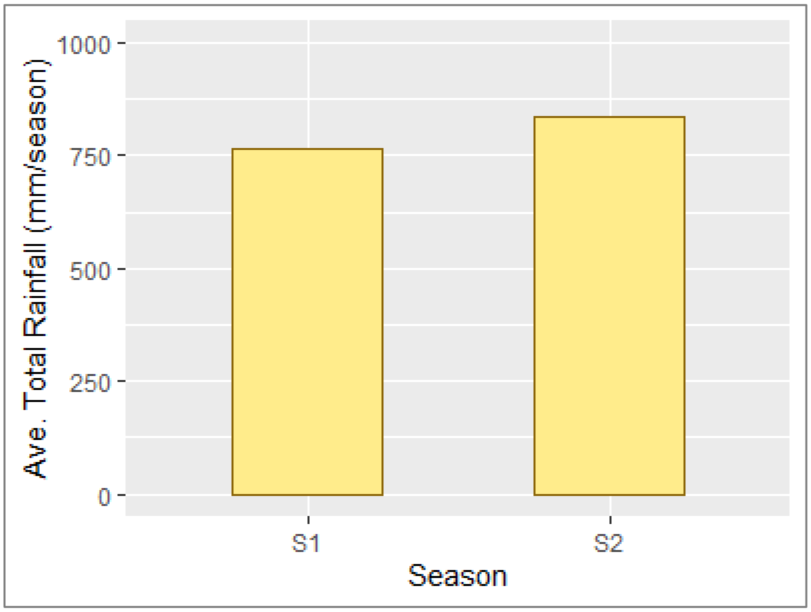

Figure 4.4. Average total rainfall received (mm) for rice planted in Season1 and Season 2

3.2.2. Response of yield from varying irrigation scenarios

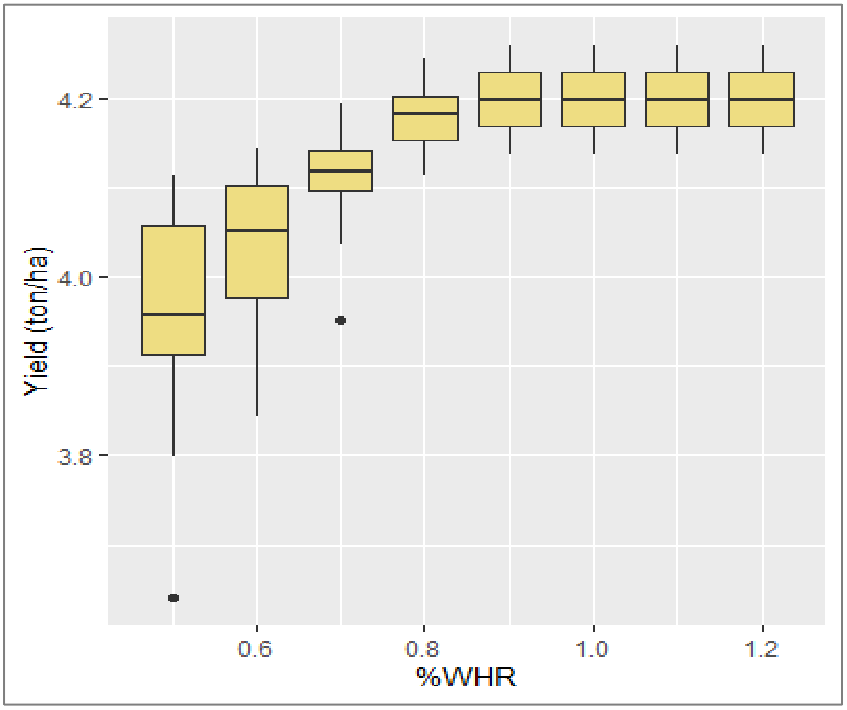

Figure 4.5. Simulated yield for rice at varying %WHR

Rice growth from 2005 to 2012 was simulated for the different irrigation scenarios. The simulated yield (in Figure 4.5) increases with increasing %WHR and plateaus upon reaching 90%WHR. While rice is quite tolerant to flooded conditions, yield does not substantially increase with higher soil-water content. The 50% to 90%WHR represent irrigation deficit systems while the 100, 110 and 120% represent continuous flooding since in these scenarios an irrigation input is kept to maintain the target %WHR.

Studies on the impact of irrigation schemes on rice yield vary widely. The works of Feng et al. (2021) and Poddar et al. (2022) have shown that when less water is used than in the traditional system of continuous flooding, the yield suffers. A field experiment in Eastern India (Poddar et al., 2022) of three irrigation schemes (continuous flooding, AWD, and fields kept at saturation (SAT)) showed that the grain yields obtained for AWD and SAT are 6 and 12% lower, respectively, compared to those obtained from continuous flooding. Their study found significant differences in yield response between the three different varieties used, denoting the significance of the variety on the effectivity of irrigation schemes. On the other hand, a study in the Rio Grande do Sul, Brazil has found that there was no significant difference in yield ($p>0.05$) between continuous irrigation and intermittent flooding scenarios (Borin et al., 2016). Similar results were also obtained in field experiments on rice in China and the Philippines (Belder et al., 2003).

To consolidate these differing responses of rice yield to irrigation schemes, a landmark review by Bouman and Tuong (2001) of 31 sets of experimental data with varying soil and rice cultivars found that yield is indeed reduced for water-saving irrigation scenarios but only when the matrix potential at 10-20 cm soil depth goes below -100 to -300 mbar. This suggests that scenarios such as intermittent irrigation, AWD and irrigation deficit can be used with minimal impact on the yield provided that a safe operational level of matrix potential or water depth is maintained in the field.

In the case of rice farming in Guyana, the yield was indeed reduced below 90%WHR. To identify if the yield reduction at 50, 60, 70 and 80% WHR is significant, a pairwise t-test was conducted. The results in Table 4.5 show no significant difference between the 80%WHR and the 90%WHR yield. When water is limited, an irrigation scheme following the 80%WHR is acceptable for efficient use of water at minimal yield loss.

Table 4.5. The T-test between yield at 90%WHR and varying %WHR irrigation scenarios.

	Scenarios (%WHR)				
	90	**80[a]**	**70[b]**	**60[b]**	**50[b]**
Average yield (tons per ha)	4.20	4.18	4.11	4.03	3.95
- p-value	ref.	0.35	4.9E-04	4.2E-10	2.0E-16
Irrigation requirement (mm per ha)	164	132	104	82	68

[a] No significant difference from yield at 90%WHR (alpha = 0.05).
[b] With significant difference from yield at 90%WHR (alpha = 0.05).

The 80% scenario is suitable for growing rice in Guyana during dry periods and the 90% WHR during regular conditions. However, there may be other considerations for the decision-maker to pick other irrigation schemes such as weed management and salinity control. Table 4.6 shows the moisture contents which can be used as thresholds, in conjunction with soil moisture sensors, to trigger irrigation operations. The minimum irrigation volume per application is also provided. It considers the field losses such as soil evaporation, runoff, and deep percolation. However, lateral seepage and conveyance losses still need to be estimated and included.

Table 4.6. Simulated crop parameters and irrigation information for each %WHR scenario

WHR	Simulated crop outputs		MC_{vol} threshold	Irrigation volume per application	Total irrigation volume per season
	Yield	WP			
(%)	(tons/ha)	(kg/m^3 H_2O)	(mm/mm)	(m^3/ha)	(m^3/ha)
60	4.03	0.823	0.4454	616	822
70	4.11	0.823	0.4608	462	1,043
80	4.18	0.825	0.4762	308	1,318
90	4.20	0.819	0.4916	154	1,643
100	4.20	0.812	0.5070	95	1,881
110	4.20	0.813	0.5224	233	3,191
120	4.20	0.813	0.5378	400	5,166

4. Conclusion

AquaCrop has been successfully calibrated and validated to simulate rice growth along the coastal frontland soils of Guyana. Field-measured data of the soil and climate had proven to be necessary for simulations alongside crop parameters obtained from local information and the AquaCrop rice file. The sensitivity analysis has shown, however, that the simulation can still be substantially improved if field measurements of the growth stage duration (e.g., days to maturity, duration of flowering, days to maximum rooting depth), percentage weed coverage and crop coefficient at maximum canopy cover could be obtained.

Irrigation scenarios were simulated of which the highest yields can be obtained at 90%WHR. In this scenario, the soil water content is allowed to decrease until 90%WHR, upon which irrigation commences until the field is back to field capacity. Meanwhile, the 80%WHR scenario seems to be the optimal method for the Guyana coastal plains when both yield and water consumption are important considerations. In this scenario, the yield is not significantly different from the maximum yield and the water consumption is lower.

The current method of irrigating rice involves flooding the fields, with up to 10mm of standing water, weekly. The simulations have shown that there is no substantial increase in yield when the soil-water content is kept above field capacity. Moreover, a higher volume of total irrigation is used for a whole season at a high %WHR.

5. Declaration of competing interest

The authors declare that they have no known competing financial interests of personal relationships that could have appeared to influence the work reported in this paper.

6. Acknowledgements

We would like to thank the following for providing data and information: Guyana Rice Development Board, NAREI, and Raffaella Maria Pilati de Carvalho and Dr. Felexce Ngwa for collecting and analyzing the soils and climate data. We acknowledge a grant from the International Development Research Centre (IDRC), Ottawa, Canada, and with the financial support of the Government of Canada provided through Global Affairs Canada, support of the NSERC and a fellowship to the senior author by the Macdonald Stewart Foundation under the Liliane and David M. Stewart Fellowship in Water Resources.

7. References

Alberto, Ma.C.R., Quilty, J.R., Buresh, R.J., Wassmann, R., Haidar, S., Correa, T.Q., Sandro, J.M., 2014. Actual evapotranspiration and dual crop coefficients for dry-seeded rice and hybrid maize grown with overhead sprinkler irrigation. Agric. Water Manag. 136, 1–12. https://doi.org/10.1016/j.agwat.2014.01.005

Alvar-Beltrán, J., Heureux, A., Soldan, R., Manzanas, R., Khan, B., Dalla Marta, A., 2021. Assessing the impact of climate change on wheat and sugarcane with the AquaCrop model along the Indus River Basin, Pakistan. Agric. Water Manag. 253, 106909. https://doi.org/10.1016/j.agwat.2021.106909

Belder, P., Bouman, B.A.M., Cabangon, R., Guoan, L., Quilang, E.J.P., Yuanhua, L., Spiertz, J.H.J., Tuong, T.P., 2003. Effect of water-saving irrigation on rice yield and water use in typical lowland conditions in Asia. Agric. Water Manag. 65, 193–210. https://doi.org/10.1016/j.agwat.2003.09.002

Borin, J.B.M., Carmona, F. de C., Anghinoni, I., Martins, A.P., Jaeger, I.R., Marcolin, E., Hernandes, G.C., Camargo, E.S., 2016. Soil solution chemical attributes, rice response and water use efficiency under different flood irrigation management methods. Agric. Water

Manag. 176, 9–17. https://doi.org/10.1016/j.agwat.2016.05.021
Bouman, B.A.M., Tuong, T.P., 2001. Field water management to save water and increase its productivity in irrigated lowland rice. Agric. Water Manag. 49, 11–30. https://doi.org/10.1016/S0378-3774(00)00128-1
Bovolo, I., 2014. Managing Flood Risk in Guyana: The Conservancy Adaptation Project, 2008 - 2013 (No. 86635). International Bank for Reconstruction and Development / The World Bank MMXIV, Washington, DC.
Braun, E.G., Derting, J.F., 1964. Map for the Reconnaissance Soil Survey of Northeast British Guiana.
Diaz, M.B., Roberti, D.R., Carneiro, J.V., Souza, V. de A., de Moraes, O.L.L., 2019. Dynamics of the superficial fluxes over a flooded rice paddy in southern Brazil. Agric. For. Meteorol. 276–277, 107650. https://doi.org/10.1016/j.agrformet.2019.107650
FAO, 2018a. AquaCrop - Mauna Loa Observatory mean atmospheric CO2.
FAO, 2018b. AquaCrop (software).
Feng, Z.Y., Qin, T., Du, X.Z., Sheng, F., Li, C.F., 2021. Effects of irrigation regime and rice variety on greenhouse gas emissions and grain yields from paddy fields in central China. Agric. Water Manag. 250, 106830. https://doi.org/10.1016/j.agwat.2021.106830
GLSC, 2013. Guyana National Land Use Plan (national plan). Guyana Lands and Surveys Commission, Georgetown, Guyana.
GLSC, 2004. Region VI Sub-Regional Land Use Plan (soil map). Guyana Lands & Surveys Commission, Georgetown, Guyana.
GRDB, 2020. Management Guidelines for the Cultivation of GRDB 16 (brochure). Guyana Rice Development Board, Georgetown, Guyana.
GRDB, 2016a. 2016 Annual Report (annual report). Guyana Rice Development Board, Georgetown, Guyana.
GRDB, 2016b. Plant Breeding [WWW Document]. Guyana Rice Dev. Board. URL https://grdb.gy/plant-breeding/ (accessed 8.22.22).
GRDB, 2016c. Agronomy [WWW Document]. Guyana Rice Dev. Board. URL https://grdb.gy/agronomy-of-rice/ (accessed 7.13.22).
GRDB, 2016d. Rice Breeding Programme in Guyana (brochure). Guyana Rice Development Board, Georgetown, Guyana.
Kim, D., Chun, J.A., Inthavong, T., 2021. Managing climate risks in a nutrient-deficient paddy rice field using seasonal climate forecasts and AquaCrop. Agric. Water Manag. 256, 107073. https://doi.org/10.1016/j.agwat.2021.107073
Linquist, B., Snyder, R., Anderson, F., Espino, L., Inglese, G., Marras, S., Moratiel, R., Mutters, R., Nicolosi, P., Rejmanek, H., Russo, A., Shapland, T., Song, Z., Swelam, A., Tindula, G., Hill, J., 2015. Water balances and evapotranspiration in water- and dry-seeded rice systems. Irrig. Sci. 33, 375–385. https://doi.org/10.1007/s00271-015-0474-4
Mahdu, O., 2019. The Impacts of Climate Change on Rice Production and Small Farmers' Adaptation: A Case of Guyana (dissertation). Virginia Polytechnic Institute and State University, Blacksburg, Virginia.
OECD, FAO, 2022. OECD-FAO Agricultural Outlook 2022-2031, OECD-FAO Agricultural Outlook. Food and Agriculture Organization of the United Nations; and Organisation for Economic Co-operation and Development, Rome, Italy; Paris, France.
Pereira, L.S., Paredes, P., Hunsaker, D.J., López-Urrea, R., Mohammadi Shad, Z., 2021. Standard single and basal crop coefficients for field crops: Updates and advances to the FAO56 crop

water requirements method. Agric. Water Manag. 243, 106466. https://doi.org/10.1016/j.agwat.2020.106466
Poddar, R., Acharjee, P.U., Bhattacharyya, K., Patra, S.K., 2022. Effect of irrigation regime and varietal selection on the yield, water productivity, energy indices and economics of rice production in the lower Gangetic Plains of Eastern India. Agric. Water Manag. 262, 107327. https://doi.org/10.1016/j.agwat.2021.107327
Raes, D., Steduto, P., Hsiao, T.C., Fereres, E., 2018. AquaCrop Reference Manual (version 6.0 - 6.1).
Raoufi, R.S., Soufizadeh, S., 2020. Simulation of the impacts of climate change on phenology, growth, and yield of various rice genotypes in humid sub-tropical environments using AquaCrop-Rice. Int. J. Biometeorol. 64, 1657–1673. https://doi.org/10.1007/s00484-020-01946-5
Roel, A., Heilman, J.L., McCauley, G.N., 1999. Water use and plant response in two rice irrigation methods. Agric. Water Manag. 39, 35–46. https://doi.org/10.1016/S0378-3774(98)00087-0
Salman, M., Garcia-Vila, M., Fereres, E., Raes, D., Steduto, P., 2021. The AquaCrop model: enhancing crop water productivity. Ten years of development, dissemination and implementation 2009-2019 (No. 47), FAO Water Report. Food and Agriculture Organization of the United Nations, Rome, Italy. https://doi.org/10.4060/cb7392en
Steduto, P., Hsiao, T.C., Fereres, E., Raes, D., 2012. Crop yield response to water, FAO Irrigation and Drainage Paper. Food and Agriculture Organization of the United Nations.
USACE, 1998. Water Resources Assessment of Guyana (Assessment). US Army Corps of Engineers, Guyana.
Xu, J., Bai, W., Li, Y., Wang, H., Yang, S., Wei, Z., 2019. Modeling rice development and field water balance using AquaCrop model under drying-wetting cycle condition in eastern China. Agric. Water Manag. 213, 289–297. https://doi.org/10.1016/j.agwat.2018.10.028

8. Appendix

Appendix A

Key: Cal = Calibrated
M = Measured
F = Field Observation and information
Con = Conservative parameter
Lit = Literature
AQ = AquaCrop default

Crop File: Paddy rice at BBP, Guyana

Table 4.A1. Simulation parameters used after calibration

PARAMETER	VALUE	SOURCE
Development:		
type of planting method	direct sowing	F
canopy size of seedling	3.0 cm2/plant	AQ
sowing rate	134.50 kg seed/ha	F, Cal
germination rate	75%	AQ
1000 seed mass	50g	AQ
maximum canopy cover (CCx)	85%	AQ, Cal
canopy decline (CDC)	13.8%/day	F
Days to emergence	21	F
Days to maturity	112	F, Cal
Duration of flowering	15 days	AQ, Cal
Days to flowering	77 days	F
soil restrictions	shallow rooted	AQ
max effective rooting depth	0.50 m	AQ, Cal
Days to max root depth	44 days	AQ, Cal
ave. root zone expansion	1.1 cm/day	AQ
effect of canopy shelter in late season	50%	Con
Evapotranspiration		
Crop coefficient at CCx (Kc tr,x)	1	AQ, Cal
Water extraction pattern - upper 1/4 - 2nd 1/4 - 3rd 1/4 - bottom ¼	40% 30% 20% 10%	AQ
Production		
Water Productivity (WP*)	19.0 g/m2	Con
Reference Harvest Index (Hio)	41%	AQ, Cal
Response to Water Stress:		
p(upper) for canopy expansion	0	Con

PARAMETER	VALUE	SOURCE
p(lower) for canopy expansion	0.4	Con
Shape factor for canopy expansion	3	Con
p(upper) for stomatal closure (psto)	0.1	AQ
Shape factor for stomatal closure	3	Con
p(upper) for early senescence (psen)	0.55	Con
Shape factor for early senescence	3	Con
Aeration threshold below saturation	0%	AQ
Positive effect on HI due to limited growth	none	Con
p(upper) for failure of pollination (ppol)	0.75	Con
Positive effect on HI due to leaf expansion	small	Con
Negative effect on HI due to stomatal closure	moderate	Con
Response to Temperature Stress		
Base temp for crop development (Tbase)	8.0 C	Con
Upper temp for crop development (Tupper)	30.0 C	Con
GD range from 0 degree-day to:	10.0 C-day	Con
Min air temp range affecting pollination: +3 C to _ C	8 Celsius	Con
Max air temp range affecting pollination: _ C to 40C	35 Celsius	Con
Response to Salinity		
Lower Ece threshold (ECEn)	3 dS/m	Con
Upper Ece threshold (ECEx)	11 dS/m	Con
Ece at 100% stress affecting canopy expansion	5.0 dS/m	Con
Ece at 100% stress affecting stomatal closure	5.0 dS/m	Con

Climate File: Black Bush Polder, Guyana from 2005 to 2012

Parameter	Value	Source
Rainfall	Daily, 2005 – 2012	M
Evapotranspiration (ETO)	Daily, 2005 – 2012	Com
Temperature	Daily, 2005 – 2012	M
CO2	Yearly, MaunaLoa	AQ

Irrigation File: rice at BBP, Guyana

Parameter	Value	Source
Irrigation Method for rice	Basin, Irrigate to FC when %TAW is reached	F
Water Quality for BBP	0.0 dS/m	F

Soil File: BBP, Guyana

Parameter	Value	Source
Horizons information (texture, thickness, PWP, FC, SAT)	3 horizons up to 0.45 m depth	M
Saturated hydraulic conductivity (Ksat)	35.0 mm/day	AQ
Curve Number (CN)	77	AQ, Cal

Field Management: Rice at BBP, Guyana

Parameter	Value	Source
Soil cover by mulches	None, 0%	F
Soil bund height for rice	0.20 m	F
Weed cover for rice	15%	F, Cal
Effect on CN by field practice (poor hydrologic condition, straight furrows)	+10%	F, Cal

Simulation parameters

Parameter	Value	Source
Planting Search Window for S1	May	F, Cal
Planting Search Window for S2	Nov	F, Cal
Initial Soil Water for rice	At Saturation	F
Initial Water Depth between bunds for rice	100 mm	F, Cal
Initial salinity for BBP	0.02 dS/m	F
Initial canopy cover (Cco)	0%	AQ
Initial Biomass	0 ton/ha	AQ
Initial root depth	0.30 m	AQ

BRIDGING TEXT

The crop simulations for rice, in Chapter IV, have shown that water-saving scenarios could be achieved with minimal impact on yield. We want to know if a similar response will be observed in sugarcane. Even with the decreasing production of sugarcane, it is still one of Guyana's major crops and still occupies large areas serviced by the existing irrigation and drainage system. Chapter V discusses the response of yield and water productivity of sugarcane to different irrigation scenarios. It will determine the suitability of the current irrigation scheme to the needs of sugarcane and identify possible ways to improve water management in the estates.

This study is in preparation for submission to *Irrigation Science*. The paper is co-authored by Guia Marie M. Mortel and Dr. Chandra Madramootoo. The contributions of each author are mentioned on page 7.

CHAPTER V

Improving water productivity of surface irrigated sugarcane estates

Abstract

Sugarcane is a traditional major crop and export of Guyana. The estates are located along the coast which is approximately one metre below sea level. Therefore, drainage canals are essential for the disposal of surface runoff which is of paramount importance as the coast experiences over 1000 mm of rain annually during two pronounced wet seasons. The crop water requirement for irrigation is a secondary priority. This I&D system, comprised of continuous open furrows, keeps the moisture within the fields at approximately 70% water-holding capacity in the rootzone (%WHR). The system within sugar estates is also used for the delivery of harvested canes from the fields to the mill via barges. This study aims to propose irrigation scenarios to maximize yield and water productivity, using the AquaCrop model. Field-measured climate and soil data, and local crop parameters were used with the model. During calibration, the yield was weakly sensitive (0.6 - 2% ΔRMSEn), to changes in crop parameter values with the maximum change observed for the maximum canopy cover and the crop coefficient (kc_{max}). The crop simulation was calibrated with actual reported yields from 2005 to 2008. The calibrated parameters were then validated using the 2009 to 2012 dataset. The good agreement (RMSE of 7.15% or 4.39 ton cane/ha) with the recorded yield during validation, and the low sensitivity of calibrated parameters indicate the acceptability of AquaCrop and the parameters used for simulations. Several irrigation scenarios were then simulated, of which no significant reduction or increase in yield was observed between 50% to 100%WHR scenarios. The I&D system can aim for an 80%WHR to obtain a slightly better yield. A threshold of 50%WHR is advisable during dry periods to avoid significant yield loss.

1. Introduction

1.1. Water productivity of sugarcane irrigation schemes

Water productivity (WP_{et}) is referred to in this paper in terms of the yield produced for each unit of water used by both evaporation and transpiration. Water productivity is an indicator of the efficiency by which a crop converts the water it uses into harvestable yield. Two main factors influence WP_{et}: crop genetics or variety characteristics, and cultural management practices. Application of soil amendments (Kalanaki et al., 2022; Zahra et al., 2021), nitrogen application rates (Cao et al., 2021) and soil textures (Fang and Su, 2019) have been shown to affect WP_{et}. In the realm of crop water management, several factors that influence water productivity are the amount of irrigation provided (Kalanaki et al., 2022), the matrix potential threshold for irrigation (dos Anjos Veimrober Júnior et al., 2022), groundwater depth (Dai et al., 2022), and irrigation method used such as between surface and subsurface drip irrigation (Aydinsakir et al., 2021).

Several studies have compared the water productivity of various irrigation methods. However, studies specific to furrow irrigation for sugarcane are sparse. It is known that for sugarcane, double-row furrow planting with mulch has been shown to increase water productivity in India (Singh et al., 2022). Reports on other irrigation methods of sugarcane are more common such as subsurface drip irrigation in Iran (Naseri et al., 2020) and India (Vaiyapuri et al., 2019), and drip irrigation in Brazil (Coelho et al., 2012).

1.2. Irrigation of sugarcane estates in Guyana

Sugarcane is a ratoon crop which is grown from shoots left by a harvested crop. In Guyana, the first crop (plant cane) is usually planted between November and January and is harvested after 40 weeks (Eastwood, 2009). A ratoon crop, meanwhile, takes only 36 weeks to be ready for harvest (Eastwood, 2009). Sugarcane is planted on beds laid out in either ridge-and-furrow or broad-bed design (GuySuCo, 2022). Most of the fields have traditionally been following the ridge-and-furrow layout, but recently, more plots are converted to broad-bed design for eventual mechanized planting and harvesting (GuySuCo, 2018).

Water is pumped from rivers and into the canals leading to the sugarcane estates. It is then routed through farm plots, and finally into the furrows within the fields. The irrigation layout is a continuous open-ended furrow system wherein water is allowed to freely enter and exit the furrows. When the water reaches the end of the furrows, it is collected by an in-field collector drain which routes and merges it with the main line (GuySuCo, 2022).

A unique feature of Guyana's I&D is the use of open canals for delivering harvested cane from the farms to the sugar mills. The inflow of these canals is regulated mainly for the conveyance of the harvested cane. A head difference must be maintained between the farms and the mill to convey the barges downstream. With this scheme, the soil water content in the fields is kept at approximately 70% water holding capacity within the first meter rooting depth.

1.3. Irrigation and drainage design priorities

The wet tropical climate (Peel et al. 2007) and clayey frontland soils (Braun and Derting 1964; GLSC 2013) of the Guyana's coast, places more emphasis on drainage for agriculture. Guyana's towns and most of its population are also located along the coast, which is generally below sea water level (USACE 1998). As such, the entire I&D system of Guyana, the conservancies, and the sea walls were designed to keep water off.

With drainage and conveyance taking priority in the I&D system design, irrigation is given the least priority. Irrigation, however, is a necessary component of fully functioning I&D system. Regulating irrigation reduces waterlogging problems and thus lessens the burden on drainage. The conveyance role of channels may mean that a large volume of water is allowed to flow, and the potential yield of sugarcane is not reached because of waterlogging. The prioritization of conveyance may also mean that during dry periods, channels leading into fields are temporarily closed to increase the channel head at the main line.

This study aims to identify the impact of the current I&D system on the sugarcane yield and water productivity obtained. We also want to investigate whether better yield and water productivity can be achieved in other irrigation scenarios. This is especially important to schedule block irrigation during the dry season.

Crop growth is modelled using AquaCrop. It is chosen because of its design to model yield response from fewer and easily measured crop parameters. Furthermore, AquaCrop has been intensively used for research and as such several crop parameters have already been measured, estimated, or calibrated. For sugarcane, the field experiments in Brazil (da Costa Faria Martins et al., 2022; da Silva et al., 2013), Australia, Swaziland (Inman-Bamber and McGlinchey, 2003) and South Africa (Olivier and Singels, 2012) have contributed to improvements to key parameters of the sugarcane crop file, specifically the crop coefficients, maximum root depth, and the threshold of soil water depletion for water stress. The default parameters for sugarcane can be found in the AquaCrop reference manual (Raes et al., 2018), while the updated crop parameters are published by Pereira et al. (2021).

AquaCrop had been used to simulate sugarcane growth to understand the crop's response to projected climate change in Pakistan (Alvar-Beltrán et al., 2021; Farooq and Gheewala, 2020); identify a suitable deficit irrigation design in Khuzestan, Iran (Bahmani and Eghbalian, 2018); and predict the impact of a shifted crop calendar considering climate projections in Phu Yen, Vietnam (Lee and Dang, 2018).

2. Methodology

2.1. Data and preparation of simulation files

The study location covers the sugarcane estates of Albion, Rose Hall, and Port Mourant in Region 6. Sugar production in Albion accounts for 55% of Guyana's total sugarcane production with 45,000 to 60,000 ha harvested annually from 2009 to 2018 (GuySuCo, 2018). Irrigation is mainly supplied by the Canje Creek which is located southwest of the sugarcane estates.

Climate data were obtained from the nearest installed automatic weather station located at 6°4'58" N, 57°15'57" W. Daily data on the rainfall, sunshine hours, wind velocity, and minimum and maximum temperature were measured from 2005 to 2012. The average monthly rainfall at the study site, in Figure , shows variability between the months. A first wet season can be observed from May to August and a second wet season from December to January. The monthly rainfall varies from the average by 50 to 200 mm. The greatest variability is observed for December until March, and May to June, which are also notably the rainy seasons. The daily reference evapotranspiration (ETo) was computed using the FAO Penman-Monteith within AquaCrop. The ETo averages 130 mm/month, with the highest variability observed from March to April, at 35 mm/month. Meanwhile, the minimum and maximum temperatures are almost constant throughout the year.

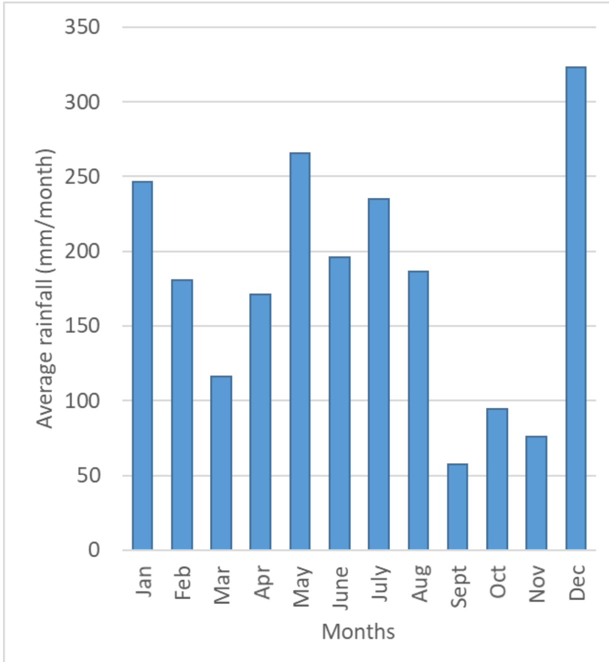

Figure 5.1. Average monthly rainfall (2005 - 2012) at the Region 6 sugarcane estates

The majority of the soil at the Region 6 sugarcane estates is a Frontland clay. It is characterized by a deep gray layer of clay and silt soil particles, poor drainage, level to nearly level relief and the presence of stratified marine deposits (Braun and Derting, 1964). Soil sampling done at four random sites confirmed a sand-silt-clay ratio of 2% – 34% – 64%. The soil characteristics and soil water retention curve from the four sampling sites were measured.

The crop parameters used were based on the sugarcane file provided in AquaCrop. When field measurements or local information are available, these values were used instead of those provided in AquaCrop's sugarcane file (Eastwood, 2009: Gaj and Madramootoo, 2017). Some of the key values used are shown in Table 4.2. The full list is provided in Table 5.A1.

Table 5.1. Some simulation parameters and the values used.

PARAMETER	VALUE	SOURCE
Soil:		
Saturated hydraulic conductivity (Ksat)	35.0 mm/day	AQ
Curve Number (CN)	77	AQ, Cal
Crop:		
Type of planting method	transplanting	F
Row spacing	1.0 m	Lit
Plant spacing	0.25	AQ, Cal
Maximum canopy cover (CCx)	90%	AQ, Cal
Days to recovered	22 DAT	F, Cal
Days to max canopy	134 DAT	F, Cal
Days to harvest	281 DAT	F, Cal
Max effective rooting depth (Zx)	0.80 m	F
Days to max root depth	181 days	F
Crop coefficient at CCx (Kc_{max})	1.1	F, Cal
Water Productivity (WP*)	30.0 g/m^2	Con
Reference Harvest Index (HIo)	35%	AQ, Cal
p(upper) for stomatal closure (psto)	0.5	AQ, Cal
Aeration threshold below saturation	3%	AQ, Cal
Management:		
Irrigation Method	Furrow	F
Water Quality	0.0 dS/m	F
Weed cover	6%	F, Cal
Effect on CN by field practice	+10%	F, Cal
Simulation:		
Planting Search Window	Nov	F, Cal
Initial Soil Water	At Saturation	F
Initial salinity	0.02 dS/m	F

* Key: Cal = Calibrated parameter, M = Measured parameter, F = Local field observation or information, Con = Conservative parameter, Lit = From literature, AQ = AquaCrop default

2.3. Calibration and validation

Calibration was first done on 13 parameters within a range of values provided in the literature or within 10% of the default or average value. The actual yield data reported by GuySuCo (2013) from 2005 to 2008 was converted to dry yield using a 30% dry matter factor (FAO, 2012). The agreement between the actual and simulated yield was determined through statistical analysis using the root mean square error, percent RMSE and mean bias error. Since these three are measures of error, the best set of calibrated parameters is the one which would give the lowest error values.

Once the calibrated parameters were finalized, they were used to simulate the yield for 2009 to 2012. An RMSEn value of 10% and an RMSE and MBE below 1.89-ton cane/ha (dry yield) confirm that the model and the parameters used were acceptable for simulating yield.

2.4. Irrigation management scenario simulations

The irrigation scenarios are all continuous open-furrow irrigation with varying maintained thresholds in terms of the water holding capacity in the rootzone (WHR). The WHR is the total amount of water in the root zone depth (Ze) held between the measured volumetric moisture content (MC_{vol}) at PWP and MC_{vol} at FC (in Equation 1). Irrigation commences when the threshold is reached, and an irrigation input is provided to return the %WHR to the threshold. There were 7 scenarios simulated, namely, 40, 50, 60, 70, 80, 90 and 100% WHR. The 100%WHR scenario corresponds to soil water content maintained at Field Capacity.

$$WHR = \left(\%MC_{vol,FC} - \%MC_{vol,PWP}\right) \times Ze \qquad (1)$$

Simulations were run for each scenario from 2009 to 2012 using the calibrated and validated parameters. A one-way ANOVA test was then conducted to determine a statistical difference between the yield distributions of the irrigation scenarios used. Afterwards, a pairwise t-test was done to identify if each scenario's simulated yield is statistically different from the highest yield.

3. Results and Discussion

3.1. Calibration and validation

The simulated yield showed the most sensitivity to the crop coefficient (kc_{max}) and maximum canopy cover (CC_{max}) for the range of values used (Table 5.2). However, the changes in the RMSEn are only up to 2%. This indicates that the crop parameters used are nearly optimal and are already representative of the conditions in the field. Notably, kc_{max} is already a field-measured value provided in the Agriculture Operation Guidelines of GuySuCo (Eastwood, 2009). The CC_{max} meanwhile is based on the indicative value provided in the AquaCrop sugarcane base file.

Table 5.2. Sensitivity of simulated yield (ΔRMSEn) to the most sensitive calibrated parameters for the range of values used

Parameter calibrated	Range of values used	Δ RMSEn (%)
Crop coefficient at maximum canopy cover (kc_{max})	1.05 to 1.15	0.6 - 1
Maximum canopy cover (CC_{max})	90 to 99%	1 – 2
Days to maximum canopy	90 to 134 DAT	0.5 – 1
Days to harvest	267 to 295 DAT	0.5 – 1
Threshold for aeration stress	3 to 6% MC_{vol} below SAT	0 – 0.8%
Reference Harvest Index (HI_o)	34 to 36%	0 – 0.5%

During the calibration of the model and the input parameters, a good agreement between the simulated and actual yield was obtained. The RMSEn, RMSE, and MBE were low and within tolerable limits. The validation between the simulated and actual yields has also shown good agreement, as shown in Table 5.3.

Table 5.3. Agreement between simulated and actual yield after calibration and validation

Simulation	RMSE ton cane/ha[a]	RMSEn %	MBE ton cane/ha[a]
Acceptable at:	<6.24	<10	<6.24
Calibration: 2005 – 2008	4.32	6.83	- 0.03
Validation: 2009 - 2012	4.39	7.15	+ 1.44

[a] in metric tonnes cane of fresh yield per hectare

3.2. Irrigation management scenario simulation

3.2.1. Response of yield for the different irrigation scenarios

The irrigation scenarios were first run from 2005 to 2012 to get the simulated yields. An ANOVA of the yields shows that there is a significant difference among the scenarios (using simple f-test at a = 0.05). The yield increases with increasing %WHR and plateaued upon reaching the maximum mean yield, of 63 ton cane/ha, at 80% WHR, as shown in Figure 5.2.

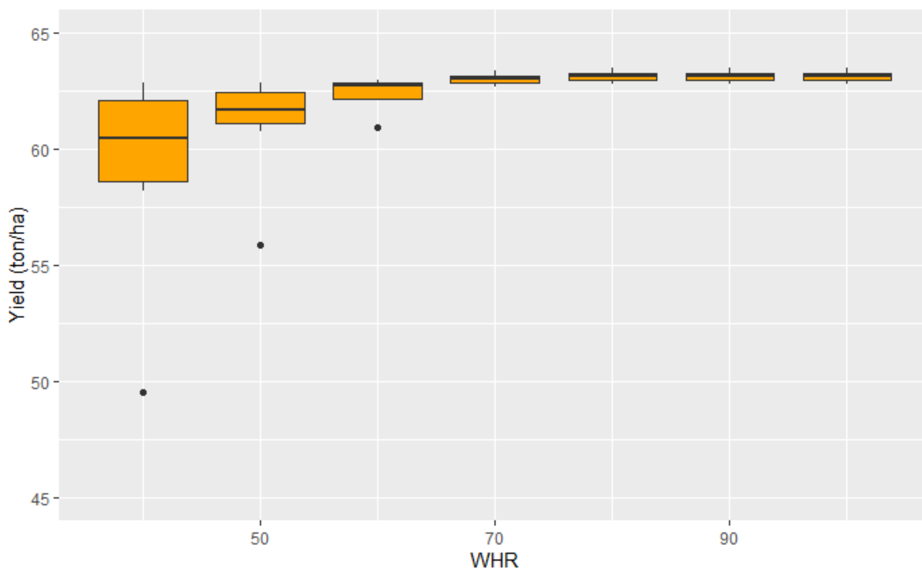

Figure 5.2. Simulated yield (ton cane/ha) obtained at varying %WHR scenarios

A one-way t-test shows that the yield distribution from 50 to 100%WHR is not significantly different from 90%WHR (Table 5.4). The t-test compares not only the mean values but also the spread of the yield distribution. As such, even though the mean yield obtained at 50%WHR is lower than the one obtained at 80%WHR, the difference is not significant since there is still the possibility that 80%WHR yields can be obtained when using the 50%WHR scenario. Meanwhile, a reduction in yield was evident and statistically significant when the 40%WHR scenario is used. This implies that, when water is limited, the soil water content can be allowed to go as low as 50%WHR without incurring a significant yield penalty.

Table 5.4. Pairwise t-test of yields of each irrigation scenario with the yield at 90%WHR

	Scenarios (%WHR)						
	100[a]	**90**	**80[a]**	**70 [a]**	**60 [a]**	**50 [a]**	**40[b]**
Mean yield (ton cane/ha)	63.13	63.13	63.13	63.01	62.38	61.08	59.18
P value at a = 0.05	1.0	reference	1.0	0.91	0.49	0.06	0.006
Irrigation requirement (mm per ha)	532	433	366	303	243	195	139

[a] no significant difference from reference at a = 0.05
[b] with significant difference from reference at a = 0.05

The current irrigation system of the sugarcane estate keeps an estimated 70%WHR within the fields. The simulated yields at 70%WHR are not significantly different from those obtained between 80 to 100%WHR. Given the variability in the field, some spots may have a lower soil water content, but the gap between the 70% and the 50%WHR provides a leeway to ensure that most crops are well irrigated.

3.2.2. Response of water productivity at varying irrigation scenarios

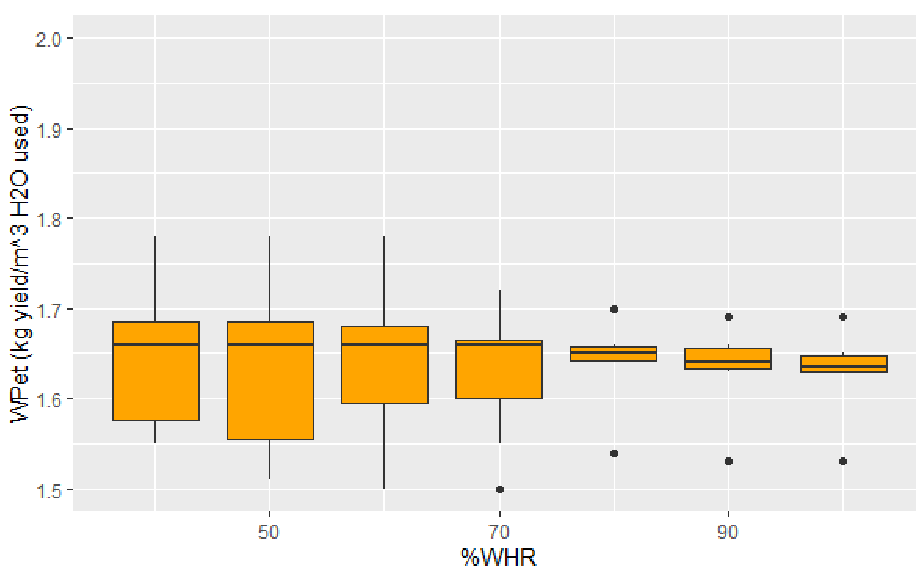

Figure 5.3. Water productivity at varying %WHR scenarios.

The highest mean WPet was obtained at 60%WHR (Figure 5.3) wherein 1.64 kg of dry biomass is produced for each cubic meter of water used by evaporation and transpiration. However, both a one-way ANOVA and pairwise t-tests have confirmed that the differences in water productivity between the scenarios were minimal and not significant p>0.05.

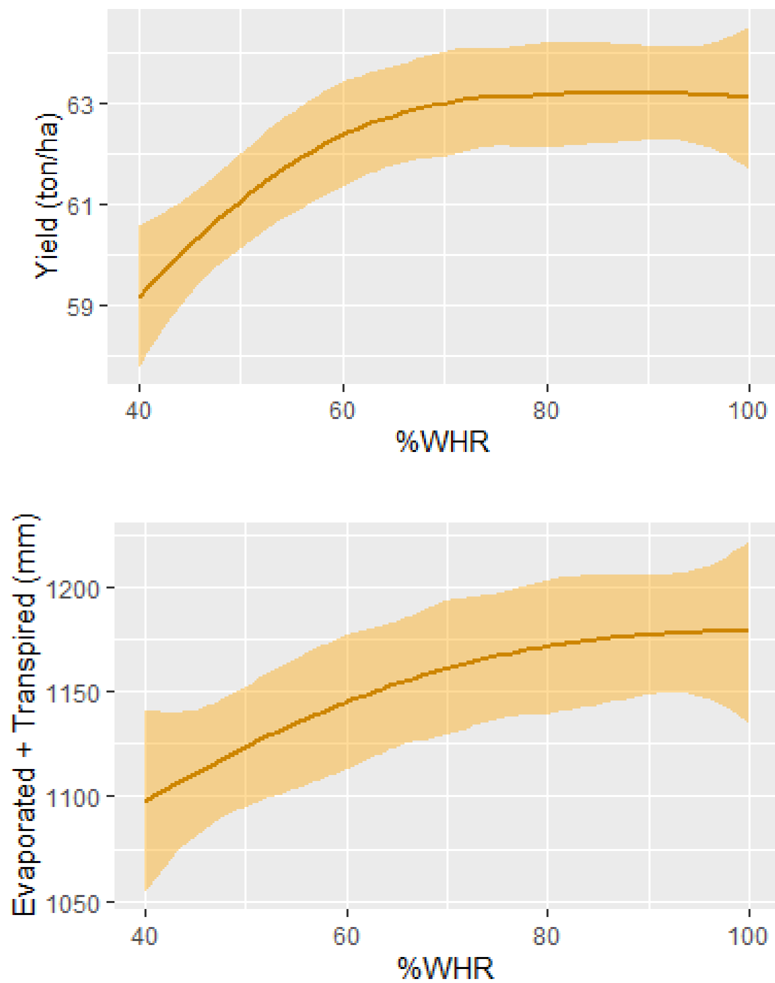

Figure 5.4. Comparison of yield (top) and water evaporated and transpired (bottom) at increasing %WHR.

The WPet is the conversion of the water used to yield, and as shown in Figure 5.4, both the yield and the amount of water used increase almost proportionally with increasing %WHR. The differences in water productivity between the different threshold are not significant. As was the case in an experiment in India in a semi-arid region with clay soils, the water productivity of sugarcane was also not significantly different between the different soil water replenishment levels applied throughout the whole season (Dingre et al., 2021).

4. Conclusion

Irrigation management scenarios were simulated for sugarcane grown along the Guyana coastal plains on heavy clay soil. In the process, the sugarcane crop file of AquaCrop was successfully calibrated with reported yields from 2005 to 2008 and validated with those from 2009 to 2012. During calibration, the simulated yield did not show high sensitivity to changes in the values of crop parameters. The most sensitive parameters are the crop coefficient and maximum canopy cover for which at most a 2% change of the RMSEn was observed. The good agreement between the simulated and the reported yields during both calibration and validation showed that AquaCrop and its sugarcane crop file can be used to reliably simulate yields when used with field-measured soil and climate data, and key crop parameters.

The current irrigation of sugarcane in Guyana, at 70% water holding capacity in the rootzone (WHR), was then assessed with other irrigation management scenarios of 40, 50, 60, 80, 90 and 100% WHR. The yield was highest at 80%WHR, but there was no significant difference in the yield distribution obtained between 50 to 100% WHR. Within the scenarios simulated, good yields of sugarcane can be obtained from the current irrigation scenario at 70%WHR. Keeping the soil-water content above 70% WHR uses more irrigation water but does not significantly increase the yield. Meanwhile, keeping between 50 to 70%WHR will reduce irrigation requirements with no significant decrease in yield during low rainfall years experiencing drought stress.

5. Acknowledgements

We would like to thank the following for providing data and information: GuySuCo, and Raffaella Maria Pilati de Carvalho and Dr. Felexce Ngwa for collecting and analyzing the soils and climate data. We acknowledge a grant from the International Development Research Centre (IDRC), Ottawa, Canada, and with the financial support of the Government of Canada provided through Global Affairs Canada, the support of the NSERC and a fellowship to the senior author by the Macdonald Stewart Foundation under the Liliane and David M. Stewart Fellowship in Water Resources.

6. References

Alvar-Beltrán, J., Heureux, A., Soldan, R., Manzanas, R., Khan, B., Dalla Marta, A., 2021. Assessing the impact of climate change on wheat and sugarcane with the AquaCrop model along the Indus River Basin, Pakistan. Agric. Water Manag. 253, 106909. https://doi.org/10.1016/j.agwat.2021.106909

Aydinsakir, K., Dinc, N., Buyuktas, D., Kocaturk, M., Ozkan, C.F., Karaca, C., 2021. Water productivity of soybeans under regulated surface and subsurface drip irrigation conditions. Irrig. Sci. 39, 773–787. https://doi.org/10.1007/s00271-021-00744-0

Bahmani, O., Eghbalian, S., 2018. Simulating the Response of Sugarcane Production to Water Deficit Irrigation Using the AquaCrop Model. Agric. Res. 7, 158–166. https://doi.org/10.1007/s40003-018-0311-0

Braun, E.G., Derting, J.F., 1964. Map for the Reconnaissance Soil Survey of Northeast British Guiana.

Briggs, L.J., Shantz, H.L., 1913. The Water Requirement of Plants. US Department of Agriculture, Washington, DC.

Cao, X., Wu, L., Lu, R., Zhu, L., Zhang, J., Jin, Q., 2021. Irrigation and fertilization management to optimize rice yield, water productivity and nitrogen recovery efficiency. Irrig. Sci. 39, 235–249. https://doi.org/10.1007/s00271-020-00700-4

Coelho, R.D., Maschio, R., Leal, D.P.V., Barbosa, F. da S., Mauri, R., 2012. Water Productivity into Biomass and Energy for 24 Brazilian Sugarcane Varieties Under Drip Irrigation, in: ASABE Paper No. 121341044. Presented at the 2012 Dallas, Texas, July 29 - August 1, 2012, ASABE, St. Joseph, MI. https://doi.org/10.13031/2013.42042

da Costa Faria Martins, S., dos Santos, M.A., Lyra, Gustavo Bastos, de Souza, J.L., Lyra, Guilherme Bastos, Teodoro, I., Ferreira, F.F., Júnior, R.A.F., dos Santos Almeida, A.C., de Souza, R.C., 2022. Actual Evapotranspiration for Sugarcane Based on Bowen Ratio-Energy Balance and Soil Water Balance Models with Optimized Crop Coefficients. Water Resour. Manag. https://doi.org/10.1007/s11269-022-03263-5

da Silva, V. de P.R., da Silva, B.B., Albuquerque, W.G., Borges, C.J.R., de Sousa, I.F., Neto, J.D., 2013. Crop coefficient, water requirements, yield and water use efficiency of sugarcane

growth in Brazil. Agric. Water Manag. 128, 102–109. https://doi.org/10.1016/j.agwat.2013.06.007
Dai, J., Li, R., Miao, Q., Li, C., Lu, Y., Hua, Z., 2022. Shallow groundwater enhances water productivity of maize in arid area. Irrig. Sci. https://doi.org/10.1007/s00271-022-00800-3
de Carvalho, R.M.P., Madramootoo, C.A., Ngwa, F., 2014. Determining Irrigation Requirements in Guyana and St Kitts using the McGill IRRIMOD© Soil Water Balance Model [WWW Document]. Margaret Gilliam Inst. Glob. Food Secur. URL https://www.mcgill.ca/globalfoodsecurity/research-initiatives/research-projects/completed-projects/caricom/outputs/abstracts (accessed 7.18.22).
Dingre, S. k., Gorantiwar, S. d., Pawar, D. d., Dahiwalkar, S. d., Nimbalkar, C. a., 2021. Sugarcane response to different soil water replenishment-based deficit irrigation treatments during different growth stages in an Indian semi-arid region*. Irrig. Drain. 70, 1155–1171. https://doi.org/10.1002/ird.2609
dos Anjos Veimrober Júnior, L.A., da Silva, A.J.P., Gheyi, H.R., do Nascimento, F.A.L., da Silva, M.G., Vellame, L.M., 2022. Water productivity of passion fruit under different forms of propagation and soil-based irrigation management criteria. Irrig. Sci. 40, 423–433. https://doi.org/10.1007/s00271-021-00766-8
DPI, 2018. GUYSUCO'S Uitvlught Estate surpasses 1st crop target. Dep. Public Inf. Guyana.
Eastwood, D., 2009. Agriculture Operations Guidelines.
Fang, J., Su, Y., 2019. Effects of Soils and Irrigation Volume on Maize Yield, Irrigation Water Productivity, and Nitrogen Uptake. Sci. Rep. 9, 7740. https://doi.org/10.1038/s41598-019-41447-z
FAO, 2012. Crop yield response to water, FAO Irrigation and Drainage Paper. FAO, Rome.
Farooq, N., Gheewala, S.H., 2020. Assessing the impact of climate change on sugarcane and adaptation actions in Pakistan. Acta Geophys. 68, 1489–1503. https://doi.org/10.1007/s11600-020-00463-8
Gaj, N., Madramootoo, C.A., 2017. Long-Term Simulations of the Hydrology for Sugarcane Fields in the Humid Tropics: Case Study on Guyana's Coastland. J. Irrig. Drain. Eng. 143, 05017002. https://doi.org/10.1061/(ASCE)IR.1943-4774.0001204
GLSC, 2013. Guyana National Land Use Plan (national plan). Guyana Lands and Surveys Commission, Guyana.
GuySuCo, 2022. Field layouts [WWW Document]. Guyana Sugarcane Corp. Inc. URL https://www.guysuco.gy/index.php?option=com_k2&view=item&id=44:field-layouts&Itemid=101&lang=en (accessed 7.13.22).
GuySuCo, 2018. Annual Report 2018 (annual report). Guyana Sugar Corporation, Georgetown, Guyana.
GuySuCo, 2013. Annual Report 2013 (annual report). Guyana Sugar Corporation, Georgetown, Guyana.
Inman-Bamber, N.G., McGlinchey, M.G., 2003. Crop coefficients and water-use estimates for sugarcane based on long-term Bowen ratio energy balance measurements. Field Crops Res. 83, 125–138. https://doi.org/10.1016/S0378-4290(03)00069-8
Kalanaki, M., Karandish, F., Afrasiab, P., Ritzema, H., Khamari, I., Tabatabai, S.M., 2022. Assessing the influence of integrating soil amendment applications with saline water irrigation on Ajwain's yield and water productivity. Irrig. Sci. 40, 71–85. https://doi.org/10.1007/s00271-021-00759-7
Lee, S.K., Dang, T.A., 2018. Application of AquaCrop model to predict sugarcane yield under the

climate change impact: A case study of Son Hoa district, Phu Yen province in Vietnam. Res. Crops 19, 310. https://doi.org/10.5958/2348-7542.2018.00047.5

Memon, M.S., Ullah, K., Siyal, A.A., Leghari, N., Tagar, A.A., Ibupoto, K.A., karim, S.T.A., Tahir, M., Memon, N., 2020. The Effect of Different Raised Bed Sizes under Furrow Irrigation Method on Salt Distribution in Soil Profile and Yield by Hydrus (2/3D). Pak. J. Agric. Res. 33. https://doi.org/10.17582/journal.pjar/2020/33.1.113.125

Naglič, B., Kechavarzi, C., Coulon, F., Pintar, M., 2014. Numerical investigation of the influence of texture, surface drip emitter discharge rate and initial soil moisture condition on wetting pattern size. Irrig. Sci. 32, 421–436. https://doi.org/10.1007/s00271-014-0439-z

Naseri, A., Boroomand-Nasab, S., Sheini-Dashtgol, A., 2020. Investigation effect of installation depths and dripper spacing on water productivity and sugarcane yield in subsurface drip irrigation. undefined.

Olivier, F.C., Singels, A., 2012. The effect of crop residue layers on evapotranspiration, growth and yield of irrigated sugarcane†. Water SA 38, 77–86. https://doi.org/10.4314/wsa.v38i1.10

Peel MC, Finlayson BL, McMahon TA (2007) Updated world map of the Koppen-Geiger climate classification. Hydrol Earth Syst Sci 11:1633–1644

Pereira, L.S., Paredes, P., Hunsaker, D.J., López-Urrea, R., Mohammadi Shad, Z., 2021. Standard single and basal crop coefficients for field crops: Updates and advances to the FAO56 crop water requirements method. Agric. Water Manag. 243, 106466. https://doi.org/10.1016/j.agwat.2020.106466

Raes, D., Steduto, P., Hsiao, T.C., Fereres, E., 2018. AquaCrop Reference Manual (version 6.0 - 6.1).

Salman, M., Garcia-Vila, M., Fereres, E., Raes, D., Steduto, P., 2021. The AquaCrop model: enhancing crop water productivity. Ten years of development, dissemination and implementation 2009-2019 (No. 47), FAO Water Report. Food and Agriculture Organization of the United Nations, Rome, Italy. https://doi.org/10.4060/cb7392en

Singh, K., Pal, R., Chalotra, N., Brar, A.S., 2022. Water Productivity of Sugarcane Influenced by Planting Techniques, Mulching and Irrigation Scheduling in Indo-Gangetic Plains of India. Sugar Tech 24, 408–418. https://doi.org/10.1007/s12355-021-01041-y

Ünlü, M., Kanber, R., Onder, S., Sezen, M., Diker, K., Ozekici, B., Oylu, M., 2007. Cotton yields under different furrow irrigation management techniques in the Southeastern Anatolia Project (GAP) area, Turkey. Irrig. Sci. 26, 35–48. https://doi.org/10.1007/s00271-007-0070-3

USACE (1998) Water Resources Assessment of Guyana. US Army Corps of Engineers, Guyana

Vaiyapuri, K., Selvakumar, S., Manivannan, V., Anbumani, S., 2019. Planting techniques in sugarcane as influenced by growth, yield and water productivity in western agro climatic zones of Tamil Nadu. undefined.

Zahra, M.B., Aftab, Z.-E.-H., Haider, M.S., 2021. Water productivity, yield and agronomic attributes of maize crop in response to varied irrigation levels and biochar–compost application. J. Sci. Food Agric. 101, 4591–4604. https://doi.org/10.1002/jsfa.11102

7. Appendix

Appendix A

Key: Cal = Calibrated parameter
M = Measured parameter
F = Field observation and information
Con = Conservative parameter
Lit = From literature
AQ = AquaCrop default

Table 5.A1. Simulation parameters used after calibration

PARAMETER	VALUE	SOURCE
Development:		
Type of planting method	transplanting	F
Canopy size of seedling	6.5 cm^2/plant	AQ
Row spacing	1.0 m	Lit
Plant spacing	0.3 m	AQ, Cal
Maximum canopy cover (CCx)	90%	AQ, Cal
Canopy decline coefficient (CDC)	7.6%/day	F
Days to recovered	22	F, Cal
Days to maximum canopy	134	F, Cal
Days to senescence	253	AQ
Days to harvest	281	F, Cal
Max effective rooting depth	0.80 m	F
Days to maximum root depth	181	F
Ave. root zone expansion	2.8 cm/day	AQ
Effect of canopy shelter in late season	60%	Con
Evapotranspiration		
Crop coefficient at CCx (Kc tr,x)	1.1	AQ, Cal
Water extraction pattern - upper 1/4 - 2nd 1/4 - 3rd 1/4 - bottom ¼	40% 30% 20% 10%	AQ
Production		
Water Productivity (WP*)	30.0 g/m2	Con
Reference Harvest Index (Hio)	35%	AQ, Cal
Response to Water Stress:		
p(upper) for canopy expansion	0.25	Con
p(lower) for canopy expansion	0.55	Con
Shape factor for canopy expansion	3	Con
p(upper) for stomatal closure (psto)	0.5	AQ, Cal
Shape factor for stomatal closure	3	Con

PARAMETER	VALUE	SOURCE
p(upper) for early senescence (psen)	0.6	Con
Shape factor for early senescence	3	Con
Aeration threshold below saturation	3%	AQ, Cal
Response to Temperature Stress		
Base temp for crop development (Tbase)	9.0 °C	Con
Upper temp for crop development (Tupper)	32.0 °C	Con
GD range from 0 degree-days to:	12.0 °C-day	Con
Response to Salinity		
Lower Ece threshold (ECEn)	2 dS/m	Con
Upper Ece threshold (ECEx)	19 dS/m	Con
Ece at 100% stress affecting canopy expansion	6.3 dS/m	Con
Ece at 100% stress affecting stomatal closure	6.3 dS/m	Con

Climate File:

Parameter	Value	Source
Rainfall	Daily, 2005 – 2012	M
Evapotranspiration (ETO)	Daily, 2005 – 2012	Com
Temperature	Daily, 2005 – 2012	M
CO2	Yearly, MaunaLoa	AQ

Irrigation File:

Parameter	Value	Source
Irrigation Method	Furrow, Irrigate to maintain %WHR	F
Water Quality	0.0 dS/m	F

Soil File:

Parameter	Value	Source
Horizons information (texture, thickness, PWP, FC, SAT)	3 horizons up to 0.45 m depth	M
Saturated hydraulic conductivity (Ksat)	35.0 mm/day	AQ
Curve Number (CN)	77	AQ, Cal

Field Management:

Parameter	Value	Source
Soil cover by mulches	None, 0%	F

Parameter	Value	Source
Weed cover	6%	F, Cal
Effect on CN by field practice (poor hydrologic condition, straight furrows)	+10%	F, Cal

Simulation parameters

Parameter	Value	Source
Planting Search Window	Nov	F, Cal
Initial soil Water	At Saturation	F
Initial soil salinity	0.02 dS/m	F
Initial canopy cover (CCo)	0%	AQ
Initial Biomass	0 ton cane/ha	AQ
Initial root depth	0.30 m	AQ

BRIDGING TEXT

The abandonment of sugarcane farms is driving the diversification to higher-value cropping systems. Chapter IV and Chapter V simulated the irrigation water requirement of rice and sugarcane. With the vegetable industry's projected expansion and prioritization, its share of water use will grow. It is necessary to obtain information on the water requirement of several vegetables. Chapter VI discusses the crop water productivity scenarios which lead to minimal yield reduction.

This study is in preparation for submission to *Irrigation & Drainage Systems Engineering*. The paper is co-authored by Guia Marie M. Mortel and Dr. Chandra Madramootoo. The contributions of each author are mentioned on page 7.

CHAPTER VI

Development of irrigation water strategies to intensify vegetable production

Abstract

Guyana aims to reinvigorate its agriculture sector by diversifying to higher value vegetable crops. Apart from ensuring food security, this also reduces the country's food import bill. Abandoned sugarcane farmlands are targeted for intensification and expansion of vegetable production. The diversification initiative comes with investments for the establishment of new farms, restoration of canals, the establishment of new water control structures and re-evaluation of the irrigation and drainage design. This study seeks to identify water-efficient irrigation scenarios and determine the irrigation requirements of vegetable farms located along the coastal lands. Field-measured soil and climate data were obtained from 2005 to 2012 and used in the AquaCrop model alongside local crop and management data of cabbage (*Brassica oleracea var. capitata*), cassava (*Manihot esculenta*), eggplant (*Solanum melongena*), hot pepper (*Capsicum frutescens*), tomato (*Solanum lycopersicum*) and bora or yardlong bean (*Vigna unguiculata*). Seven scenarios of varying irrigation thresholds (40, 50, 60, 70, 80, 90 and 100% water holding content at the rootzone [WHR]) were tested in a deficit irrigation management. Results show that at 40, 50 and 60% WHR, a decreasing irrigation requirement but no significant reduction in yield (pairwise t-test, $p > 0.05$) were observed. The water savings can be used to irrigate potential production areas, thereby assisting in the expansion of the vegetable industry. The choice of planting season does not affect the yield (ANOVA, $p > 0.05$).

1. Introduction

1.1. Crop diversification

The shift of priorities towards vegetable production came with the Agriculture Export

Diversification Program (AEDP) which was designed to promote the production and export of non-traditional crops. Activities planned or done under the crop diversification initiative include the increased support for existing non-traditional crops; the establishment of farms, the introduction of new varieties; and the introduction of new crops. The diversification program initially focused on the 4Ps (pepper, plantain, pineapple and pumpkin) and 4Cs (coconut, citrus, cassava and carrots) (Ministry of Agriculture 2013). Soybean and corn have also been given importance for their use as protein sources in the poultry industry. Meanwhile, coconut, mango, pumpkin, watermelon, pineapple, and pepper lead the top non-traditional agricultural exports (Ministry of Agriculture 2013; NAREI 2021).

Irrigation and drainage are necessary to manage the poor internal drainage of Guyana's coastal soils, however, for the 1.7 million hectares of agricultural land, only 0.2 million hectares have adequate drainage and irrigation (Ministry of Agriculture 2013). To improve the productivity of vegetable crops and increase the area cultivated, the diversification program is complemented by increased investments in the I&D system to restore canals in abandoned areas and train farmers in the maintenance and rehabilitation of structures (GLSC 2013).

This paper seeks to contribute to the effort on diversification and improvement of Guyana's water resources management by providing the irrigation requirements of several vegetables for several recommended irrigation scenarios. Specifically, we want to identify factors which influence yield (irrigation thresholds, and planting season); understand the representativeness of the simulations to other coastal farmland areas of Guyana; examine the potential of the vegetables to achieve maximum yield, and recommend an irrigation scenario for efficient use of water. .

1.2. The AquaCrop model

This study uses the AquaCrop model to simulate crop growth. It is a water-driven model wherein yield is a function of the evapotranspiration and availability of water. Computation of the crop evapotranspiration are conducted first using the FAO-Penman Monteith. Modules on root growth and soil-water movement simulate the available soil water for uptake. Parameters characterizing the soil, climate, crop, water quality, and field management practices are used to ultimately simulate the yield. Stresses are not computed in detail but instead AquaCrop relies on indicator parameters to determine the intensity of stress. Details of the model's structure and formulae are discussed in the FAO Irrigation and Drainage Paper #66 (Steduto et al. 2012).

AquaCrop has been designed for a wide range of practitioners and thus aims to minimize complexity in the crop parameters required and the use of the software. Apart from the 15 crop files in the system, it provides a crop template for fruit/grain-producing crops, leafy vegetable crops, and root and tuber crops. Within 10 years after its release, AquaCrop has been implemented in 46 different crops (Salman et al. 2021). Apart from development and evaluation studies (i.e., calibration and validation), it has often been used in application studies such as agronomic management, environmental changes assessment and policy (Salman et al. 2021). AquaCrop has also been used in Guyana for the crop suitability study in Region 3 and Region 9, under climate scenarios RCP 4.5 and RCP 8.5 (Navarette-Frias et al. 2021).

2. Materials and Methods

2.1. Data input

2.1.1. Location, soil and climate

The study covers Parika, Guyana which is a town situated at the outlet of the Essequibo River, in the northern portion of Guyana's coastal farmlands. It is a part of administrative Region 3 and is a main port along the Essequibo River (GLSC 2013). The presence of the port drives the trade of several goods at the local market. It is also this trading which has assisted in increasing the production of vegetables at farms in and around the town. The agricultural area expanse, known as ‘Parika Back’, starts at approximately 5 km from the settlement areas and extends 6 to 8 km inwards to the Boerasirie Conservancy (Central Housing & Planning Authority [CHPA] 2006).

The soil in Parika is silty clay with a sand-silt-clay percentage of 1% - 53% - 46%. Its properties were identified by sampling 2 sites in Parika with 2 samples taken at each site at 0 - 15, 15 - 30, and 30 – 45 cm depth. The soil is acidic with a pH averaging at 4. For the 3 depth horizons, the moisture content at field capacity (FC) ranges between 43 to 48%, and between 38 to 43% for the moisture content at the permanent wilting point (PWP). This gives total available water (TAW) of approximately 49 mm per meter of soil.

The climate information, meanwhile, was gathered from an automatic weather station located at 6.84° N, -58.4° W. The daily rainfall, minimum and maximum temperature, wind velocity at 2 m and sunshine hours duration were obtained from 2005 to 2012. The climate at Parika follows the general climate of the coastal plains of Guyana. It is characterized by high rainfall throughout the year, and almost constant minimum and maximum temperatures. The rainiest months, as shown in Figure 6.1, occur from May to July, and December to January. The start of the two rainy seasons signals the two planting seasons in Guyana: April to May and November to December. These two rainy seasons are also when the rainfall shows the most variability with as high as 400mm/month difference from the average. The reference evapotranspiration (ETo) was calculated in AquaCrop using the Penman-Monteith and the climate data provided. The ETo is less than the rainfall for most of the year except in September when the ETo is higher than the monthly rainfall. It is consistent across the year averaging at 127 mm/month. Throughout the simulation period, it was observed to vary between 85 to 164 mm/month.

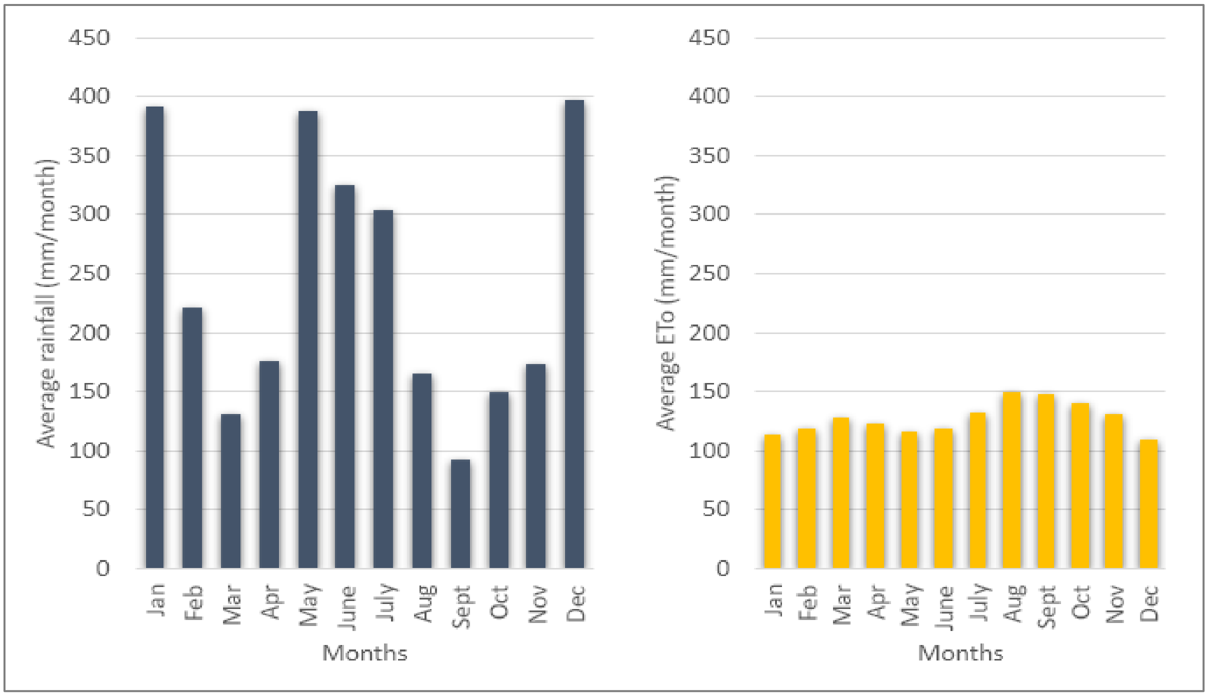

Figure 6.1. Average monthly rainfall and reference evapotranspiration (ETo) at the study site (Parika, Guyana) from 2005 to 2012.

The Boerasirie Conservancy provides freshwater to Parika. However, the irrigation water at Parika is slightly more brackish because of the gradual mixing of fresh and seawater at the outlet, tidal influence, salt-water intrusion, and salinity of some patches of soil (USACE 1998).

2.1.2. Vegetables

The vegetables focused on for the simulations were cassava (*Manihot esculenta*), eggplant (*Solanum melongena*), yardlong or bora bean (*Vigna unguiculata*), cabbage (*Brassica oleracea var. capitata*), tomato (*Solanum lycopersicum*), and hot pepper (*Capsicum frutescens*). These vegetables were selected because of their part in the government's diversification program, their suitability to the present and future climate of Guyana, and the role they play in Guyana's top exports, as discussed in Section 1. Among these crops, only tomato has a crop file in AquaCrop.

The rest did not have their crop files, as such, AquaCrop's templates were used as the base file. These crops, however, had substantial research of their crop parameters as used in AquaCrop. The parameters identified in these studies were noted and used in their respective crop files. As much as possible, only studies done in areas having the same climate, latitude or crop variety as coastal Guyana are included. Lastly, local information on the variety and management of these vegetables was obtained, and these were also incorporated in the final crop files. Table 6.1 lists the secondary sources of crop parameter data for each vegetable. The complete list of crop parameters used is shown in Table 6.A1.

Table 6.1. Secondary sources of crop parameter data.

Crop	Source	Location of Experiment
All crops	National Agricultural Research and Extension Institute (NAREI)	Guyana
	Updated standards for vegetables by Pereira et al. (2021)	Various locations
	AquaCrop Reference Manual by Raes et al. (2018)	Various locations
	FAO Irrigation and Drainage Paper by Steduto et al. (2012)	Various locations
Tomatoes (*S. lycopersicum* 'Heatmaster')	Tomato crop file by FAO (2018)	Various locations
	Uzun (2006)	Laboratory
Eggplant (*S. melongena*)	Carvalho et al. (2012)	Seropédica-RJ, Brazil
	Uzun (2006)	Laboratory
	Shabetya et al. (n.d.)	Laboratory
	Paula et al. (2003)	Laboratory
Hot Pepper (*C. frutescens* var. *Maiwiri)*	Miranda et al. (2006)	Ceara, Brazil
	Adegoke et al. (1996)	Ibadan, Nigeria
Bora Bean	Cavalcante Jr. et al. (2016)	Grande do Note, Brazil

Crop	Source	Location of Experiment
(*V. unguiculata* subsp. *sesquipedalis*)	Miranda and Campelo Jr. (2010)	Rondonia, Brazil
	Ofori and Klogo (2005)	Legon, Ghana
Cabbage (*B. oleracea* var. *capitata*)	Zhang et al. (2021)	Wellesbourne, UK
	Tayyeb et al. (2017)	Laboratory
Cassava (*M. esculenta*)	Wellens et al. (2022)	Colombia, Togo, Nigeria
	Maraphum et al. (2021)	Laboratory

The AquaCrop model version 7.0 (FAO 2018) was used. The input files for the climate, crop, soil, management and simulation parameters were prepared. Calibration and validation were not done as there were no available recorded data on the yield of the vegetables at the regional scale from 2005 to 2012.

2.2. Irrigation management scenarios

The growth of the vegetables was simulated for varying thresholds of water-holding capacity (WHR). The WHR is the total amount of water held in the root zone between the field capacity and the permanent wilting point. AquaCrop takes another unit of measure of soil-water content, the readily available water (RAW), as an input. The relationship between WHR and RAW is shown in Figure 6.2 (a-d). The RAW is a part of the WHR that is easily accessible to plants. The accessibility of this water is defined by the psto, which is a threshold of soil water depletion (Dr). The Dr is the inverse of the WHR such that when Dr is equal to 0, there is no water depletion and WHR is equal to 100%. Meanwhile, when Dr is equal to 1, the soil-water is fully depleted and the WHR is 0%. When the water depletion is below the psto value, water is accessible, while above psto, water is more difficult to extract, even if the moisture content is still above PWP.

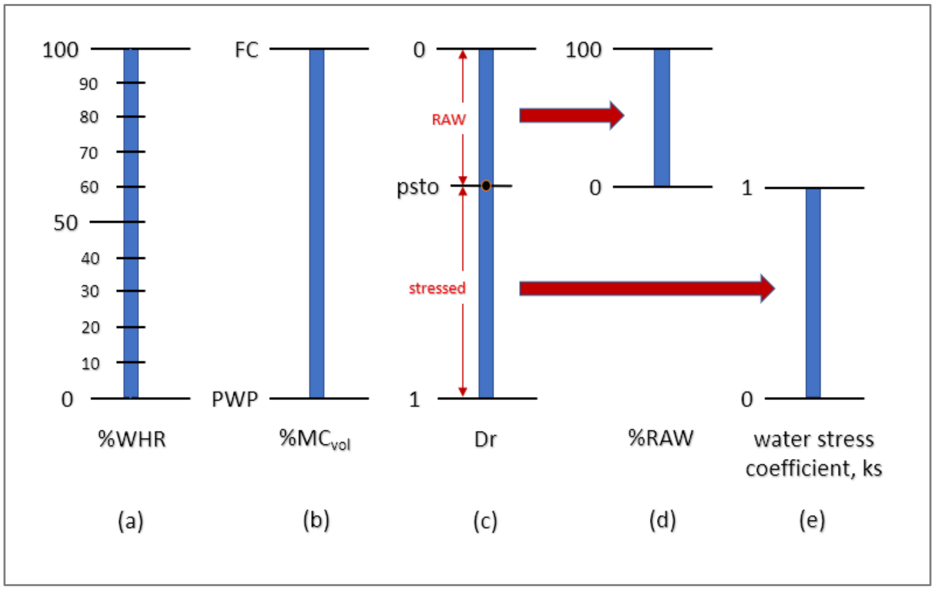

* a = water holding content at the rootzone, b = moisture content by volume, c = Dr, fraction of water depletion at the rootzone, psto = threshold of Dr, d = readily available water, e = water stress coefficient

Figure 6.2. Relationship between units of measure* of soil water content.

The value of psto is specific to the crop, with drought-resilient crops having a higher psto value than the others. Among the vegetables in this study, cassava has the highest value, and hot pepper has the lowest. The psto is used in Equation 1 to convert the %WHR to the RAW input required by AquaCrop. For consistency, the %WHR is used to represent soil-water content throughout this paper.

$$RAW\ depletion = \ (1 - WHR)/psto \qquad \text{(Eq. 1)}$$

The irrigation scenarios were designed such that irrigation is triggered once the threshold %WHR is reached. Then, an irrigation amount was applied to return the soil-water content to 100%WHR, or field capacity. There were 7 thresholds used: 40%, 50%, 60%, 70%, 80%, 90% and 100% WHR.

An ANOVA was conducted to test the dependency of yield on the varying scenarios used, planting season, and crops planted. To determine if the yield response is replicable or representative of other farm sites in coastal Guyana, simulations were also replicated in Black Bush Polder, another coastal agricultural area at 6°4'58" N, 57°15'57" W. The Black Bush Polder study site is characterized by a tropical rainforest climate and clayey soils.

The crop growth simulations were done using the AquaCrop software (FAO 2018). The R language (R Core Team 2022) was used for statistical analysis (ANOVA and t-test).

3. Results and Discussion

3.1. Irrigation management scenario simulation

The yield was simulated for the 6 vegetables for 8 years and 2 planting seasons. While we are focused on the impact of the varying irrigation thresholds on yield, we also want to identify if other conditions, such as the planting season and location are important factors. A one-way ANOVA was conducted for the two planting season groups, and the results show that the yields obtained are not significantly different from each other (at a = 0.05). Since the two planting times coincide with the two wet seasons, almost the same amount of rainfall is provided for a whole crop season, as shown in Table 6.2. Both planting seasons provide a good opportunity to get good yields.

Table 6.2. Comparison of the two planting seasons based on the total rainfall received (mm) through a whole crop growing period

Planting Season	Average Total Rainfall Received (mm/ cropping season)
Season 1 (Apr. to May planting)	1 509
Season 2 (Nov. to Dec. planting)	1 673

To study the impact of location on the yield, simulations were also done for 2005 – 2012 using the soil and climate dataset of Black Bush Polder, Guyana. The ANOVA result has shown that the yields obtained between Black Bush Polder and Parika were significantly different (at a = 0.05). Notably, the whole of coastal Guyana can be generalized as having a wet tropical rainforest climate and front land clay soils. Yet, the location-specific differences between Parika and Black Bush Polder in terms of the rainfall patterns, water quality and the different soil texture and layer characteristics have impacts on the location's potential yield.

The rainfall pattern at BBP and Parika both fall under wet tropical climate under the Koppen-Geiger classification (Peel, Finlayson, and McMahon 2007). The more detailed climate map by the Hydromet Department of Guyana (GLSC 2013) classifies the two under different precipitation regimes: very wet for Parika, and moist for BBP. The difference in monthly rainfall between the two locations are shown in Figure 6.3. For the 8 years of observation data gathered, the average yearly rainfall for Parika is at 2,912 mm and for BBP, it is 2,147 mm.

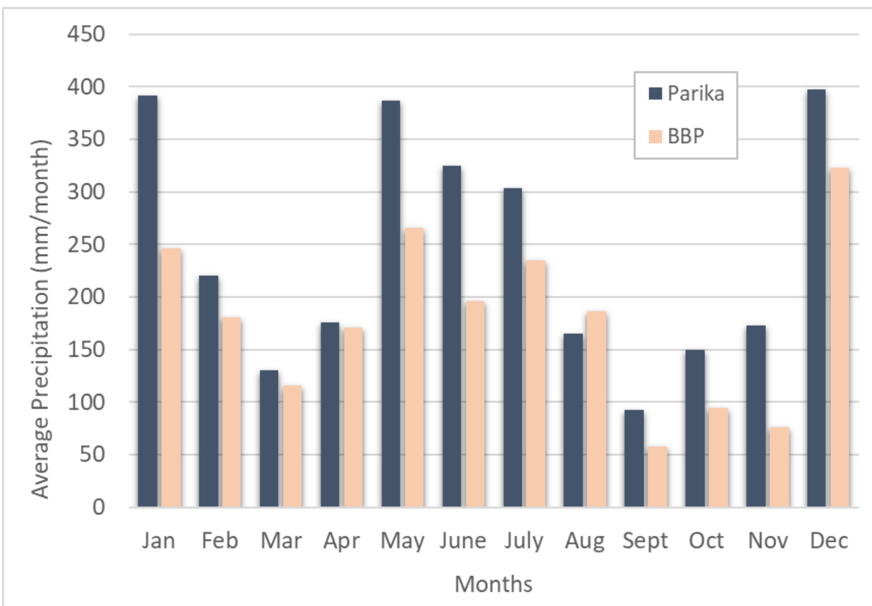

Figure 6.3. Average monthly precipitation (mm) at Parika and Black Bush Polder.

The soils of the two locations also are classified as hydraquents or marine phase 'frontland clay' (Braun and Derting 1964). There are differences between the two locations. As shown by the soil series mapping (Steele 1966; GLSC 2004), the soil in BBP is categorized under the drained phase Corentyne clay while the soil in Parika falls under Brickery clay. Further examination of the samples obtained at the two locations shows a difference between their moisture retention curves

(Figure 6.4). The field capacity is reached by the BBP soils at a higher moisture content than the Parika soils, but the moisture content at PWP is higher for Parika than for BBP. This shows a lower water holding capacity of Parika soils because of the smaller gap between its FC and PWP, as compared to the BBP soil. This is consistent with the characteristics of clayey soils for the BBP, and the silty clayey soil at Parika. These difference affects both locations available soil-water and water balance computations.

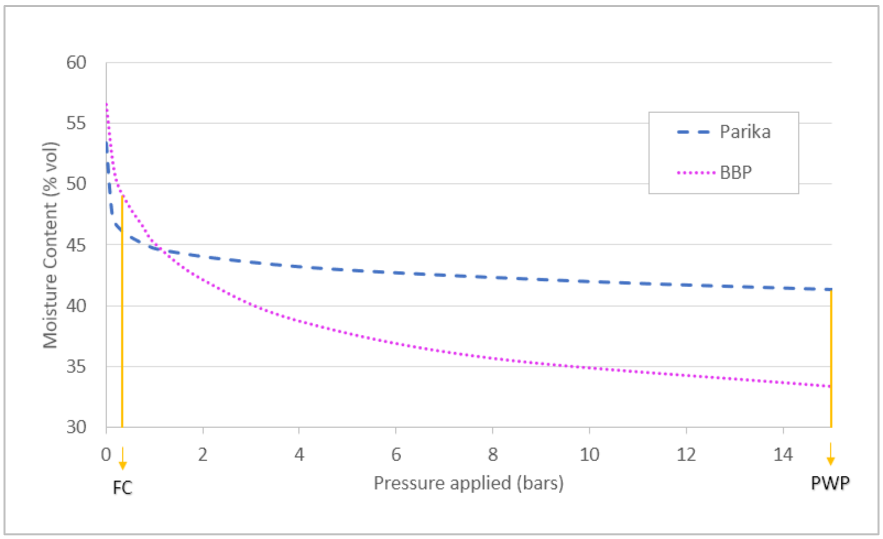

Figure 6.4. Soil moisture retention curves of soil samples from Parika and BBP.

The significant difference in yield between the two locations highlights the importance of location-specific data for crop simulations, especially soil and climate data. For a regional or town scale of analysis, such as was done in this paper, the results of crop simulations could not be generalized over broad climate and soil classifications. More detailed classification systems such as the soil series, and national climatic regimes are better alternatives to expand the results of a simulation to nearby locations.

3.2. Response of vegetable growth and yield to the irrigation scenarios

The capacity of the vegetables to reach their potential production can be expressed by the relative biomass (Brelative). The Brelative is the percentage of aboveground biomass relative to the biomass which can be produced if stresses are absent (Raes et al. 2018). The Brelative for the vegetables for all irrigation scenarios range mostly between 75 to 100% (Figure 6.5). This confirms that values near the potential can be obtained in Parika even with the crop stresses which can be experienced at this site.

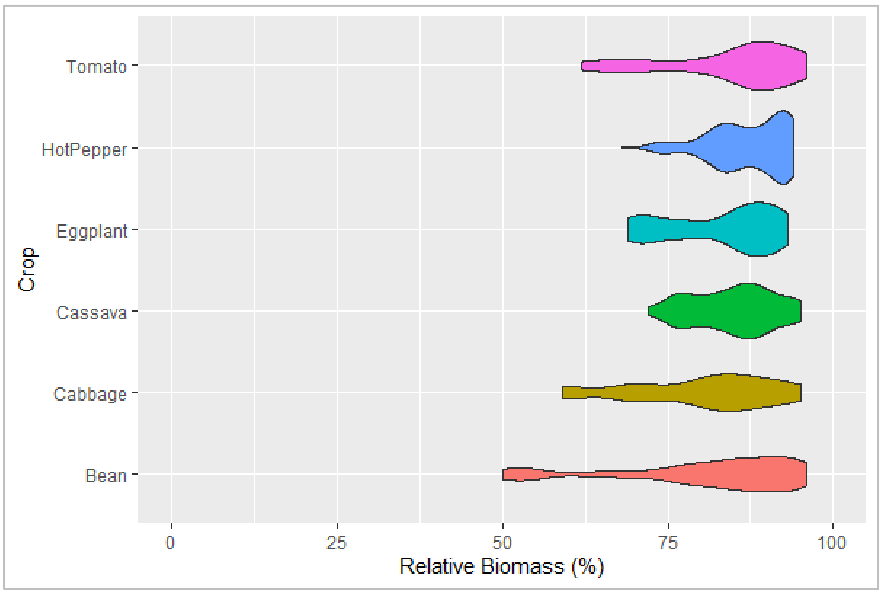

Figure 6.5. Predicted biomass production relative to potential biomass (%) of vegetables crops grown in Parika, Guyana for various irrigation scenarios.

The harvest index partitions the biomass into its harvestable component, the yield. A one-way ANOVA found no significant difference (at a = 0.05) between the yields obtained from the different irrigation scenarios for each vegetable. Figure 6.6 shows the relationship between the simulated yield for the different scenarios. There are instances that with a decreasing %WHR, the yield also decreased such as for hot pepper and tomato or increased as observed in cassava and bora bean. A pairwise t-test was done to check if these variations in the yields were significant. The yields of all scenarios were compared to the yields obtained at 90% WHR. The 90%WHR was chosen as it reflects more the current irrigation management as compared to the 100%WHR wherein the fields are always kept at field capacity (100% WHR). The t-test (in Table 6.3) confirms that differences in yield were indeed minimal and insignificant. This indicates that lower %WHR thresholds can be used to trigger irrigation without suffering any major reduction in yield.

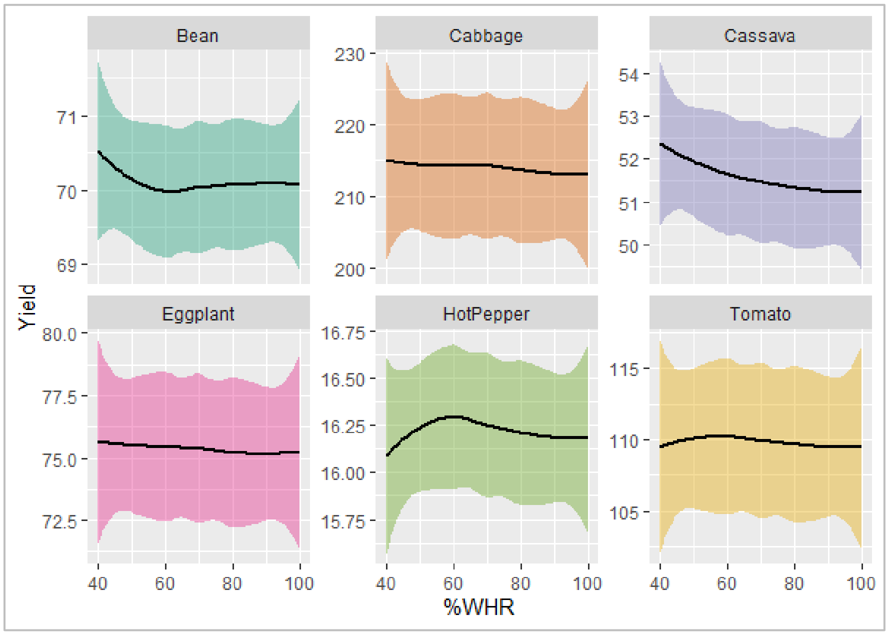

Figure 6.6. Yield of various vegetables at varying %WHR at Parika, Guyana

Table 6.3. P-values of the pairwise t-test of yield relative to yield at 90% for vegetable farming in Parika.

Crop	**P-values of pairwise t-test**						
Irrigation scenario (% WHR)	**100**	**90**	**80**	**70**	**60**	**50**	**40**
Cabbage	0.99	REF	0.99	0.85	0.95	0.91	0.84
Cassava	0.99	REF	0.97	0.84	0.81	0.62	0.44
Eggplant	0.99	REF	0.98	0.94	0.93	0.96	0.87
Hot Pepper	0.99	REF	0.99	0.82	0.85	0.78	0.78
Tomato	0.99	REF	0.98	0.90	0.93	0.86	1.00
Bora Bean	0.98	REF	0.96	0.95	0.97	0.98	0.59
Significant difference in yield (at a <0.05)	No	REF	No	No	No	No	No

The low %WHR scenarios, such as the 40%, 50% and 60% WHR, seem to be viable due to the frequency and amount of its rainfall. As shown in Figure 6.7, the average rainfall received by each crop throughout its whole growing cycle is more than the crop water requirement (transpiration and evaporation). Even the driest years, shown by the error bars, are still sufficient. There were instances of dry days when the available water in the soil has to be supplemented with irrigation. In the 90%WHR scenario, the irrigation supplies only 30 to 49% of the crops' water requirement. This small contribution to the crops' requirement makes it possible for low %WHR scenarios, such as the 40%, 50% and 60% WHR, to have minimal impact on the yield. Moreover, even with the low %WHR thresholds, frequent rains replenish the soil, and the threshold would be rarely reached.

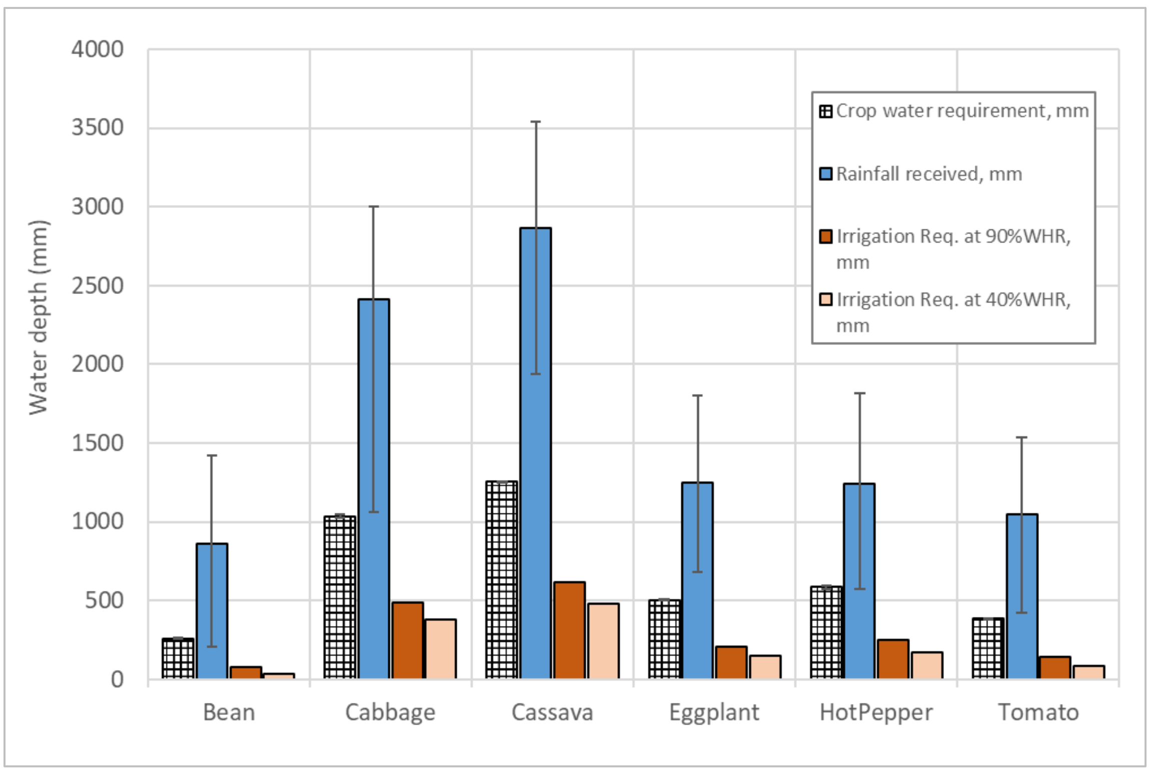

Figure 6.7. Comparison of crop water requirement (mm), rainfall received throughout a growing season (mm), and irrigation water requirement (mm) of the 90% and 40%WHR scenarios for various vegetables at Parika

The low %WHR scenarios require less irrigation water within one whole crop cycle, as shown in Table 6.4. The irrigation requirements include losses from soil evaporation, runoff and deep percolation. An allowance must be added to cover losses not included in the simulation such as lateral seepage and conveyance losses. A 1 ha field using the 60%WHR will require 20 to 50% less irrigation than 90%WHR. The water savings can be used for the irrigation of another field. As such, for the same amount of irrigation, a larger area can be irrigated.

Table 6.4. The average irrigation requirement (in m^3) * for one hectare of a vegetable farm using different irrigation scenarios.

Crop	Total irrigation requirement (in m^3) of 1-hectare plot							Crop cycle (months)
Irrigation scenario (% WHR)	**100**	**90**	**80**	**70**	**60**	**50**	**40**	-
Cabbage	4,890	4,860	4,710	4,490	4,260	4,060	3,830	9.0
Cassava	6,290	6,150	5,790	5,450	5,190	4,920	4,780	12.0
Eggplant	2,150	2,090	1,950	1,780	1,650	1,610	1,500	4.5
Hot Pepper	2,600	2,520	2,320	2,150	2,010	1,890	1,730	4.7
Tomato	1,450	1,390	1,270	1,140	1,050	930	860	3.4
Bean	810	770	690	590	580	480	350	2.5

* The irrigation requirement considers losses from soil evaporation, runoff and deep percolation.

4. Conclusion

This study sought to provide the irrigation requirements of several vegetable crops grown in the coastal farmlands of Guyana. The dataset from 2005 to 2012 obtained at Parika was used to simulate the growth of cabbage, cassava, eggplant, hot pepper, tomato and bora or yardlong bean. In the process of predicting the irrigation requirements, factors affecting the yield of vegetables were explored, and the following key findings were found:

a. ***The 40%, 50% and 60% WHR are recommended to be used as thresholds of deficit irrigation.*** There was no significant difference between the yields obtained from the irrigation scenarios (40, 50, 60, 70, 80, 90 and 100%WHR). The low %WHR scenarios

(40, 50 and 60%WHR) seem to be favourable because of the area's frequent and moderate to high amount of rainfall. The irrigation requirement of these three scenarios ranges from 140 to 473 m^3 per hectare per month, inclusive of soil evaporation, run-off and deep percolation losses.

b. ***No significant difference between the two planting seasons.*** The yields which can be obtained from the two planting seasons in Guyana are not significantly different from each other because of the equally high rainfall received for both planting seasons.

c. ***A significant difference between two coastal farmland sites.*** When the simulated yield at Parika was compared with the results of simulations at Black Bush Polder, Guyana, notable differences were found. Even with the similar soil type and climate of both Parika and Black Bush Polder, the different environments at the two sites affected the yield. The results show that care must be observed when generalizing or expanding the scope of crop simulation results to other areas. It also highlights the importance of measuring climate and soil data in the study site for crop simulations.

d. An irrigation deficit strategy can be used to efficiently use water while getting high yields. The water saved can be used to expand the production area, cultivate abandoned farmlands, and aid in intensifying vegetable production in Guyana.

5. Limitations & Recommendations for Future Studies

This study is an application of AquaCrop and does not seek to develop calibrated and validated crop parameters. We recommend a field experiment of the 40, 50 or 60%WHR irrigation scenarios in Parika, Guyana. The hypothesis of its suitability in Guyana can be tested out through field experiments on cassava, bora bean, and hot pepper, which are the crops with the lowest p-values in the pairwise t-test. It is also good to consider one crop for the three crop types in

AquaCrop: leafy vegetable, fruit-producing crop (i.e. tomato, hot pepper, beans), and root or tuber crop. The timing of irrigation deficit with the crop stage can be explored. Research should also be conducted to evaluate other irrigation methods in coastal Guyana such as sprinkler irrigation, drip irrigation, alternate-furrow, fixed-furrow irrigation as was done by Abera et al. (2020) for onion production in Ethiopia.

The comparison of simulations at BBP and Parika show that broad classifications could not be used to define similar zones for simulation. A simulation can be done for a location having the same soil series and climate regime as Parika to note if statistical difference is present for this more detailed classification.

6. Acknowledgements

We would like to thank the following for providing data and information: NAREI, and Larissa Jarvis and Raffaella M. P. de Carvalho for collecting and analyzing the soils and climate data. We acknowledge a grant from the International Development Research Centre (IDRC), Ottawa, Canada, and with the financial support of the Government of Canada provided through Global Affairs Canada, the support of the NSERC and a fellowship to the senior author by the Macdonald Stewart Foundation under the Liliane and David M. Stewart Fellowship in Water Resources.

7. Conflict of Interest

The authors declare and confirm no known personal associations or relationships that might create a conflict of interest or influence the work reported in this paper.

8. References

Abera, Messay, Aemro Wale, Yalelet Abie, and Tilahun Esubalew. 2020. "Verification of the Efficiency of Alternate Furrow Irrigation on Amount of Water Productivity and Yield of Onion at Sekota Woreda." *Irrigation & Drainage Systems Engineering* 9 (4).

https://doi.org/10.37421/idse.2020.9.248.

Adegoke, G.O., A.E. Allamu, J.O. Akingbala, and A.O. Akanni. 1996. “Influence of Sundrying on the Chemical Composition, Aflatoxin Content and Fungal Counts of Two Pepper Varieties - Capsicum Annum and Capsicum Frutescens.” *Plant Foods for Human Nutrition* 49 (February): 113–17. https://doi.org/10.1007/BF01091967.

Braun, E.G, and J.F. Derting. 1964. “Map for the Reconnaissance Soil Survey of Northeast British Guiana.” Soil map. Rome, Italy: Food and Agriculture Organization of the United Nations. https://esdac.jrc.ec.europa.eu/content/map-reconnaissance-soil-survey-northeast-british-guiana.

Bubbico, Antonio, Michael Keller, and Cristian Morales Opazo. 2020. *Perspectives on Diversification Prospects for the Agrifood Industry in Guyana*. FAO Agricultural Development Economics Technical Study 6. Rome, Italy: Food and Agriculture Organization of the United Nations. https://doi.org/10.4060/ca9754en.

Carvalho, Daniel F. de, Marcio E. de Lima, Alexsandra D. de Oliveira, Hermes S. da Rocha, and José G. M. Guerra. 2012. “Crop Coefficient and Water Consumption of Eggplant in No-Tillage System and Conventional Soil Preparation.” *Engenharia Agrícola* 32 (4): 784–93. https://doi.org/10.1590/S0100-69162012000400018.

Cavalcante Jr., Edmilson G., José F. de Medeiros, José Espínola Sobrinho, Vladimir B. Figueirêdo, João P. N. da Costa, and Wesley de O. Santos. 2016. “Development and Water Requirements of Cowpea under Climate Change Conditions in the Brazilian Semi-Arid Region.” *Revista Brasileira de Engenharia Agrícola e Ambiental* 20 (9): 783–88. https://doi.org/10.1590/1807-1929/agriambi.v20n9p783-788.

CHPA. 2006. “Parika Development Plan 2006 - 2016.” Central Housing & Planning Authority. http://guyana2030.com/wp-content/uploads/2015/03/PARIKA-DEVELOPMENT-PLAN.pdf.

FAO. 2018. “AquaCrop (Software).” Windows. Rome, Italy: Food and Agriculture Organization of the United Nations. https://www.fao.org/aquacrop/software/aquacropstandardwindowsprogramme/en/.

GLSC. 2004. “Region VI Sub-Regional Land Use Plan.” Soil map. Georgetown, Guyana: Guyana Lands & Surveys Commission. https://www.forestcarbonpartnership.org/system/files/documents/Guyana_Region_VI_Sub-Regional_Land_Use_Plan_0.pdf.

GLSC. 2013. “Guyana National Land Use Plan.” National plan. Georgetown, Guyana: Guyana Lands and Surveys Commission. https://glsc.gov.gy/wp-content/uploads/2017/05/Summary-Booklet-of-the-National-Land-Use-Plan.pdf.

Maraphum, Kanvisit, Khwantri Saengprachatanarug, Seree Wongpichet, Arthit Phuphuphud, Panmanas Sirisomboon, and Jetsada Posom. 2021. “Modified Specific Gravity Method for Estimation of Starch Content and Dry Matter in Cassava.” *Heliyon* 7 (7): e07450. https://doi.org/10.1016/j.heliyon.2021.e07450.

Ministry of Agriculture. 2013. “A National Strategy for Agriculture in Guyana 2013 - 2020.” Ministry of Agriculture, Guyana. https://caricom.org/documents/11264-moa_agriculture_strategy_2013-2020_-_cd.pdf.

Miranda, F.R., R.S. Gondim, and C.A.G. Costa. 2006. “Evapotranspiration and Crop Coefficients for Tabasco Pepper (Capsicum Frutescens L.).” *Agricultural Water Management* 82 (1–2): 237–46. https://doi.org/10.1016/j.agwat.2005.07.024.

Miranda, Marcelo Notti, and José Holanda Campelo Jr. 2010. “Soma térmica para o subperíodo semeadura-maturação de feijão cv. carioca em Colorado do Oeste, Rondônia." *Pesquisa Agropecuária Tropical* 40 (2): 180–85. https://revistas.ufg.br/pat/article/view/6790.

NAREI. 2021. "Guyana Records 9% Increase in Export of Non-Traditional Agricultural Commodities in 2020." Government. National Agricultural Research and Extension Institute. February 2, 2021. https://narei.org.gy/guyana-records-9-increase-in-export-of-non-traditional-agricultural-commodities-in-2020/.

Navarette-Frias, Carolina, Miguel Lizarazo, Anton Eitzinger, Caroline Mwongera, Danny Sandoval, Judith Rosales, Pauline Bullen, Louisa Daggers, Dina Benn, and Satesh Nanlall. 2021. "Climate-Smart Agriculture Investment Portfolios in Guyana: A Way Forward." Alliance of Biodiversity International and CIAT. https://hdl.handle.net/10568/114178.

Ofori, K., and P.Y. Klogo. 2005. "Optimum Time for Harvesting Yardlong Bean (Vigna Sesquipedalis) for High Yield and Quality of Pods and Seeds." *Journal of Agriculture & Social Sciences* 1 (2): 86–88. https://www.fspublishers.org/published_papers/63552_..pdf.

Paula, V.A. de, M.R. Schuck, G. Duarte, A. Deibler, C. Aldrighi, A.V. da Costa, and M.G. Mendez. 2003. "Evapotranspiração Máxima e Coeficiente de Cultura Da Berinjela Em Ambiente Protegido." In . Pelotas.

Peel, M C, B L Finlayson, and T A McMahon. 2007. "Updated World Map of the Koppen-Geiger Climate Classification." *Hydrology and Earth System Sciences* 11: 1633–44. www.hydrol-earth-syst-sci.net/11/1633/2007/.

Pereira, L.S., P. Paredes, R. López-Urrea, D.J. Hunsaker, M. Mota, and Z. Mohammadi Shad. 2021. "Standard Single and Basal Crop Coefficients for Vegetable Crops, an Update of FAO56 Crop Water Requirements Approach." *Agricultural Water Management* 243 (January): 106196. https://doi.org/10.1016/j.agwat.2020.106196.

R Core Team. 2022. "R: A Language and Environment for Statistical Computing." Vienna, Austria: R Foundation for Statistical Computing. https://www.R-project.org/.

Raes, Dirk, Pasquale Steduto, Theodore C. Hsiao, and Elias Fereres. 2018. "AquaCrop Reference Manual (Version 6.0 - 6.1)." Food and Agriculture Organization of the United Nations. https://www.fao.org/aquacrop/resources/referencemanuals/en/.

Salman, Maher, Margarita Garcia-Vila, Elias Fereres, Dirk Raes, and Pasquale Steduto. 2021. "The AquaCrop Model: Enhancing Crop Water Productivity. Ten Years of Development, Dissemination and Implementation 2009-2019." 47. FAO Water Report. Rome, Italy: Food and Agriculture Organization of the United Nations. https://doi.org/10.4060/cb7392en.

Shabetya, O.N., N.V. Kotsareva, A.M. Nasser, A G Katskaya, and A.A.H. Al-Maidi. 2020. "Biochemical Composition of Eggplant and Its Change during Storage." *Plant Archives* 20 (Supplement 2): 385–88. http://www.plantarchives.org/SPL%20ISSUE%2020-2/64__385-388_.pdf.

Steduto, Pasquale, Theodore C. Hsiao, Elias Fereres, and Dirk Raes. 2012. *Crop Yield Response to Water*. FAO Irrigation and Drainage Paper 66. Food and Agriculture Organization of the United Nations. https://www.fao.org/3/i2800e/i2800e00.htm.

Steele, J.G. 1966. "Report to the Government of Guyana on Soil Surveys." TA2243. Rome: Food and Agriculture Organization of the United Nations. https://edepot.wur.nl/483994.

Tayyeb, Muhammad, Nadeem Rashid, Safi Ullah Khan Achakzai, Saif Ur Rehman, Waseem Akhtar, Kamran Baseer, and Muhammad Sabir. 2017. "Mineral Profile and Proximate Analysis of Fresh and Wastewater Irrigated Cabbage from Quetta Balochistan." *Pure and Applied Biology* 6 (3): 882–88. https://doi.org/10.19045/bspab.2017.60093.

USACE. 1998. "Water Resources Assessment of Guyana." Assessment. Guyana: US Army Corps of Engineers. https://www.sam.usace.army.mil/Portals/46/docs/military/engineering/docs/WRA/Guyana/Guyana%20WRA.pdf.

Uzun, Sezgin. 2006. “The Quantitative Effects of Temperature and Light on the Number of Leaves Preceding the First Fruiting Inflorescence on the Stem of Tomato (Lycopersicon Esculentum, Mill.) and Aubergine (Solanum Melongena L.).” *Scientia Horticulturae* 109 (2): 142–46. https://doi.org/10.1016/j.scienta.2006.04.006.

Wellens, Joost, Dirk Raes, Elias Fereres, Jan Diels, Cecilia Coppye, Joy Geraldine Adiele, Kodjovi Senam Guillaume Ezui, et al. 2022. “Calibration and Validation of the FAO AquaCrop Water Productivity Model for Cassava (Manihot Esculenta Crantz).” *Agricultural Water Management* 263 (April): 107491. https://doi.org/10.1016/j.agwat.2022.107491.

Zhang, Huanxue, Yuji Wang, Jiali Shang, Mingxu Liu, and Qiangzi Li. 2021. “Investigating the Impact of Classification Features and Classifiers on Crop Mapping Performance in Heterogeneous Agricultural Landscapes.” *International Journal of Applied Earth Observation and Geoinformation* 102 (October): 102388. https://doi.org/10.1016/j.jag.2021.102388.

9. Appendix

Appendix A

Key:

M	= Measured parameter	Lit	= From literature
F	= Field observation and information	AQ	= AquaCrop default
Con	= Conservative parameter	n/a	= Not applicable
Com	= Computed		

Table 6.A1. Crop simulation parameters used after calibration

PARAMETER	SOURCE	Tomato	Eggplant	Hot Pepper	Bora Bean	Cabbage	Cassava
Development:							
Type of planting method	F	transplanting	transplanting	direct sowing	direct sowing	transplanting	transplanting
sowing rate (kg seed/ha)	F	n/a	n/a	1.33	3.67	n/a	n/a
Row spacing (m)	Lit, F	1.5	1.4	n/a	n/a	1.5	1.5
Plant spacing (m)	Lit	0.2	0.7	n/a	n/a	1.0	0.67
Maximum canopy cover (CCx) (%)	AQ	75	85	85	85	85	85
Canopy decline coefficient (CDC) (%/day)	Con, Lit	0.4	8.0	8.0	8.0	8.0	4.1
Days to recovered (days)	AQ, Lit	3	7	7	17	65	10
Days to maximum canopy (days)	AQ, Lit	53	67	120	35	164	70
Days to senescence (days)	AQ, Lit	82	105	140	70	245	300
Days to maturity (days)	AQ, Lit, F	102	134	140	76	270	360
Duration of flowering	AQ, Lit	40	74	60	26	n/a	250
Days to flowering (days)	AQ, Lit	28	30	90	35	n/a	80
Max effective rooting depth (m)	AQ, Lit	0.90	1.0	0.75	0.95	0.4	0.65
Days to maximum root depth (days)	AQ	46	60	65	35	135	135
Evapotranspiration							
Effect of canopy shelter in late season (%)	Con	60	60	60	60	60	60
Crop coefficient at CCx (Kc tr,x)	AQ, Lit	1.1	1.05	1.1	1.1	1.05	1.0
Production							
Water Productivity (WP*) (g/m^2)	Con	18.0	17.0	17.0	17.0	17.0	17.0
Reference Harvest Index (Hio) (%)	AQ, Lit	63	50	50	50	85	60
Response to Water Stress:							
p(upper) for canopy expansion	Con	0.15	0.25	0.25	0.25	0.25	0.25
p(lower) for canopy expansion	Con	0.55	0.55	0.55	0.55	0.55	0.60
Shape factor for canopy expansion	Con	3	3	3	3	3	3
p(upper) for stomatal closure (psto)	AQ, Lit	0.4	0.45	0.3	0.45	0.4	0.5

PARAMETER	SOURCE	Tomato	Eggplant	Hot Pepper	Bora Bean	Cabbage	Cassava
Shape factor for stomatal closure	Con	3	3	3	3	3	3
p(upper) for early senescence (psen)	Con	0.7	0.85	0.85	0.85	0.85	0.5
Shape factor for early senescence	Con	3	3	3	3	3	3
Aeration threshold below saturation (% vol)	AQ	5	5	5	5	5	5
Harvest index adjustment							
Water stress during vegetative (unitless)	Con, Lit	0	+ 10	+ 10	+ 10	n/a	+ 4
P(upper) for failure of pollination (unitless)	Con	0.92	0.9	0.9	0.90	n/a	n/a
Stress affecting leaf expansion (unitless)	Con, Lit	+ 0	+ 10	+ 10	+ 10	n/a	+ 4
Stress affecting yield formation (unitless)	Con, Lit	-3	- 8	- 8	- 8	n/a	- 10
Max. HI adjustment (%)	Com	15	15	15	15	n/a	15
Response to Temperature Stress							
Base temp for crop development (°C)	AQ, Lit	7	10	10	10	10	10
Upper temp for crop development (°C)	AQ, Lit	28	35	30	35	30	30
Min. air temp affecting pollination (°C)	Con	10	8	8	8	n/a	n/a
Max. air temp affecting pollination (°C)	Con	45	40	40	40	n/a	n/a
Response to Salinity							
Lower Ece threshold (ECEn) (dS/m)	Con, Lit	1.7	2	2	4.9	1.4	2.0
Upper Ece threshold (ECEx) (dS/m)	Con, Lit	12.8	15	9	13.2	10.1	12.0
Ece affecting canopy expansion (dS/m)	Con	4.8	5.3	3.8	7.0	4.0	4.5
Ece affecting stomatal closure (dS/m)	Con	4.8	5.3	3.8	7.0	4.0	4.5

Table 6.A2. Other simulation parameters used after calibration

Parameter	Source	Value
A. Climate File:		
Rainfall	M	Daily, 2005 – 2012
Evapotranspiration (ETO)	Com	Daily, 2005 – 2012
Temperature	M	Daily, 2005 – 2012
CO2	AQ	Yearly, MaunaLoa
B. Irrigation File:		
Irrigation Method	F	Furrow
Irrigate back to	F	Field Capacity
Water Quality	F	2.0 dS/m
C. Soil File:		
Horizons information (texture, thickness, PWP, FC, SAT)	M	3 horizons up to 0.45 m depth
Saturated hydraulic conductivity (Ksat)	AQ	35.0 mm/day
Curve Number (CN)	AQ, Cal	72
D. Field Management:		
Soil cover by mulches	F	None, 0%
Weed cover	F, Cal	5%
Effect on CN by field practice (poor hydrologic condition, straight furrows)	F, Cal	+10%
E. Simulation parameters:		
Planting Search Window	F, Cal	May for Season 1 Nov for Season 2
Initial soil Water	F	At 80% TAW
Initial soil salinity	F	2.00 dS/m
Initial canopy cover (CCo)	AQ	0%
Initial Biomass	AQ	0 ton cane/ha
Initial root depth	AQ	0.30 m

CHAPTER VII: COMPREHENSIVE DISCUSSION

1. Application of new developments in remote sensing for crop inventory mapping

The assessment of single-date, single-sensor images has shown high accuracy of Landsat8 for classifying sugarcane areas, and Sentinel2 for rice. The spatial and spectral resolution of the satellite images have played a role in crop identification, The fusion of Sentinel2 and RCM images provided a better accuracy (95 to 100%) for both crops. An accuracy analysis for May, June and October 2021, and January 2022 have helped identify the crop stages which are suitable for a crop inventory. During the tillering stage for rice and the establishment stage for sugarcane, the crops are too short and sparse to be identified properly. Meanwhile, harvested rice fields and late maturity stage and harvested sugarcane fields are not suitable for a crop inventory as these areas are misclassified with mixed vegetation. The best stages to conduct a crop inventory are late vegetative to ripening stages for rice and tillering to early maturity for sugarcane. If planting follows the usual cropping calendar, these stages dominate the fields from January to March, and June to August.

The crop inventory and irrigation water requirement work in tandem for the operational design of an irrigation and drainage system. The results of a crop inventory can be used alongside data on watershed or irrigation service area boundaries to identify the hectarage of rice and sugarcane within their bounds.

The field practice of irrigation for rice and sugarcane is represented by the 100% WHR and 70%WHR scenarios respectively. For these current irrigation regimes, a rice field will require roughly 504 m^3 ha^{-1} $month^{-1}$ and a sugarcane plot will require 323 m^3 ha^{-1} $month^{-1}$. The field water requirement of rice and sugarcane multiplied with the production area and the I&D system efficiencies will provide us with the minimum volume of water needed per month. This amount can be compared with the available water from the conservancy or the pump discharge to determine additional potential irrigation areas. These are also possible expansion areas for either rice, sugarcane or vegetable production. However, the volume comparison between the water supply and agriculture demand might also show that the water storage capacity of the conservancy or the pump discharge rate is not sufficient for the current production area's needs. In this case, the water-saving scenarios discussed in Chapters III, IV and V can be explored alongside developments in the conservancy design and pumping capacity.

2. The applicability of AquaCrop for crop simulations at a regional scale

The rice and sugarcane calibration and validation exercise have shown that the AquaCrop can be used to simulate the yield of these crops at a regional scale. But for this to work, the modeller needs at least the field-measured data on the soil and climate. As such, the results of a simulation can be expanded to areas having similar soil, climate type, water quality, and agricultural management practice. The paper in Chapter VI on vegetables has shown, however, that modellers need to be careful in expanding the coverage of a simulation's results.

General classifications such as the USDA and FAO Subgroup and Family Soil Classification, and the Koppen-Geiger climate classification are too broad for simulations smaller than the country scale. A paper by (Pasquel et al., 2022) has expounded on the hazards of using classifications and parameters for modelling at various scales. The scale at which a simulation is analyzed should ideally be the same scale at which the model parameters are generalized. As such, a general parameter value or grouping which describes large portions of the world, as was the case of the Koppen-Geiger, would not capture the variability of the parameter at smaller scales. In the same way, a parameter measured at one plot or farm may represent only that specific farm and not adequately represent the general characteristics of the crop for a region.

The analysis and recommendations of Chapters IV, V, and VI are for the scale of a region or a conservancy service area. A more detailed classification such as the climatic regimes defined by the Hydromet Department of Guyana (GLSC, 2013), and the soil series mapping (Steele, 1966) may be a better categorical system with which to expand the results of a simulation.

3. Sensitivity of crop parameters

The calibration of rice and sugarcane has shown that simulated yield is more sensitive to some parameters than others. Big errors or changes to these parameters will decrease the simulation's congruence with the actual yields. These parameters are the crop stage duration and the crop coefficient.

The crop stage duration is the days or growing-degree-days from planting or transplanting until maximum canopy and maturity. This information is important for an AquaCrop simulation since they contribute to computations of the effective canopy cover and effective rooting depth (Ze). The crop stage duration also affects the crop's exposure to flooding or drought, especially those occurring near the end of a growing season.

The crop coefficient, meanwhile, is directly used in the computation of crop transpiration. As it is among the first computations done in the model, errors in the crop coefficient will compound in the succeeding computations. Compared to the crop stage duration whose information is provided for each cultivar by breeding centers, or easily measurable in the fields by the farmers themselves, the crop coefficient is more tedious to measure. The kc values are usually determined through research, and as such, may be accurate for the cultivar or climate conditions that it was measured. Steps to make the kc values transferable are delineated by (Allen et al., 1998), however, the review by (Pereira, Paredes, López-Urrea, et al., 2021) has shown that few studies have met the pristine and standard requirements to obtain transferable crop coefficients. It is thus helpful to use kc values measured locally, if possible, or from locations having the same climate regime, and calibrate the kc before scenario simulations are done.

Aside from these two parameters, it is also important to get field measurements of the maximum rooting depth (Zx) and experiments or calibration of the root zone depletion threshold of water stress for stomatal closure (psto). The Zx influences the effecting rooting depth, and thus the computations of the soil water uptake. The psto meanwhile is important in the simulation of the impact of water stress. The psto defines the boundary above which plants start to experience water stress as discussed in Chapter II.

One of the key features of AquaCrop is its provision of conservative and default parameters for the simulations. Experimental research into the kc and psto values of different crops would contribute to confirming or improving the conservative parameters used. It would also assist in developing new parameter files outside of the 15 crop files in AquaCrop.

4. Response of yield to varying %WHR irrigation thresholds

The simulations for rice, sugarcane and vegetables have all shown that water-saving scenarios can be efficiently used without incurring significant ($p > 0.05$) yield losses. Vegetables can use as low as 40%WHR deficit irrigation, 50%WHR for sugarcane and 80%WHR for rice.

One possible reason for these low limits is the coastal farms' environment. The rainfall is abundant, wet days are frequent, and the soils have high water-holding capacities. The high rainfall received is evident in the coastal area's need for drainage, which has been the main purpose of Guyana's canals for several years. Yet even when rainfall is high, there are dry days in between when a crop needs water. Even at the lowest threshold, at 40%WHR, for all the crops studied, an irrigation requirement is still simulated. Both irrigation and drainage are essential considerations for a functioning agricultural water management system.

CHAPTER VIII: CONCLUSION

1. Summary and overall conclusion

This research aims to contribute to the design of agricultural water management practices in Guyana by establishing a methodology for a crop inventory and assessing irrigation scenarios for rice, sugarcane and vegetables.

For the component of the crop inventory, we have identified satellite data products and dates of image acquisition for the methodology of a crop inventory in Guyana. Between single-date images of Landsat8, Sentinel2, and RCM, Landsat8 was the most accurate in classifying sugarcane areas, while for rice, Sentinel2 was better. The fusion of Sentinel2 and RCM gave better accuracies for a simultaneous inventory of rice and sugarcane. The analysis by image acquisition date has shown that among the crop growth stages, the images acquired two to months after planting for rice, and three to twelve months for sugarcane were adequate for a crop inventory. Rice and sugarcane are undistinguishable in the satellite images during their early growth stages (tillering for rice and establishment for sugarcane) and at late maturity.

Crop water productivity and yield simulations were also conducted for several crops. AquaCrop has been proven to reliably simulate the yield at a regional scale based on the validation of rice and sugarcane simulations. Sensitivity analyses of the rice and sugarcane simulations have identified the crop stage duration, maximum rooting depth (Zx), crop coefficient (kc) and threshold of water stress affecting stomatal closure (psto) as important crop parameters for crop simulations. Measurement or calibration of these values will help improve the accuracy of future crop simulation studies.

Deficit irrigation scenarios of varying soil-water thresholds were simulated and analyzed. The 80%WHR scenario for rice, 50% WHR for sugarcane and 40%WHR for vegetables were assessed to be suitable water-saving irrigation methods at the coastal farms. In these scenarios, there is no significant decrease ($p>0.05$) in yield, and irrigation requirements are lower compared to current irrigation schemes.

The planting season does not affect the yields obtained for rice, sugarcane and vegetables. The location, meanwhile, contributes to yield differences observed between Black Bush Polder and Parika. These two locations have the same front land clay soils and wet tropical climates but have different soil series and national-level climate regimes. More detailed soil and climate classifications, such as the soil series and national climate regime, are a better basis for expanding the results of a simulation as compared to broad global classifications.

The future climate for Guyana is forecasted to be drier. However, the current climate over the coast is still very wet, and as such drainage is the most important component equal focus on both irrigation and drainage will help ensure that Guyana's agriculture is adapted to the future climate while protecting it from the risks of the present.

2. Recommendations

2.1. Policy

Use remote sensing technologies for crop monitoring. The work on the crop inventory has shown that it is possible to use remote sensing for crop monitoring in Guyana. Before the technology could be adapted, the Ministry of Agriculture, or any of its divisions, has to be enabled in using this technology such as through the hiring or training of personnel on GIS; acquisition of processing equipment; and participation in further research to improve and apply the methodology.

Give incentives for farmers to employ water-saving irrigation schemes. The use of water-saving irrigation regimes such as deficit irrigation is useful in improving the efficiency of the system and saving irrigation water which can then be used to irrigate other farms. This is especially helpful when the agriculture sector seeks to expand the production area. However, these benefits are more felt in the community than at the farmer level. The recommended irrigation scenarios predict no significant decrease in yield, but at the same time, there is also no significant increase in yield. For a farmer, water-saving regimes do not benefit his harvest. An incentive provided through an irrigation association, or deduction of conservancy fees may help encourage the farmer to participate.

Create a long-term adaptation plan for agriculture Lower annual rainfall is forecasted in the next 50 years in Guyana, but at the same time sea levels are also expected to rise (Government of Guyana, 2012). These may reduce the existing agricultural area or spurn the gradual expansion of agricultural land further inwards or. Yet, there is a limit to inward expansion as the boundaries of the soils suitable for agriculture and the existing conservatories are reached. The results of this thesis can be used in developing a long-term adaptation plan to make full use of the country's resources.

2.2. Further research

Test and apply the %WHR scenarios recommend by this study. A field experiment in Guyana which compares the conventional irrigation methods and the recommended %WHR scenarios for rice, sugarcane and vegetables would be helpful to confirm the simulated effect on yield. This will also assist in establishing more confidence in these proposed irrigation thresholds.

Measure the crop growth stage durations and rooting zone depth of vegetables grown in Guyana. Field measurement of these two parameters is important for crop simulations. Key crop parameters for rice are provided by the GRDB whenever a new cultivar is released, while for sugarcane, these parameters have already been studied. However, there is a gap in information about vegetables. These parameters can be determined by the breeding center or agricultural extension program during their field trials for the introduction of new crops, varieties or cultivars.

Water productivity of various furrow irrigation schemes: In this paper, we have not seen any significant difference in water productivity between the %WHR thresholds used. Improvements to water productivity may be more pronounced when comparing continuous flow irrigation with deficit irrigation. Different methods of irrigation may also be compared as was done by Ünlü et al. (2007) for cotton by comparing continuous flow irrigation, alternate furrow irrigation, surge irrigation, cutback irrigation, and tailwater reuse system. Other irrigation methods such as sprinklers, center pivot or subsurface irrigation can also be studied and compared with the current irrigation methods in Guyana to determine if the water productivity is improved.

Use remote sensing-based indexes to estimate parameter values. One research area forward is the combination of satellite images and crop modelling. The recent advances in the field have tried to determine crop model parameters such as maximum canopy cover, relative biomass (B_{rel}) (Han et al., 2020), and aboveground biomass (Kim & Kaluarachchi, 2015; Mohamed Sallah et al., 2019) from satellite-derived indexes. Research on this area is still relatively and much can still be done to identify the relationship between the many remote-sensing indexes, and crop parameters. This field of research also assists in identifying general crop parameters which are representative of the characteristics at the study area's scale.

Irrigation design for broad-bed layouts. Farm labour issues in Guyana push an inevitable shift of the sugarcane farm layouts from the furrow-and-ridge into the more machinery-friendly broad-bed design. The shift from furrows to a broad-bed layout will alter the wetting pattern of the soil. There are not a lot of studies comparing the wetting pattern of the furrow-and-ridge and the broad-bed configuration, more so specifically for sugarcane or heavy clay soils. Yet, it is known that water expands more in the horizontal direction in clay soils than in course-textured soils

(Naglič et al., 2014), but as beds become wider drier spots appear at the center (Memon et al., 2020). It will be helpful to understand the wetting pattern of a typical sugarcane broad-bed plot under furrow irrigation in Guyana. This helps determine if changes in the field irrigation method need to be done to ensure that the driest part of a plot still gets the appropriate amount of moisture.

CHAPTER IX: REFERENCE LIST

Abera, M., Wale, A., Abie, Y., & Esubalew, T. (2020). Verification of the Efficiency of Alternate Furrow Irrigation on Amount of Water Productivity and Yield of Onion at Sekota Woreda. *Irrigation & Drainage Systems Engineering*, *9*(4). https://doi.org/10.37421/idse.2020.9.248

Ahmadzadeh Araji, H., Wayayok, A., Khayamim, S., Teh, C. B. S., Fikri Abdullah, A., Amiri, E., & Massah Bavani, A. (2019). Calibration of the AquaCrop Model to Simulate Sugar Beet Production and Water Productivity under Different Treatments. *Applied Engineering in Agriculture*, *35*(2), 211–219. https://doi.org/10.13031/aea.12946

Akinro, A. O., Olufayo, A. A., & Oguntunde, P. G. (2012). Crop Water Productivity of Plantain (Musa Sp) in a Humid Tropical Environment. *Journal of Engineering Science and Technology Review*, *5*, 19–25.

Allen, R. G., Periera, L. S., Raes, D., & Smith, M. (1998). *Crop evapotranspiration—Guidelines for computing crop water requirements*. Food and Agriculture Organization of the United Nations. https://www.fao.org/3/x0490e/x0490e00.htm#Contents

Alvar-Beltrán, J., Heureux, A., Soldan, R., Manzanas, R., Khan, B., & Dalla Marta, A. (2021). Assessing the impact of climate change on wheat and sugarcane with the AquaCrop model along the Indus River Basin, Pakistan. *Agricultural Water Management*, *253*, 106909. https://doi.org/10.1016/j.agwat.2021.106909

Bahmani, O., & Eghbalian, S. (2018). Simulating the Response of Sugarcane Production to Water Deficit Irrigation Using the AquaCrop Model. *Agricultural Research*, *7*(2), 158–166. https://doi.org/10.1007/s40003-018-0311-0

Bayisa, G. D., Hordofa, T., Tezera, K., Tesfaye, A., Ashame, G., & Wondimu, T. (2021). Maize Yield and Water Use Efficiency Under Different Irrigation Levels and Furrow Irrigation Methods in Semiarid, Tropical Region. *Air, Soil and Water Research*, *14*, 11786221211058176. https://doi.org/10.1177/11786221211058177

Biswal, P., Swain, D. K., & Jha, M. K. (2022). Straw mulch with limited drip irrigation influenced soil microclimate in improving tuber yield and water productivity of potato in subtropical India. *Soil and Tillage Research*, *223*, 105484. https://doi.org/10.1016/j.still.2022.105484

Blango, M. M., Cooke, R. A. C., & Moiwo, J. P. (2019). Effect of soil and water management practices on crop productivity in tropical inland valley swamps. *Agricultural Water Management*, *222*, 82–91. https://doi.org/10.1016/j.agwat.2019.05.036

Brar, H. S., & Singh, P. (2022). Pre-and post-sowing irrigation scheduling impacts on crop phenology and water productivity of cotton (Gossypium hirsutum L.) in sub-tropical north-western India. *Agricultural Water Management*, *274*, 107982. https://doi.org/10.1016/j.agwat.2022.107982

Braun, E. G., & Derting, J. F. (1964). Map for the Reconnaissance Soil Survey of Northeast British Guiana [Soil map]. Food and Agriculture Organization of the United Nations. https://esdac.jrc.ec.europa.eu/content/map-reconnaissance-soil-survey-northeast-british-guiana

Bubbico, A., Keller, M., & Opazo, C. M. (2020). Perspectives on diversification prospects for the agrifood industry in Guyana. Food and Agriculture Organization of the United Nations. https://doi.org/10.4060/ca9754en

Camargo Rodriguez, A. V., & Ober, E. S. (2019). AquaCropR: Crop Growth Model for R. *Agronomy*, *9*(7), Article 7.

Chai, Y., Chai, Q., Yang, C., Chen, Y., Li, R., Li, Y., Chang, L., Lan, X., Cheng, H., & Chai, S. (2022). Plastic film mulching increases yield, water productivity, and net income of rain-fed winter wheat compared with no mulching in semiarid Northwest China. *Agricultural Water Management*, *262*, 107420. https://doi.org/10.1016/j.agwat.2021.107420

Chen, S., Woodcock, C. E., Bullock, E. L., Arévalo, P., Torchinava, P., Peng, S., & Olofsson, P. (2021). Monitoring temperate forest degradation on Google Earth Engine using Landsat time series analysis. *Remote Sensing of Environment*, *265*, 112648. https://doi.org/10.1016/j.rse.2021.112648

Corbari, C., Ben Charfi, I., & Mancini, M. (2021). Optimizing Irrigation Water Use Efficiency for Tomato and Maize Fields across Italy Combining Remote Sensing Data and the AquaCrop Model. *Hydrology*, *8*(1), 39. https://doi.org/10.3390/hydrology8010039

CSA. (2021, November). *RADARSAT Constellation Mission* [Government]. Canadian Space Agency. https://www.asc-csa.gc.ca/eng/satellites/radarsat

Dhanapal, R., Tayade, A. S., Bhaskaran, A., & Geetha, P. (2019). Efficient Water Management in Sugarcane with Composted Coir Pith and Sugarcane Trash Under Tropical Indian Conditions. *Sugar Tech*, *21*(2), 256–264. https://doi.org/10.1007/s12355-018-0593-3

Dingre, S. k., Gorantiwar, S. d., Pawar, D. d., Dahiwalkar, S. d., & Nimbalkar, C. a. (2021). Sugarcane response to different soil water replenishment-based deficit irrigation treatments during different growth stages in an Indian semi-arid region*. *Irrigation and Drainage*, *70*(5), 1155–1171. https://doi.org/10.1002/ird.2609

Dou, F., Soriano, J., Tabien, R. E., & Chen, K. (2016). Soil texture and cultivar effects on rice (Oryza sativa, L.) grain yield, yield components and water productivity in three water regimes. *PLOS ONE*, *11*(3), 12. https://doi.org/10.1371/journal.pone.0150549

Elsheikh, E. R. A. (2015). *Water productivity of sunflower under different irrigation regimes on Gezira clay soil, Sudan*.

ESA. (2012, June 14). *Copernicus: Sentinel-1*. EoPortal. https://www.eoportal.org/satellite-missions/copernicus-sentinel-1

ESA. (2022a). *Sentinel-2 MSI User Guide*. Sentinel Online. https://sentinels.copernicus.eu/web/sentinel/user-guides/sentinel-2-msi

ESA. (2022b). *TerraSAR-X and TanDEM-X - Earth Online* [Government]. Earth Online. https://earth.esa.int/eogateway/missions/terrasar-x-and-tandem-x

FAO. (2018). *AquaCrop (software)* (Version 7.0) [Windows]. Food and Agriculture Organization of the United Nations. https://www.fao.org/aquacrop/software/aquacropstandardwindowsprogramme/en/

Feranec, J., Šúri, M., Ot’ahel’, J., Cebecauer, T., Kolář, J., Soukup, T., Zdeňková, D., Waszmuth, J., Vâjdea, V., Vîjdea, A.-M., & Nitica, C. (2000). Inventory of major landscape changes in the Czech Republic, Hungary, Romania and Slovak Republic 1970s – 1990s. *International Journal of Applied Earth Observation and Geoinformation*, *2*(2), 129–139. https://doi.org/10.1016/S0303-2434(00)85006-0

GLSC. (2004). Region VI Sub-Regional Land Use Plan [Soil map]. Guyana Lands & Surveys Commission. https://www.forestcarbonpartnership.org/system/files/documents/Guyana_Region_VI_Sub-Regional_Land_Use_Plan_0.pdf

GLSC. (2013). *Guyana National Land Use Plan*. Guyana Lands and Surveys Commission. https://glsc.gov.gy/wp-content/uploads/2017/05/Summary-Booklet-of-the-National-Land-Use-Plan.pdf

Government of Guyana. (2012). *Guyana 2nd National Communication to the UNFCCC*. Government of Guyana. https://unfccc.int/sites/default/files/resource/guync2.pdf

GuySuCo. (1999). History—Guyana Sugar Corporation Inc [Government]. Guyana Sugarcane Corporation Inc. https://guysuco.gy/index.php?option=com_k2&view=item&id=2:history&Itemid=216&lang=en

GuySuCo. (2018). Annual Report 2018. Guyana Sugar Corporation. https://guysuco.gy/index.php?option=com_k2&view=item&id=786:2018-report&Itemid=262&lang=en

Han, C., Zhang, B., Chen, H., Liu, Y., & Wei, Z. (2020). Novel approach of upscaling the FAO AquaCrop model into regional scale by using distributed crop parameters derived from remote sensing data. *Agricultural Water Management*, *240*, 106288. https://doi.org/10.1016/j.agwat.2020.106288

Hoffman, G. J., Howell, T., & Solomon, K. A. (Eds.). (1990). *Management of Farm Irrigation Systems*. American Society of Agricultural Engineers.

Jägermeyr, J., Gerten, D., Schaphoff, S., Heinke, J., Lucht, W., & Rockström, J. (2016). Integrated crop water management might sustainably halve the global food gap. *Environmental Research Letters*, *11*(2), 025002. https://doi.org/10.1088/1748-9326/11/2/025002

Karandish, F., & Hoekstra, A. Y. (2017). Informing National Food and Water Security Policy through Water Footprint Assessment: The Case of Iran. *Water*, *9*(11), Article 11. https://doi.org/10.3390/w9110831

Kim, D., & Kaluarachchi, J. (2015). Validating FAO AquaCrop using Landsat images and regional crop information. *Agricultural Water Management*, *149*, 143–155. https://doi.org/10.1016/j.agwat.2014.10.013

Lorite, I. J., García-Vila, M., Santos, C., Ruiz-Ramos, M., & Fereres, E. (2013). AquaData and AquaGIS: Two computer utilities for temporal and spatial simulations of water-limited yield with AquaCrop. *Computers and Electronics in Agriculture*, *96*, 227–237. https://doi.org/ 10.1016/j.compag.2013.05.010

Marais-Sicre, C., Fieuzal, R., & Baup, F. (2020). Contribution of multispectral (optical and radar) satellite images to the classification of agricultural surfaces. *International Journal of Applied Earth Observation and Geoinformation*, *84*, 101972. https://doi.org/10.1016/j.jag.2019.101972

McGowan, W. (2008, November 6). The beginnings of rice cultivation in Guyana (Part 2).

Stabroek News. https://www.stabroeknews.com/2008/11/06/features/the-beginnings-of-rice-cultivation-in-guyana-part-2/

Memon, M. S., Ullah, K., Siyal, A. A., Leghari, N., Tagar, A. A., Ibupoto, K. A., Karim, S. T. A., Tahir, M., & Memon, N. (2020). The Effect of Different Raised Bed Sizes under Furrow Irrigation Method on Salt Distribution in Soil Profile and Yield by Hydrus (2/3D). *Pakistan Journal of Agricultural Research*, *33*(1). https://doi.org/10.17582/journal.pjar/2020/33.1.113.125

Ministry of Agriculture. (2013). A National Strategy for Agriculture in Guyana 2013—2020. Ministry of Agriculture, Guyana. https://caricom.org/documents/11264-moa_agriculture_strategy_2013-2020_-_cd.pdf

Mitchell, D. (2006). *Sugar In The Caribbean: Adjusting To Eroding Preferences*. The World Bank. https://doi.org/10.1596/1813-9450-3802

Mohamed Sallah, A.-H., Tychon, B., Piccard, I., Gobin, A., Van Hoolst, R., Djaby, B., & Wellens, J. (2019). Batch-processing of AquaCrop plug-in for rainfed maize using satellite derived Fractional Vegetation Cover data. *Agricultural Water Management*, *217*, 346–355. https://doi.org/10.1016/j.agwat.2019.03.016

Naglič, B., Kechavarzi, C., Coulon, F., & Pintar, M. (2014). Numerical investigation of the influence of texture, surface drip emitter discharge rate and initial soil moisture condition on wetting pattern size. *Irrigation Science*, *32*(6), 421–436. https://doi.org/10.1007/s00271-014-0439-z

NASA. (2022a). *MODIS Specifications*. MODIS - Moderate Resolution Imaging Spectroradiometer. https://modis.gsfc.nasa.gov/about/specifications.php

NASA. (2022b). *NISAR L-Band SAR*. Earth Science Data Systems, NASA; Earth Science Data Systems, NASA. http://www.earthdata.nasa.gov/sensors/nisar-l-band-sar

Pasquel, D., Roux, S., Richetti, J., Cammarano, D., Tisseyre, B., & Taylor, J. A. (2022). A review of methods to evaluate crop model performance at multiple and changing spatial scales. *Precision Agriculture*, *23*(4), 1489–1513. https://doi.org/10.1007/s11119-022-09885-4

Peel, M. C., Finlayson, B. L., & McMahon, T. A. (2007). Updated world map of the Koppen-Geiger climate classification. Hydrology and Earth System Sciences, 11, 1633–1644. www.hydrol-earth-syst-sci.net/11/1633/2007/

Pereira, L. S., Paredes, P., Hunsaker, D. J., López-Urrea, R., & Mohammadi Shad, Z. (2021). Standard single and basal crop coefficients for field crops: Updates and advances to the FAO56 crop water requirements method. *Agricultural Water Management*, *243*, 106466. https://doi.org/10.1016/j.agwat.2020.106466

Pereira, L. S., Paredes, P., López-Urrea, R., Hunsaker, D. J., Mota, M., & Mohammadi Shad, Z. (2021). Standard single and basal crop coefficients for vegetable crops, an update of FAO56 crop water requirements approach. *Agricultural Water Management*, *243*, 106196. https://doi.org/10.1016/j.agwat.2020.106196

Pfitzner, K., Bartolo, R., Whiteside, T., Loewensteiner, D., & Esparon, A. (2022). Multi-temporal spectral reflectance of tropical savanna understorey species and implications for hyperspectral remote sensing. *International Journal of Applied Earth Observation and*

Geoinformation, *112*, 102870. https://doi.org/10.1016/j.jag.2022.102870

Poddar, R., Acharjee, P. U., Bhattacharyya, K., & Patra, S. K. (2022). Effect of irrigation regime and varietal selection on the yield, water productivity, energy indices and economics of rice production in the lower Gangetic Plains of Eastern India. *Agricultural Water Management*, *262*, 107327. https://doi.org/10.1016/j.agwat.2021.107327

Rallo, G., Paço, T. A., Paredes, P., Puig-Sirera, À., Massai, R., Provenzano, G., & Pereira, L. S. (2021). Updated single and dual crop coefficients for tree and vine fruit crops. *Agricultural Water Management*, *250*, 106645. https://doi.org/10.1016/j.agwat.2020.106645

Raoufi, R. S., & Soufizadeh, S. (2020). Simulation of the impacts of climate change on phenology, growth, and yield of various rice genotypes in humid sub-tropical environments using AquaCrop-Rice. *International Journal of Biometeorology*, *64*(10), 1657–1673. https://doi.org/10.1007/s00484-020-01946-5

Salman, M., Garcia-Vila, M., Fereres, E., Raes, D., & Steduto, P. (2021). *The AquaCrop model: Enhancing crop water productivity. Ten years of development, dissemination and implementation 2009-2019* (No. 47; FAO Water Report). Food and Agriculture Organization of the United Nations. https://doi.org/10.4060/cb7392en

Sandhu, S. S., Mahal, S. S., & Kaur, P. (2015). Calibration, validation and application of AquaCrop model in irrigation scheduling for rice under northwest India. *Journal of Applied and Natural Science*, *7*(2), 691–699. https://doi.org/10.31018/jans.v7i2.668

Singh, T. (2021). Study of the socio-economic impact of the closure of GUYSUCO sugar estates on sugar workers in Guyana. International Labour Organization. https://guyana.un.org/sites/default/files/2021-06/Socio%20economic%20impact%20of%20estate%20closures%20on%20GUYSUCO%20sugar%20workers_0.pdf

Steduto, P., Hsiao, T. C., Fereres, E., & Raes, D. (2012). *Crop yield response to water*. Food and Agriculture Organization of the United Nations. https://www.fao.org/3/i2800e/i2800e00.htm

Steduto, P., Hsiao, T. C., Raes, D., & Fereres, E. (2009). AquaCrop—The FAO Crop Model to Simulate Yield Response to Water: I. Concepts and Underlying Principles. *Agronomy Journal*, *101*(3), 426–437. https://doi.org/10.2134/agronj2008.0139s

Steele, J. G. (1966). *Report to the Government of Guyana on Soil Surveys* (No. TA2243; p. 250). Food and Agriculture Organization of the United Nations. https://edepot.wur.nl/483994

Ünlü, M., Kanber, R., Onder, S., Sezen, M., Diker, K., Ozekici, B., & Oylu, M. (2007). Cotton yields under different furrow irrigation management techniques in the Southeastern Anatolia Project (GAP) area, Turkey. *Irrigation Science*, *26*(1), 35–48. https://doi.org/10.1007/s00271-007-0070-3

USACE. (1998). Water Resources Assessment of Guyana. US Army Corps of Engineers. https://www.sam.usace.army.mil/Portals/46/docs/military/engineering/docs/WRA/Guyana/Guyana%20WRA.pdf

USGS. (2022). *Landsat Frequently Asked Questions*. USGS - Mapping, Remote Sensing, and Geospatial Data. https://www.usgs.gov/landsat-missions/landsat-frequently-asked-questions

Vélez-Sánchez, J. E., Balaguera-López, H. E., & Rodríguez Hernández, P. (2022). The water status of pear (Pyrus communis L.) under application of regulated deficit irrigation in high tropical latitudinal conditions. *Journal of the Saudi Society of Agricultural Sciences*, *21*(7), 460–468. https://doi.org/10.1016/j.jssas.2021.12.003

Verma, A., Kumar, A., & Lal, K. (2019). Kharif crop characterization using combination of SAR and MSI Optical Sentinel Satellite datasets. *Journal of Earth System Science*, *128*(8), 230. https://doi.org/10.1007/s12040-019-1260-0

Waser, L. T., & Schwarz, M. (2006). Comparison of large-area land cover products with national forest inventories and CORINE land cover in the European Alps. *International Journal of Applied Earth Observation and Geoinformation*, *8*(3), 196–207. https://doi.org/10.1016/j.jag.2005.10.001

Wellens, J., Raes, D., Fereres, E., Diels, J., Coppye, C., Adiele, J. G., Ezui, K. S. G., Becerra, L.-A., Selvaraj, M. G., Dercon, G., & Heng, L. K. (2022). Calibration and validation of the FAO AquaCrop water productivity model for cassava (Manihot esculenta Crantz). *Agricultural Water Management*, *263*, 107491. https://doi.org/10.1016/j.agwat.2022.107491

Zhuo, L., Mekonnen, M. M., & Hoekstra, A. Y. (2016). Benchmark levels for the consumptive water footprint of crop production for different environmental conditions: A case study for winter wheat in China. *Hydrology and Earth System Sciences*, *20*(11), Article 11. https://doi.org/10.5194/hess-20-4547-2016